



**UNIVERSIDAD DE INVESTIGACIÓN DE  
TECNOLOGIA EXPERIMENTAL YACHAY**

**Escuela de Ciencias de la Tierra, Energía y Ambiente**

**TÍTULO: GEOLOGIC CHARACTERIZATION OF  
SALINAS DE IBARRA: DISCOVERING THE ORIGIN OF  
SALT.**

Trabajo de integración curricular presentado como requisito para  
la obtención del título de Geólogo.

**Autor:**

Chusin Cunuhay Rubén Ricardo

**Tutor:**

Ph.D. Vazquez Taset Yaniel Misael

**Co-Tutor:**

Ph.D. Ávila Sosa Edward Ebner

Urcuquí, julio 2023

## **AUTORIA**

Yo, **CHUSIN CUNUHAY RUBÉN RICARDO**, con cédula de identidad 0504827668, declaro que las ideas, juicios, valoraciones, interpretaciones, consultas bibliográficas, definiciones y conceptualizaciones expuestas en el presente trabajo; así cómo, los procedimientos y herramientas utilizadas en la investigación, son de absoluta responsabilidad de el autor del trabajo de integración curricular. Así mismo, me acojo a los reglamentos internos de la Universidad de Investigación de Tecnología Experimental Yachay.

Uruguay, julio del 2023.



---

Rubén Ricardo Chusin Cunuhay

CI: 0504827668

## AUTORIZACIÓN DE PUBLICACIÓN

Yo, **CHUSIN CUNUHAY RUBÉN RICARDO**, con cédula de identidad 0504827668, cedo a la Universidad de Investigación de Tecnología Experimental Yachay, los derechos de publicación de la presente obra, sin que deba haber un reconocimiento económico por este concepto. Declaro además que el texto del presente trabajo de titulación no podrá ser cedido a ninguna empresa editorial para su publicación u otros fines, sin contar previamente con la autorización escrita de la Universidad.

Asimismo, autorizo a la Universidad que realice la digitalización y publicación de este trabajo de integración curricular en el repositorio virtual, de conformidad a lo dispuesto en el Art. 144 de la Ley Orgánica de Educación Superior.

Urcuquí, julio del 2023



---

Rubén Ricardo Chusin Cunuhay

CI: 0504827668

## **DEDICATORY**

I dedicate this work to my grandparents, who are up there in heaven; they always supported me. I also dedicate this work to my family, Chusin & Cunuhay, who helped me during my college career, especially my mother, Maria, my father, Ricardo, and my siblings, Jonathan, Gloria, and Annabel. In addition, I dedicate this work to my uncles, especially Daniel Chusin, who is always looking out for my academic and emotional situation.

Thanks to all of them throughout my university life, I was able to finish my studies at the excellent Yachay Tech University.

Chusin Cunuhay Rubén Ricardo

## ACKNOWLEDGMENTS

First, I want to thank God for always protecting me in all the processes of my life.

I want to thank my family for always being attentive to my college life.

I want to thank my tutor Yaniel Vázquez and my co-tutor Edward Ávila who were my guide and support in my thesis project. Without a doubt, they are excellent professors and people.

I am grateful to each of the professors who were and are part of Yachay Tech with whom I shared excellent moments, especially Germán Martín, Felipe Carlosama, Sebastián Gallegos, Cristian Panchana, Raúl Davalos, Rafael Almeida, Anna Foster, Wayra Simbaña, Elisa Piispa, Celine Mandon, Carlos Loyo, Elizabeth Mariño, Mariela Rodríguez, Milena Gonzalez and Karla Freire.

I am grateful to each of my university classmates with whom I was able to share with whom I was able to share unforgettable moments, especially Luis Zhinin, Jenny Gonzales, Evelyn Guiz, Nicole Jara, Johana Criollo, Gabriel Cofre, Truman Tapia, and T2-12 house, who were part of the University from the beginning. I also thank Erika, Javier, Karol, Angie, BatiFamiliy, and B31 House. They were an essential part of these last times in my university stage to excel at any time. I thank all my friends and acquaintances who always brightened the day with any activity that motivated me to keep fighting for my goals.

Finally, I thank the GeoclubYT that was part of my life; it allowed me to generate more confidence and experience in leading an amiable group. Also, I would like to thank the Chuchin&AsociadosYT soccer team with which I became champion, and I feel happy for each achievement.

Chusin Cunuhay Rubén Ricardo

## RESUMEN

El proceso de explorar, encontrar y usar la sal ha evolucionado junto con el avance de la humanidad, convirtiéndola en un componente necesario en la Tierra. En esta investigación se ha estudiado los minerales de las sales de la parroquia Santa Catalina de Salinas debido a que la zona, en siglos anteriores fue considerada uno de los mayores productores de sal del Norte del País; sin embargo, el contexto geológico del origen de la sal no ha sido muy estudiado. Este estudio ha sido desarrollado mediante la recopilación de muestras de suelo, costras de sal y agua; en la cual se encuentran en las diferentes zonas de Tolas, afloramientos, vertientes naturales y superficiales. Por lo tanto, para determinar el contexto geológico del área de estudio se realizó una investigación de campo, considerando las diferentes unidades geológicas, para posteriormente representarlas en un mapa geológico. De esta manera, se aplicaron varios procesos, tales como, un análisis del pH del agua para identificar la clasificación de la misma, una caracterización mineralógica de las muestras de suelo mediante la difracción de rayos X (DRX). El análisis de tamizado fue usado para separar las fracciones granulométricas de las muestras obtenidas en las 24 Tolas. Posteriormente, las muestras de las Tolas fueron seleccionadas aleatoria mediante dos métodos basados en Python; con el primer método, se seleccionaron siete Tolas y con el empleo del segundo método fue seleccionada la Tola de la cual se extrajo la sal de forma artesanal; en esta muestra se aplicó un análisis semicuantitativo de la fase de composición mineralógica mediante DRX, con el fin de comprender la concentración salina de la muestra. Gracias a estos análisis, se identificó que las muestras de suelo se clasifican como arena fina a gruesa; presentando concentraciones, principalmente, de sales solubles en fracciones de arena fina. Además, los grupos funcionales químicos reconocidos fueron sulfatos, carbonatos, cloruros, boratos, fosfatos y nitratos; siendo los sulfatos, el grupo químico funcional más predominante con la mineral thenardita ( $\text{Na}_2\text{SO}_4$ ); seguido por el grupo de los carbonatos con la mineral calcita ( $\text{CaCO}_3$ ), y el borato con el sassolite ( $\text{H}_3\text{BO}_3$ ). Los resultados permitieron determinar el origen de la sal, correspondiente a precipitaciones en suelos salinos de origen continental, asociados a depósitos vulcanoclasticos asociados a colapsos de edificios volcánicos, que formaron terrazas indiferenciadas, específicamente con material volcánico de Chachimbiro, fase de erupción 2 (CH-2) y Yanahurco.

**PALABRAS CLAVES:** Santa Catalina de Salinas, fracciones granulométricas, sales solubles, difracción de rayos x (DRX), fases de minerales, origen de depósitos de sal, y materiales volcánicos.

## ABSTRACT

The process of exploring, finding, and utilizing salt has evolved alongside the progress of humanity, rendering it an indispensable element on Earth. This research focuses on studying the salt minerals in the parish of Santa Catalina de Salinas, as this region was once renowned as one of the major salt industries in northern Ecuador. However, the geological context regarding the origins of salt in this area remains unexplored. This study involved the collection of soil samples, salt crusts, and water from various areas including Tolas, outcrops, and natural springs. The collected samples were then utilized to determine the geological context of the study area. To achieve this, fieldwork was conducted to investigate other geological units, which were subsequently represented on a geological map. Various procedures were implemented as part of the research. For instance, pH analysis was conducted on water samples to determine their classification. Soil samples underwent mineralogical characterization using X-ray diffraction (XRD) methodology. Sieving analyses were used in order to separate the granulometric fractions of the 24 samples taken from the Tolas. After that the Tola samples were randomly selected using two methods based on Python; in the first method, seven tolas were selected, and in the second method, one sample was chosen to extract the salt using artisanal methods. Semi-quantitative analysis of the mineral phase composition was conducted through XRD in order to determine the concentration of the salts and a better understanding of their distributions. Finally, analyzing these results, it was possible to identify the grain size classification of the samples, obtained that the samples had a fine to coarse sand classification, with high concentrations of soluble salts in fine sand fractions. Additionally, the chemical functional groups recognized were sulfates, carbonates, chlorides, borates, phosphates, and nitrates, being sulfates the most predominant chemical functional group, with 27% of thenardite mineral, ( $\text{Na}_2\text{SO}_4$ ), follow by carbonate with calcite mineral, ( $\text{CaCO}_3$ ), and borate with sassolite, ( $\text{H}_3\text{BO}_3$ ). Based on the results, we were able to determine the origin of the salt. It is derived from soluble salts found in saline soils of continental origin, which are associated with volcanoclastic deposits resulting from the collapse of volcanic edifices. These deposits have formed undifferentiated terraces, specifically related to the Chachimbiro volcanic eruption phase 2 (CH-2) and the Yanahurco volcanic activity.

**KEY WORDS:** Santa Catalina de Salinas, granulometric fractions, soluble salts, X-ray diffraction (XRD), mineral phases, salt deposits origin, and volcanic materials.

## Table of Contents

<b>DEDICATORY</b> .....	iii
<b>ACKNOWLEDGMENTS</b> .....	iv
<b>ABSTRACT</b> .....	vi
<b>List of Figures</b> .....	ix
<b>List of Tables</b> .....	xi
<b>1. Chapter 1. Introduction</b> .....	1
<b>1.1 The history and formation of the salt</b> .....	1
<b>1.2 Salt deposits production processes Worldwide</b> .....	2
<b>1.3 History of salt production in Ecuador</b> .....	3
<b>1.4 Salt in Santa Catalina de Salinas (Imbabura province)</b> .....	4
<b>1.5 Background information</b> .....	5
1.5.1 Salt classification in the environment .....	6
1.5.2 Origin of salt crystallization .....	10
1.5.3 Saline or sodic soil classification .....	14
<b>1.6 Statement of the Problem</b> .....	15
<b>1.7 Objectives</b> .....	15
1.7.1 General objective .....	15
1.7.2 Specific objective .....	16
<b>1.8 Introduction to study area</b> .....	16
<b>1.9 Geomorphology</b> .....	19
<b>1.10 Climate conditions</b> .....	20
<b>2 Chapter 2. Geological Framework</b> .....	22
<b>3 Chapter 3. Experimental procedure</b> .....	29
<b>3.1 Materials and Equipment</b> .....	29
<b>3.2 Methodology</b> .....	29
3.2.1 Laboratory work .....	32



3.2.2	pH analysis .....	32
3.2.3	Salt sample separation .....	32
3.2.4	Sieving methods .....	33
3.2.5	Granulometric analysis .....	35
3.2.6	Artisanal extraction of salt .....	39
3.2.7	Crushing process .....	41
3.2.8	X-ray diffraction analysis (XRD) .....	42
<b>4.</b>	<b>Chapter 4. Result and Discussion .....</b>	<b>45</b>
<b>4.1</b>	<b>Stratigraphic column of the study area .....</b>	<b>45</b>
<b>4.2</b>	<b>Granulometric analysis .....</b>	<b>47</b>
<b>4.3</b>	<b>pH analysis.....</b>	<b>48</b>
<b>4.4</b>	<b>X- Ray Diffraction result.....</b>	<b>49</b>
4.4.1	Second methodology: Salt extraction .....	54
4.4.2	Salt Crusts Samples .....	58
<b>4.5</b>	<b>Discussion.....</b>	<b>63</b>
4.5.1	Salt deposits based on the stratigraphy of the area .....	63
4.5.2	Granulometric fractions .....	64
4.5.3	Mineral phase group of the samples .....	65
<b>5.</b>	<b>Chapter 5. Conclusions and Recommendation.....</b>	<b>74</b>
<b>5.1</b>	<b>Conclusions .....</b>	<b>74</b>
<b>5.2</b>	<b>Recommendations .....</b>	<b>75</b>
<b>6.</b>	<b>References .....</b>	<b>75</b>

## List of Figures

- Figure 1.** Location map and elevation model of the study area within the province of Imbabura at a scale of 1:50,000 (A). Sample collection site of the 24 Tolas and salt crusts. Additionally, six water samples from natural and surface springs near and around Santa Catalina de Salinas (B) and (C). ..... 18
- Figure 2.** Representation of the geomorphological map of Santa Catalina de Salinas with a scale of 1:25000. This parish is settled on terraces filled with volcaniclastic materials. The most represented formations are mountainous volcanic reliefs and plains of volcanic deposits from the Chachimbiro and Yanahurco volcanoes. Modified from García, 2020 and Instituto Geográfico Militar, 2016. .... 21
- Figure 3.** Tectonic setting of Ecuador. Model showing the structural subdivisions of the Andes Mountains in Ecuador: Cordillera Occidental, Inter-Andean Valley, Cordillera Real. Quaternary deposits are shown in the Inter-Andean depression, where the study area is recorded with the blue box. Modified from Morocco & Winter, 1997..... 22
- Figure 4.** Geological map of Santa Catalina de Salinas, Imbabura province. The most representative units are the undifferentiated terraces such as Chachimbiro (CH-V-2) and Yanahurco volcanic (Yh-V). These units are associated with alluvial deposits in terrace fills. Adapted from Instituto de Investigación Geológico and Energético, 2018; Pupiales,2021. .... 24
- Figure 5.** The main points of interest in the sample collection. (A) The zone of tolal resulting from the residues of soil piles from the salt extraction process, (B) Tolal showing heights up to 10 meters, and (C) Water sampling zone in natural springs. .... 30
- Figure 6.** Different points where the samples were collected, (A) Samples of 1kg salts with sediments in soils, (B) Salt crusts in natural water sources, (C) Areas made up of salts in the soil, (D) Salt zones with fragments of volcanic rocks such as pumice and volcanic tuffs. .... 33
- Figure 7.** The sieving method, (a) Sieving mechanic with different mesh size, (b) Measuring range to samples analysis. Figure 7b; modified from Retsch GmbH Haan (2016). .... 34
- Figure 8.** The samples are dried in an incubator at 85° for 4 hours (A). B) After drying, the samples can be sieved on sieves from 10 to 450 mesh. .... 35
- Figure 9.** It consists of an online Python programming language to identify random samples. The random code generates random numbers that fit a uniform distribution over a range of integers (1,24). .... 38
- Figure 10.** It consists of an online Python programming language to identify random samples. The random code generates random numbers that fit a uniform distribution over a range of integers (2,24). .... 38

<b>Figure 11.</b> Workflow of the artisanal salt extraction process in Santa Catalina de Salinas and in the laboratories of Yachay Tech University. This diagram shows the different processes from soil collection to salt production. ....	40
<b>Figure 12.</b> Crushing of samples using the disc mill (A). The pieces must be well dried so the crushing is homogeneous (B) and not mixed with organic matter. ....	41
<b>Figure 13.</b> Sample preparation by crushing the agate mortar (A). Samples should be turned into a powder so they are passed on the 450-mesh sieve.....	42
<b>Figure 14.</b> Processes to prepare the samples and then put them in the XRD. (A), drying of samples moisture. (B) Crushing in the agate mortar. (C) Passing through the smallest sieve to obtain a powder-type sample. (D) Placing in the sample holder. (E) Analyze the samples for 4 hours according to the XRD parameters. Finally, analyze by Match program the mineralogical composition phases (F). ....	44
<b>Figure 15.</b> The stratigraphic position of the samples in the undifferentiated terrace which has a thickness of 103m. Image a) represents the upper part of the column composed of pyroclastic flows between tuffs, lapilli, and Cangahua. b) represents blocks of andesitic lava flows with ash-supported matrix. c) represents a channel filled with the lenticular body through conglomerate lenses. d) represents the base of the terrace with the presence of volcanic breccias. ....	46
<b>Figure 16.</b> Representation of fractions recorded on all tolas according to their accumulation in the established fractions. ....	47
<b>Figure 17.</b> The salt concentration was obtained for each fraction according to the sieve mesh size. The highest salt concentration is in fractions 18 and 35 and the lowest in 230 mesh size. ....	48
<b>Figure 18.</b> Diffractogram determined with the XRD pattern of the sample T23P26-230M medium. It is constituted that the presence of the highest intensity peaks of the minerals, such as halite, dolomite, calcite and andesine (silicate group).....	51
<b>Figure 19.</b> XRD percentage of the mineral phase composition versus sieve mesh size classification of 21 mineral phases of the saline soils. In this samples, there are higher concentrations of salt minerals such as dolomite, thenardite, halite and calciolangbeinite. ....	53
<b>Figure 20.</b> Percentage concentrations of functional chemical groups of 21 mineral phases within the T23P26 - medium. Considering the silicate groups as the main chemical functional group of the whole tola samples, but the main chemical functional groups for the salts are carbonate and sulfates. ....	54
<b>Figure 21.</b> Diffractogram determined with the XRD pattern of the T16M20P19-60M- Top sample. It can be observed that the presence of the highest intensity peaks of the minerals, such as syngenite, nitratine, halite, and anhydrite .....	55
<b>Figure 22.</b> Represents the percentages of mineral phase composition versus sieve mesh size classification. In addition, twenty-seven mineral phases were identified by X-ray	

*diffraction analysis (XRD). The studied samples were extracted by the salt leaching process in saline soils. .... 57*

**Figure 23.** *Percentage concentrations of functional chemical groups of 27 mineral phases within the T16P19 – top salt. Considering the main chemical functional group for the salts are found as sulfates, chlorides, carbonates and nitrates. .... 58*

**Figure 24.** *Diffraction pattern determined with the XRD pattern of the M4P4 Salts samples. It can be observed that the presence of the highest intensity peaks of the minerals, such as thenardite, sylvite, ezcurrite, and albite. .... 59*

**Figure 25.** *It represents the percentages of the mineral phases' composition identified with the samples of crusts and secondary salts. In addition, twenty-one mineral phases were identified by X-ray diffraction analysis (XRD). The studied samples were collected at different sampling points, such as in areas of Tolas and natural springs..... 61*

**Figure 26.** *Represents the percentage concentrations of chemical functional groups of 21 mineral phases in the Crusts and salts samples. Considering the main chemical functional groups are found as sulfates, carbonates, nitrates, borates, chlorides, silicates, and oxides. .... 63*

**Figure 27.** *The presence of soluble salt crusts on the surface is due to the capillarity process in areas with saline soils. This process can occur more frequently in dry precipitation due to the evaporation-transpiration of water to the surface. This saline soil is located in Tolas Zone (T17M21P20; see Figure 1B). .... 67*

**Figure 28.** *It represents the percentage of functional chemical concentrations of eight tolas and five salt crust samples. The main groups are sulfates, carbonates, and borates, marked in a red box because they are the most predominant in the area. Each group is represented by minerals such as thenardite, calcite, dolomite, and sassolite, identified semi-quantitatively by x-ray diffraction..... 71*

**Figure 29.** *Geologic map of the different volcanic deposits, especially the Chachimbiro volcano of the eruptive phase 2 (CH-2) and Yanahurco volcanic deposits. In the study area, it can be seen that there is a higher concentration of debris flow deposits due to the eruptive activity. The geomorphological formation of Santa Catalina is a plateau of volcanic deposits. The different samples collected in the area are within the CH-2 polygon. Modified from Bernard et al., 2011 and Bellver-Baca et al., 2019..... 73*

## List of Tables

**Table 1.** *Approximate production of salt mines in tons and world salt reserves. Modified from U.S. Geological Survey, Mineral Commodity Summaries, 2023. .... 2*

**Table 2.** *The main chemical functional groups of salt are associated with different environments. Modified from: Ibañez et al., 2004 and Salvany, 1989. .... 7*

<b>Table 3.</b> <i>The most representative minerals of the chloride group and the geological setting from which are generated in the Earth's crust. Information compiled from RRUFF Project in collaboration with the International Mineralogical Association (IMA),2005.</i>	8
<b>Table 4.</b> <i>The most representative minerals of the sulfates group and the geological origin from which are generated in the Earth's crust. Information compiled from RRUFF Project in collaboration with the International Mineralogical Association (IMA), 2005.</i>	9
<b>Table 5.</b> <i>The most representative minerals of the carbonate group and the geological environments from which are generated in the Earth's crust. Information compiled from RRUFF Project in collaboration with the International Mineralogical Association (IMA), 2005</i>	9
<b>Table 6.</b> <i>The most representative minerals of the Nitrates group and the geological environments from which are generated in the Earth's crust. Information compiled from RRUFF Project in collaboration with the International Mineralogical Association (IMA), 2005.</i>	10
<b>Table 7.</b> <i>The most representative minerals of the chloride group and the geological origin from which are generated in the Earth's crust. Information compiled from RRUFF Project in collaboration with the International Mineralogical Association (IMA), 2005.</i>	10
<b>Table 8.</b> <i>Materials used to carry out research work both in the field and laboratory ..</i>	29
<b>Table 9.</b> <i>Equipment used to carry out research work both in the field and laboratory.</i>	29
<b>Table 10.</b> <i>Description of samples collected from Santa Catalina of Salinas, Ibarra. Samples of water, soil, and salt crusts are present in the study area.</i>	31
<b>Table 11.</b> <i>Classification of sediments by grain size proposed in 1922 by C. K. Wentworth. Adapted from Ingemmet, 2015.</i>	36
<b>Table 12.</b> <i>Representing to the data of the total weight of the sample and the total weight remaining for each particle size fraction. The light blue row is from the first method and the yellow row is from the second method.</i>	37
<b>Table 13.</b> <i>Result of the classification of water by pH. There is a higher concentration of natural spring water, so it is neutral.</i>	49
<b>Table 14.</b> <i>General detail of the mineral phases detected in the T23P26-Medium sample divided into each granulometric fraction.</i>	52
<b>Table 15.</b> <i>General detail of the mineral phases detected in the T23P26-Medium sample divided into each granulometric fraction.</i>	56
<b>Table 16.</b> <i>General detail of the mineral phases detected in the Crusts and salts samples divided into each granulometric fraction.</i>	60
<b>Table 17.</b> <i>The most predominant compositional phase per semi-quantitative XRD analysis. The most common functional groups are sulfate, carbonate, and borates. The most predominant minerals are thenardite, calcite, calciolangbeinite, sassolite, and gypsum. These minerals represent the soluble salts in the study area.</i>	66

# **1. Chapter 1. Introduction**

## **1.1 The history and formation of the salt**

The process of exploring, finding, and utilizing salt has evolved alongside the progress of humanity, rendering it an indispensable element on Earth. Therefore, salt is a main ingredient in food and conservation in the history of humanity because salt can explain various aspects of the general world, such as the rise and fall of populations, wars of repression, and rebellion within the history of humans, especially in the Indian War of Independence (Cirillo et al., 1994). In addition, the earliest records of salt being used in food date back to China's emperor Huangdi's reign in 2670 BC (Cuello, 2009). One of the first salt mines discovered for human use is in the northern Shanxi Province, surrounded by mountains and saltwater lakes. According to Cuello (2009) mentions that the Xia dynasty recorded the first methods of extracting salt by hand in 800 BC. At that time, seawater was put into earthenware vessel containers exposed to the flame until the crystals were separated by evaporation (Kurlansky, 2011; Cuello, 2009). The production and use of salt came to have greater prominence in the life of humanity because they generated customs and laws that continue to be used today. In contrast, others have ended due to technological development. The use of salt in minimal quantities for humans and animals, in which researchers conduct several experiments, has suggested that man needs about 5g of salt per day or about 2kg per year to continue human development (Bloch, 1976).

In Ancient Egypt, salt was used to preserve mummies, which dated back to 3000 BC, and was preserved using salt sands from deserts (Cuello, 2009). The Egyptians were already specialists in exporting raw foods, but salt's ability to preserve food allowed them to increase the variety of items that could be sold. They were making them the first exporters of salted fish in antiquity (Sadoul et al., 1998). The Hallei salt mines in Salzburg, Austria, one of the first continental contributions to the salt trade, were mined by the Celts throughout Europe. Eventually, According to Cuello (2009), the Romans were aware of the method used to extract salt and believed that every man was entitled to a portion of the common salt. However, the amount of salt provided to Roman legionaries as payment for their labor is where the word "salary," derived from the Latin "salarium," originates.

Salt is a mineral compound of sodium and chloride (NaCl) with a white color, crystalline aspect, low toxicity, and non-flammable. Salt contains several elements in

different percentages, such as sodium, up to 40%, and 60% chloride for every gram of salt in industrial salt (The EU-China Energy and Environment Programme, 2009). Therefore, salt has been a fundamental pillar in food preparation worldwide from ancient times of prehistory to the present because it is added to food manufacturing as a color, flavor, and texture enhancer. In addition, salt is still an essential daily diet to the progress of the human race. Salt is used in several manufacturing industries of chlorine and sodium hydroxide, which are used to make polyvinyl chloride, plastics, and paper manufactured from sodium hydroxide (Durack et al., 2008).

## 1.2 Salt deposits production processes Worldwide

Several nations worldwide have ample salt deposits and reserves, allowing for sufficient consumption to meet human demands. According to U.S. Geological Survey (2023), the nations with the highest production of salt mines are the United States, Australia, Canada, Chile, China, Germany, and others (Table 1). The United States is the primary producer of salt in the world, and various states, including Kansas, Michigan, Texas, and Louisiana, use brine salt and rock salt extraction. However, Arizona, California, Nevada, New Mexico, Oklahoma, and Utah have salt factories that use solar evaporation and saline lakes.

**Table 1.** *Approximate production of salt mines in tons and world salt reserves. Modified from U.S. Geological Survey, Mineral Commodity Summaries, 2023.*

<b>Country</b>	<b>2021</b>	<b>2022</b>
United States	42,000	42,000
Australia	12,200	13,000
Brazil	7,400	7,400
Canada	11,800	11,000
Chile	8,570	9,000
China	64,000	64,000
Germany	15,000	15,000
India	45,000	45,000
México	9,000	9,000
Russia	6,500	6,000
Spain	4,200	4,200
Other Countries	31,000	32,000

Besides, there are three specific classifications of salt production, such as direct mining of rock salts like halite, solar evaporation of seawater, and thermal evaporation of brines. Rock salt is obtained as halite deposits underground or in veins and domes on the

surface. In addition, rock salt is a sedimentary rock that belongs to the Evaporite group (The EU-China Energy and Environment Programme, 2009).

The evaporation of inland seas results in naturally occurring rock salt formation. This salt contains the minerals in that particular body of water, primarily sodium, chloride, calcium, magnesium, potassium, and sulfate (Titler et al., 2011). Therefore, salt deposits that were initially bedded may appear in veins. Salt domes are vertical diapirs created when the pressure of the Earth forces salt up through cracks (The EU-China Energy and Environment Programme, 2009). These salt beds exist due to the weight of the rock that lies above them at depths between 100 and 1500 meters.

Vacuum pan salt is made by thermally evaporating brines created from subsurface deposits in natural event locations or following the leaching process of the rocky mass. In this process, the water that has evaporated from the brine is pumped to the surface because it uses multiple-effect or electric-powered vapor recompression evaporators (The EU-China Energy and Environment Programme, 2009).

Seawater is related to saline lakes and oceans; salt extraction is natural evaporation. In addition, saltwater can identify in ponds where the sun evaporates seawater (The EU-China Energy and Environment Programme, 2009). This method is carried out in warm climates where evaporation causes salt crystallization (Andrusikiewicz & Tora, 2016).

There are several salt deposits worldwide, such as the United States, with different origins of salt environments, followed by Australia and Brazil leading the list of significant salt producers (U.S. Geological Survey, 2023). On the other hand, several salt crystallization deposits exist in different continental and marine environments in Andean countries, such as Chile, Bolivia, Ecuador, and others. In this same context, history of salt production in Ecuador, salt extraction processes have been developing in several regions, such as in the Sierra Region, Salinas de Guaranda, Bolivar Province and Santa Catalina de Salinas, Imbabura Province, and the Coastal region as Isla Puna, Guayas Province and Santa Elena Province (Salazar, 2010).

### **1.3 History of salt production in Ecuador**

In Ecuador, the salt deposits are considered an essential step from the past to the present day because the salt was called white gold for the Ecuadorian communities (Salazar, 2010). Salt was the most significant economic enhancement product because it allowed bartering with other provinces carrying salt and other edible products. Besides,



According to Quinapallo and Ochoa (2019), the production of salt deposits in Ecuador has involved several places within the country, such as the Coastal region, the Santa Elena area, and Puna Island. In Sierra region, Salinas de Guaranda, Bolívar province and Santa Catalina de Salinas, Imbabura province. Each of these places has a history in their production and marketing. In the Coastal region, salt production occurs more frequently in the Santa Elena Peninsula. One of the processes of salt extraction is through the evaporation of salt water of marine origin, where only the salt is left and then dried with high-temperature equipment. In the Sierra region, salt production was done by collecting soil and water from the different salt springs and then pouring the water over the salt beds to obtain the salt (Pomeroy, 1988).

#### **1.4 Salt in Santa Catalina de Salinas (Imbabura province)**

In previous decades, the parish of Santa Catalina of Salinas, Imbabura Province, has gained notoriety for being regarded as an Otavalo ethnic group's more affluent settlement in the sixteenth century. This area was considered the most potential among the northern parishes of the province of Imbabura because it had a product of greater social consumption, such as salt (Caillavet, 2000). At Santa Catalina de Salinas, salt production has specific refinement techniques that start with collecting salt-containing soil in specific locations of a dissected irrigation layer. Then, it is given by the filtered mixture of soil loaded with salt and salty spring water to get the salt (Maldonado & Mendieta, 2018). In addition, the saltwater springs originated from springwater wells along the ravine running through the village. Salt extraction occurred in open-pit mines (Quinapallo & Ochoa, 2019). In this way, in ancient times, the Santa Catalina de Salinas population considered that the production and trade of salt were prosperous. There was considerable trade in this product throughout the northern region. In the sixteenth century, Santa Catalina de Salinas was one of the wealthiest settlements in the regions of the Audiencia of Quito (Pomeroy, 1988).

In the 17th century, the first inhabitants of Salinas arrived in this area, a group of Afro-Americans. Later, the first Spanish landowners arrived and recruited the indigenous people to work in the agricultural activities of the area. However, the indigenous people were exploited for labor, so they abandoned the town. As a result, new settlers arrived in the town, such as the Afro-Ecuadorians who still live in Santa Catalina de Salinas (Caillavet, 2000). The history of the village's name has been given by several versions,

such as that it is named after the surname of the hero Juan de Salinas. However, the other version is that the Jesuits mentioned to their superiors in Quito that there was a mineral called salt and that it could be found in the basin of the Mira River and especially in the salt mines of Santa Catalina de Salinas. Therefore, the name Salinas is given by the salt mines located in the area. The salt production activity was one of the highest economic incomes of the parish and is currently considered a tangible heritage for all its history in its production and use (Cevallos, 2015).

Ecuador's Andean salt produced approximately less than 500 tons annually. At the Salinas site, salt production was estimated that 200 to 300 tons might have been produced annually (Pomeroy, 1988; Caillavet, 2000). During colonial times salt was considered one of the most traded products because it was used to exchange salt for gold, chili bell pepper, and cotton. Another use was that salt was considered a currency for commercial transactions in places like Salinas-Lita. In addition, the salt of Salinas was a product used as a traditional medicine to alleviate muscular pains and for export to Nueva Granada and Peru. Therefore, the parish of Salinas became the richest in the country's northern region (Cevallos, 2015).

Salt manufacturers went to look for saline soils in some villages of Santa Catalina de Salinas, such as Palenque, Carrillos, San Juan, Santa Rosa, El Salado, and San Jorge (Caillavet, 2000; Cevallos, 2015). In a desert environment with evidence of large piles of earth, it is called salt tola as vestiges of salt exploitation. The parish of Santa Catalina de Salinas inhabited the Otavalo ethnic group but later came of Afro-American origin who worked in the sugar plantations and salt factories. Later, only two salt manufacturers remained because the other families dedicated themselves to other activities due to the low salt consumption. Caillavet (2000) mentions that in the parish, the exploitation of salt is not sea salt or rock salt but salt that permeates the soil of the valley and the water systems present in the area.

## **1.5 Background information**

In this research work, it is necessary to know the theory of the topics related to the research objective to develop and apply the different methods and techniques. In recent years, there have been several research advances on issues of soil classification, classification of mineral groups, the methods of X-ray diffraction, and others. In this way,

science is developing, and we must investigate new bibliographic sources to identify relevant information to study the salts of Santa Catalina de Salinas. Because of this, we will explain some relevant information to bring the theory and methodology together.

### **1.5.1 Salt classification in the environment**

The classification of minerals by each chemical functional group was suggested in 1768 by Carolus Linnaeus, who considered that the external form of the mineral crystals gives the classification. Also, it suggested that the minerals should be grouped by the type of rocks that contain them. On the other hand, there is a classification where it is considered essential to classify by anions, anionic complexes, or cations because it allows determining the class of the mineral using the chemical formula (Perkins, 2001).

In order to talk about the classification of minerals present in the salts is very variable and depends on several aspects, such as the temperature and humidity of the medium where each crystallizes (Ibañez et al., 2004). Several species of minerals are differentiated by the degree of hydration of the molecule and with the possibility that mixed salts are formed where there is the presence of more than one cation. Salts' most representative chemical functional groups are sulfates, carbonates, chlorides, borates, and nitrates (Dexter, 2001; see Table 2). These can also be classified as primary and secondary minerals.

According to Salvany (1989), minerals are classified as primary minerals consisting that have precipitated directly from a brine until reaching the saturation limit. In addition, these minerals tend to develop at various interfaces, such as the water-air of a lake, and then fall to the bottom and settle out or in water sediment and finally among soft sediments such as shale, carbonate, or gypsum. These minerals are generated in sedimentary environments; in other cases, they are preserved in ancient formations once they reach the present day. Secondary minerals form after an already-developed mineral, such as a primary or secondary mineral. This mineral transformation is due to the unstable state of the mineral in a change of chemical and physical conditions. In addition, these minerals can form in the diagenetic phases of an evaporite formation, such as in the continental sedimentary environment, during burial or exhumation. Moreover, various mineral classifications exist within the main carbonates, sulfates, phosphates, nitrates,

borates, and chlorides and can be found in continental evaporite media, groundwater of continental origin, and ancient formations (see Table 2).

**Table 2.** The main chemical functional groups of salt are associated with different environments. Modified from: Ibañez et al., 2004 and Salvany, 1989.

<b>Carbonates</b>		<b>Phosphates</b>	
<b>Minerals</b>	<b>Chemical Formula</b>	<b>Minerals</b>	<b>Chemical Formula</b>
Calcite	CaCO <sub>3</sub>	Berlinite	AlPO <sub>4</sub>
Dolomite	Ca Mg (CO <sub>3</sub> ) <sub>2</sub>	Fluorapatite	Ca <sub>5</sub> (PO <sub>4</sub> ) <sub>3</sub> F
Magnesite	MgCO <sub>3</sub>	Amblygonite	LiAl (PO <sub>4</sub> )F
Natron	Na <sub>2</sub> CO <sub>3</sub> · 10H <sub>2</sub> O	<b>Chlorides</b>	
Thermonatrite	Na <sub>2</sub> CO <sub>3</sub> · H <sub>2</sub> O	Halite	NaCl
Trona	Na <sub>3</sub> H(CO <sub>3</sub> ) <sub>2</sub> · 2H <sub>2</sub> O	Sylvite	KCl
Aragonite	CaCO <sub>3</sub>	Antarcticite	CaCl <sub>2</sub> · 6H <sub>2</sub> O
<b>Sulfates</b>		Carnalite	KCl · MgCl <sub>2</sub> · 6H <sub>2</sub> O
Gypsum	CaSO <sub>4</sub> · 2H <sub>2</sub> O	<b>Borates</b>	
Anhydrite	CaSO <sub>4</sub>	Sassolite	H <sub>3</sub> BO <sub>3</sub>
Celestina	SrSO <sub>4</sub>	Ezcurrite	Na <sub>4</sub> B <sub>10</sub> O <sub>17</sub> · 7H <sub>2</sub> O
Thenardite	Na <sub>2</sub> SO <sub>4</sub>	Ulexita	NaCaB <sub>5</sub> O <sub>6</sub> (OH) <sub>6</sub> · 5H <sub>2</sub> O
Mirabilite	Na <sub>2</sub> SO <sub>4</sub> · 10H <sub>2</sub> O	<b>Nitrates</b>	
Epsomite	MgSO <sub>4</sub> · 7H <sub>2</sub> O	Niter	KNO <sub>3</sub>
Bassanite	Ca (SO <sub>4</sub> ) · 0.5H <sub>2</sub> O	Nitratine	NaNO <sub>3</sub>

Furthermore, the concentration of salts are ionic crystalline compounds formed by a cation (+), such as mainly sodium (Na), magnesium (Mg), and calcium (Ca); on the other hand, an anion (-), such as sulfate (SO<sub>4</sub><sup>2-</sup>), carbonate (CO<sub>3</sub><sup>2-</sup>), chloride (Cl<sup>-</sup>), and in some cases nitrate (NO<sub>3</sub><sup>-</sup>), and borate (BO<sub>3</sub><sup>3-</sup>) (Bauder, 2014). For this study, it should be taken into account that the minerals of the salt present in the study area are soluble salts which are saline soils that could have evaporitic, continental, marine, or volcanic origins. Therefore, to understand the chemical functional groups belonging to soluble salts, such as chlorides, sulfates, carbonates, nitrates, and borates, are described in the following paragraph.

### **Chlorides (Cl<sup>-</sup>)**

Chlorides are salts of a combination of an anion (-) chloride with a cation (+) such as sodium (Na), potassium (K), and calcium (see Table 2). Chloride is present in the form of (Cl<sup>-1</sup>) an ion, considered one of the primary inorganic anions in water that are

generated by natural or surface water (Iowa Department of Natural Resources, 2009). In addition, like salts, rainfall is the primary source of the higher concentration of chlorides found in groundwater and saline lakes in coastal regions. The most soluble natural minerals in the chemical functional groups are sodium chloride, potassium chloride, calcium chloride, or potassium magnesium chloride (see Table 3). They are associated with the marine environment by seawater, rainwater in very arid climates, and anthropic origin by drainage wastewater (Huggett, 2011). However, saline soils concentrate the highest amount of salt; hence, the mineral halite (NaCl) is the most common salt in this soil type. Its presence affects the solubility of other salts because they infiltrate at shallow depths (Padilla,2014).

**Table 3.** *The most representative minerals of the chloride group and the geological setting from which are generated in the Earth's crust. Information compiled from RRUFF Project in collaboration with the International Mineralogical Association (IMA),2005.*

<b>Bane of Mineral</b>	<b>Chemical Formula</b>	<b>Geological environments</b>
Halite	NaCl	Sedimentary rocks of evaporite association, or volcanic sublimates.
Sylvite	KCl	Sedimentary basins or volcanic fumaroles.
Carnalite	KCl · MgCl <sub>2</sub> · 6H <sub>2</sub> O	Saline marine deposits.

**Sulfates ( $SO_4^{2-}$ )**

Sulfates are minerals composed of an anion (-) that can form salts with potassium, sodium, magnesium, and other cations (+) (Bauder, 2014). The sulfate group is distributed in the earth's crust, mainly in natural groundwater (Iowa Department of Natural Resources, 2009; Moreno et al.,2011). Thus, the most representative minerals are gypsum, thenardite, mirabilite, epsomite, and anhydrite, are found in marine and continental environments or associated with volcanism (see Table 4). For example, calcium sulfate can be generated in various environments, such as marine aerosols, wind-deposited salts from rock metamorphosis, volcanic emissions, and surface and groundwater (Cosentino & Jordan, 2012). Finally, in saline soils, a high concentration of soluble salts can be identified, such as sodium sulfate and magnesium sulfate, which are influenced by temperature and are transported to the soil surface in warm periods (Ibañez et al., 2004).

**Table 4.** The most representative minerals of the sulfates group and the geological origin from which are generated in the Earth's crust. Information compiled from RRUFF Project in collaboration with the International Mineralogical Association (IMA), 2005.

<b>Bane of Mineral</b>	<b>Chemical Formula</b>	<b>Geological environments</b>
Gypsum	CaSO <sub>4</sub> · 2H <sub>2</sub> O	Sedimentary rocks (marine salt deposits).
Anhydrite	CaSO <sub>4</sub>	Sedimentary evaporite deposits, igneous rocks, fumaroles, and seafloor hydrothermal chimneys.
Thenardite	Na <sub>2</sub> SO <sub>4</sub>	Lacustrine evaporite deposits in arid regions, crusts, and efflorescence or fumaroles.
Mirabilite	Na <sub>2</sub> SO <sub>4</sub> · 10H <sub>2</sub> O	Salt pans, playas, and saline lakes, caves and volcanic fumaroles.
Epsomite	MgSO <sub>4</sub> · 7H <sub>2</sub> O	Salts deposits, caves, and outcrops of sulfide-bearing magnesian rocks, and mineral springs.

### **Carbonates (CO<sub>3</sub><sup>-2</sup>)**

Carbonate minerals are salts formed by the radical anion (CO<sub>3</sub><sup>-2</sup>), and the reaction of carbonite acid with Mg<sup>+2</sup>, Zn<sup>+2</sup>, Fe<sup>+2</sup>, and Mn<sup>+2</sup> cations, among others. Carbonates are present in the Earth's crust but mainly in association with other minerals to give rise to rocks of sedimentary origin (Moreno, 2011; Libretexts,2014). According to Mackenzie (2016), the most abundant carbonate group minerals consist mainly of calcites and aragonite, which are more abundant in the younger sedimentary mass, while dolomite is more abundant in the geologically older sequences (see Table 5).

**Table 5.** The most representative minerals of the carbonate group and the geological environments from which are generated in the Earth's crust. Information compiled from RRUFF Project in collaboration with the International Mineralogical Association (IMA), 2005

<b>Bane of Mineral</b>	<b>Chemical Formula</b>	<b>Geological environments</b>
Calcite	CaCO <sub>3</sub>	Clastic sedimentary rocks, and hydrothermal veins, in alkalic to mafic igneous rocks and speleothems in caves.
Dolomite	Ca Mg (CO <sub>3</sub> ) <sub>2</sub>	Hypersaline sedimentary environments, carbonatites and ultramafic rocks.
Aragonite	CaCO <sub>3</sub>	Converts to calcite over geologic time and evaporite deposit.

### **Nitrates (NO<sub>3</sub><sup>-</sup>)**

Nitrates are salts of nitric acid and isolated (NO<sub>3</sub><sup>-</sup>) anions. The essential nitrate mineral, nitratine, is analogous to calcite, while niter shows an aragonite structure (Okrusch & Frimmel, 2019; see Table 6). According to Franzosi and Montagna (2007), nitrates can occur in various environments and through human activities, however in geological origin, nitrates are found in the world's largest deposits in northern Chile, and

their origin is given by emplacement in rock or alluvial deposits. Nitrates are rare salts that are rapidly lost in the soil because they are highly soluble in saline and arid soils (Padilla, 2014).

**Table 6.** *The most representative minerals of the Nitrates group and the geological environments from which are generated in the Earth's crust. Information compiled from RRUFF Project in collaboration with the International Mineralogical Association (IMA), 2005.*

<b>Bane of Mineral</b>	<b>Chemical Formula</b>	<b>Geological environments</b>
Niter	KNO <sub>3</sub>	Caves, seeping groundwater; an efflorescence on soils or cliff faces in arid regions.
Nitratine	NaNO <sub>3</sub>	Bedded deposits formed in playas, caves, and seeping groundwater leaching nitrates from overlying rocks.

### **Borates ( $BO_3^{3-}$ )**

Borates are composed of boric acid, and classified into endogenous borates formed by metasomatism, such as tourmaline, Fe, Mn, Sn, Be, and other elements (Table 7). Exogenous borates are of marine or continental origin, such as magnesium borate. In addition, borates are found throughout the Andean zone, as is the case of Chile, which has the highest concentration of borates (Alonso, 2017).

**Table 7.** *The most representative minerals of the chloride group and the geological origin from which are generated in the Earth's crust. Information compiled from RRUFF Project in collaboration with the International Mineralogical Association (IMA), 2005.*

<b>Bane of Mineral</b>	<b>Chemical Formula</b>	<b>Geological environments</b>
Sassolite	H <sub>3</sub> BO <sub>3</sub>	An evaporite or sublimate around hot spring lagoons and volcanic fumaroles.
Ezcurrite	Na <sub>4</sub> B <sub>10</sub> O <sub>17</sub> · 7H <sub>2</sub> O	Dehydration of borax in a discordant deposit in folded playa siltstones and sandstones.

### **1.5.2 Origin of salt crystallization**

The origin of the minerals belonging to the formation of salt crusts occurs in areas constituted as depressions are the local base level with the intermountain disposition are fundamental for the natural refuge of erosion and evaporation products, generating a plain of different salt crusts in great extension without strong slopes (Martínez et al., 2020). The occurrence of salts and the salinization process can be generated in different ways of entry of salts to soils, being able to distinguish between the access from the surface and the one that occurs from the bottom of the profiles (Lavado & Taboada, 2009). Finally, to

know the origin of salt on the earth's surface, the natural or anthropic factors of occurrence must be identified.

### **1.5.2.1 Natural environment salt**

The presence of salts in the environment can be of natural origin due to weathering of the soil containing minerals and releasing many saline minerals, e.g., bedrock is gypsum and releases sulfate minerals. According to Torres (2018), soluble salts in soil is common in arid and semi-arid regions of the world where evapotranspiration exceeds precipitation. The primary source of salts in these environments is groundwater or water table. The main salts involved in this process are chlorides ( $\text{Cl}^-$ ) and sulfates ( $\text{SO}_4^{2-}$ ), especially of  $\text{Na}^+$ , and to a lesser extent carbonates ( $\text{CO}_3^{2-}$ ), ( $\text{Ca}^{2+}$  and  $\text{Mg}^{2+}$ ). Soluble salts can be generated by the washing of crystalline rocks, which is the process responsible for the accumulation of salts in soils, sediments, and continental waters, so the chemical composition of the solutions formed in this washing will depend on the mineral composition of the rocks themselves (Montañes,1977). Additionally, in the case of the natural environment, the origin of soluble salts is subdivided into two environments: continental and marine.

#### ***Continental environment***

Continental environment is related to the concentration of salts in soils and waters resulting from the weathering of igneous and sedimentary rocks or to deposition zones of surface and groundwater discharges (Flores, 2014). According to Montañes (1977), when salts come from the parent rock itself, it is called a continental cycle of primary accumulation. It is called a continental cycle of secondary accumulation when they come from a redistribution of those that have previously accumulated in sediments. In order to identify the different groups of saline minerals, the following processes are considered washing processes that act on rocks (granites, gneiss, and others.) that are not very weatherable; the resulting solution contains mainly carbonates, sulfates, chlorides, and alkaline silicates (Torres,2018). On the contrary, the washing process acts on basic rocks (limestones, marls, and others.) whose weathering is more intense; the water carries carbonates, sulfates, calcium, and magnesium silicates.



According to Gilbert and Lane (1994), another factor of salt accumulation was identified as volcanic events that the presence of salts in volcanic and environmental gases and fluids could cause salt precipitation on volcanic ash surfaces. Also, the fluids on the surface of the particles in the eruption plumes are stable acid solutions. Calcium sulfate and sodium chloride are secondary minerals that precipitate before the impact of the accretionary lapilli on the ground. The salts are formed by condensing acidic liquid droplets (or aerosols) on ash surfaces (Rose, 1977). Finally, salt concentrations during volcanic eruption events can be generated by fresh or saltwater precipitation, outgassing, hydrothermal alteration, or interaction with rainwater (Colombier et al., 2019).

### ***Marine environment***

The marine environment is related to the accumulation of salts in areas of the coastal region where salinization processes are found due to the transport of salts from the sea. This process may be due to the formation of salt-rich aerosols, which are transported and deposited inland by subterranean infiltration of seawater, or to the redissolution of fossil salts (Villas, 1992). Besides, the salts that accumulate the most are sodium chloride (NaCl), which originate in dry lowland areas, seawater, or areas with rocks of maritime origin (Herczeg et al., 2001). On the other hand, soils closer to the sea are called coastal areas flooded with seawater, which are more salt concentrations to give rise to saline soils (Courel, 2019). In addition, saline minerals were formed by the evaporation of large volumes of seawater imprisoned in the continents by orogenic or transgressive phenomena.

Enclosed seas or endorheic basins are one of the main components of endorheic water systems in arid regions (Jiang et al., 2022). Endorheic lakes result from the non-evacuation of quantities of water neither by surface runoff nor by infiltration into other water bodies such as rivers or the sea. The endorheic basins are classified due to the large extension; if the lakes are large, they are called a closed sea, or if they are in small extension, they are called saline lakes. For example, the Mediterranean, Caspian, and Black Seas are the enclosed seas surrounding the European continent. In addition, in these endorheic basins or enclosed seas, the salinity increases and is usually higher than in the outer ocean. Besides, it contains a high salinity when saline lakes are formed, giving rise to salt flats due to dissolved salt conditions by different hydrological systems, climatic conditions, and precipitation (Barale & Grade, 2008). On the other hand, high-altitude

endorheic basins show a decrease in salinity due to various conditions such as rapid accumulation of water mass about humidity and climate conditions, which does not allow extensive crystallization of salts in endorheic regions (Song et al., 2022; Barale & Grade, 2008).

### ***Evaporitic basins***

The evaporite basin is related to marine and continental waters, where it accumulates in and around a more saline residual brine. In addition, these brines are found in non-marine evaporitic lake environments (Warren, 2016). Evaporites originate initially from rainfall, and the salts are enriched during surface or subway circulation through igneous, metamorphic, or sedimentary rocks, allowing them to surround evaporitic basins. Evaporites occur in dry climatic conditions where the temperature can be very varied. However, it can also occur in warm regions or arid zones with high latitudes. For example, we have the Campos Basin in the coastal zone of Brazil, which is constituted by sedimentary environments such as evaporites (Spalletti, 2006).

According to Salvany (1989), water sources can be volcanic and other types of deep emanations, which allow the origin of continental basins in the evaporitic environment, such as subway flow, which consists of a more significant amount of water and salt content because it has a slow circulation that passes through the rocks and sediments that surround the evaporitic environment. Surface runoff refers to water formation through rainfall on the reliefs around the evaporite basin. The waters begin to descend through the mouths and valleys in the basin through alluvial fans. In other words, it has the form of non-channelized streams loaded with detrital sediments and dissolving salts. Rainfall falling directly on the evaporitic medium is a process that is less frequent in the evaporitic basin due to the recharge of water over the lakes. Finally, springs close to the evaporitic medium consist of small springs found at the foot of alluvial fans and about fractures or points of weakness in the basin that feed the lake with salts such as travertine.

#### **1.5.2.2 Anthropogenic salinity**

The anthropic origin is considered secondary salinization due to various human activities that impact nature (Villas, 1992). The concentration of salts is due to man's

ignorance of the fundamental laws governing the movement and accumulation of salts in the soil (Montañes, 1977). According to Flores (1991), the origin of salinity due to anthropic activity is the severe mistake made during human economic activity because it allows soil salinity to increase due to deficient washing of saline areas by irrigation, and irrigation with mineralized water, excessive use of fertilizers, which increase the concentration of chlorides such as sylvinite (KCl) and halite (NaCl). In addition, in the salt origin record, it is essential to know the classification of soils to see how the crystallization of soluble salts occurs in the environment, whether continental, marine, or anthropic.

### **1.5.3 Saline or sodic soil classification**

#### ***Saline soil***

Saline soils develop through the salinization process that requires the presence of a saline water table at a shallow depth where the upper part of the supported capillary layer reaches the soil surface; the water evaporates, and the soluble salts precipitate (Flores, 1991). Salts are found in saline soils, mainly neutral salts such as sodium, calcium, magnesium, potassium, and chloride sulfates. Nitrates may sometimes be present as carbonates, and bicarbonates are usually absent. In addition, most saline soils contain appreciable amounts of gypsum in the lower part of the profile (Osman, 2018). For this study, the soils in the parish of Santa Catalina de Salinas would be constituted by saline soils because crusts of white soluble salts are present in most sampling zones. Therefore, to interpret the salinity in the soil, it is measured by the electrical conductivity in the soil solution and the threshold to consider that soil has many salts (Courel, 2019)

#### ***Sodic soils***

Sodic (non-saline) soils contain a high proportion of exchangeable sodium ions on the colloidal surfaces that keep the particles dispersed. This soil has a dense clay layer that occurs at or near the surface of sodic soils (Osman, 2018). Sodic soils are dominated by carbonates and bicarbonates of sodium, calcium, and magnesium (Courel, 2019). To identify sodic soils, the electrical conductivity is greater than 4dS m<sup>-1</sup>, and the pH is usually 8.5 or lower (Torres, 2018).

## **1.6 Statement of the Problem**

Surface salt accumulation and salinity-affected soils severely affect humans, water, and agriculture (Buder et al., 2014). These salts can harm agricultural productivity and the quality of soil and spring water. Ecuador is an excellent area for identifying and evaluating the impact of salt crystallization in arid and semi-arid soils. It is caused by regional geology and the fluctuating climate (Chesworth, 2008). In Ecuador, salt was considered one of the most exploited resources for generating economic and nutritional survival because it could be found in sea salt, continental, or rock salt in various areas. During the previous century, Santa Catalina de Salinas was one of the communities that extracted and processed the most salt (Garcia, 2020).

Nowadays, salt is no longer processed in the parish of Salinas as it was in the last century, but large mounds of earth, or salt Tola, have been left as evidence. The community exploited salt for a long time. However, they needed to learn the origin of the salt since community originators have commented that the salt originated from an arm of the sea. Therefore, determining the origin of the salt in the parish of Santa Catalina de Salinas helps the community to know the formation and origin of the salt in the area. In addition, the study of salt allows for generating relevant geological information about the geosite Salinas- Lita within the Imbabura Geopark, especially in the knowledge of the geology, cultural and natural heritage associated with sustainable geotourism. According to Wicke et al. (2011) mention that if salt's origin and the minerals' relevant characteristics are known, salt may have considerable economic potential if adequately managed. Therefore, this study aims to identify all these processes of concentration and composition of saline minerals to determine the origin of the Santa Catalina de Salinas salts.

## **1.7 Objectives**

### **1.7.1 General objective**

This project aims to carry out geological characterization to determine the origin of the salt of Santa Catalina de Salinas using extraction, characterization, and classification methods of the samples according to their mineral phases. The x-ray diffraction approach will make it possible to discover specific details of the crystallographic structure of salt samples to ascertain the soluble salts' environment. Besides, through this investigation, the parish of Santa Catalina de Salinas learns more about the geological setting in which salt was extracted, providing the local populace with

detailed knowledge that will aid in preserving their cultural heritage and geotourism or increase their agricultural fields.

### **1.7.2 Specific objective**

- To carry out a bibliographic review of the geological context of the study area.
- To describe the different geological units and salt deposits employing a detailed geological map in Santa Catalina de Salinas.
- To study the soils of that extracted salt through methods and characterization processes to identify phase composition minerals in the samples.
- To identify the leading chemical functional group of the salt and its possible origin.
- To quantify the salt concentration for future studies to improve agricultural production in the area.

## **1.8 Introduction to study area**

The study area is located in the Inter-Andean depression in the northern Sierra region of Ecuador, around 25.5 km from the city of Ibarra, Imbabura Province (Figure 1). The Santa Catalina de Salinas parish was created on June 25, 1824. It has an area of 77.79 km<sup>2</sup> (Pupiales, 2021). The parish of Santa Catalina de Salinas has a flat sub-horizontal geomorphology. In addition, the parish is located between the Ambí River and is limited by the Cordillera Occidental, where the Chachimbiro and Yanahurco volcanic necks are present (Cevallos, 2015). This parish belongs to the Ibarra canton, which is bordered the south by the Urcuquí canton, to the north by the Juan Montalvo and La Carolina parishes, and to the west by the Cahuasqui, Pablo Arenas, and Tumbabiro parishes and to the east by the Ibarra and Mira cantons (see Figure 1). This research area is important because it is one of the geosites of the first global geopark in Ecuador, named Imbabura Geopark. This parish is considered one of the sites with geological and cultural interest because it helps us to know the region's geological history and the main events that have made this community a place of scientific, touristic, social, and cultural interest

Several hydrographic systems, such as permanent natural groundwater, carry water throughout the year in the parish of Santa Catalina de Salinas. In contrast, the intermittent courses that make up the drainage and surface water do not carry permanent

water and only in times of rain. Therefore, the hydrological network of the area is classified by rivers and streams. The main rivers of the parish are the Palacara, Amarillo, Ambí, Mira, Salado, and Jerónimo, which originate at the heights of Piñán (Figure 1). Other streams in the rural and urban areas include Cachiyacu, Chuspihuaycu, El Rancho, La Banda, El Pedregal, Pigunchuela, San Guillermo, San Lorenzo, and Yuya Pamba. These primary and secondary rivers drain surface water from the Andes mountains, part of the Mira River basin (Wolf T, 1892; Garcia, 2020).

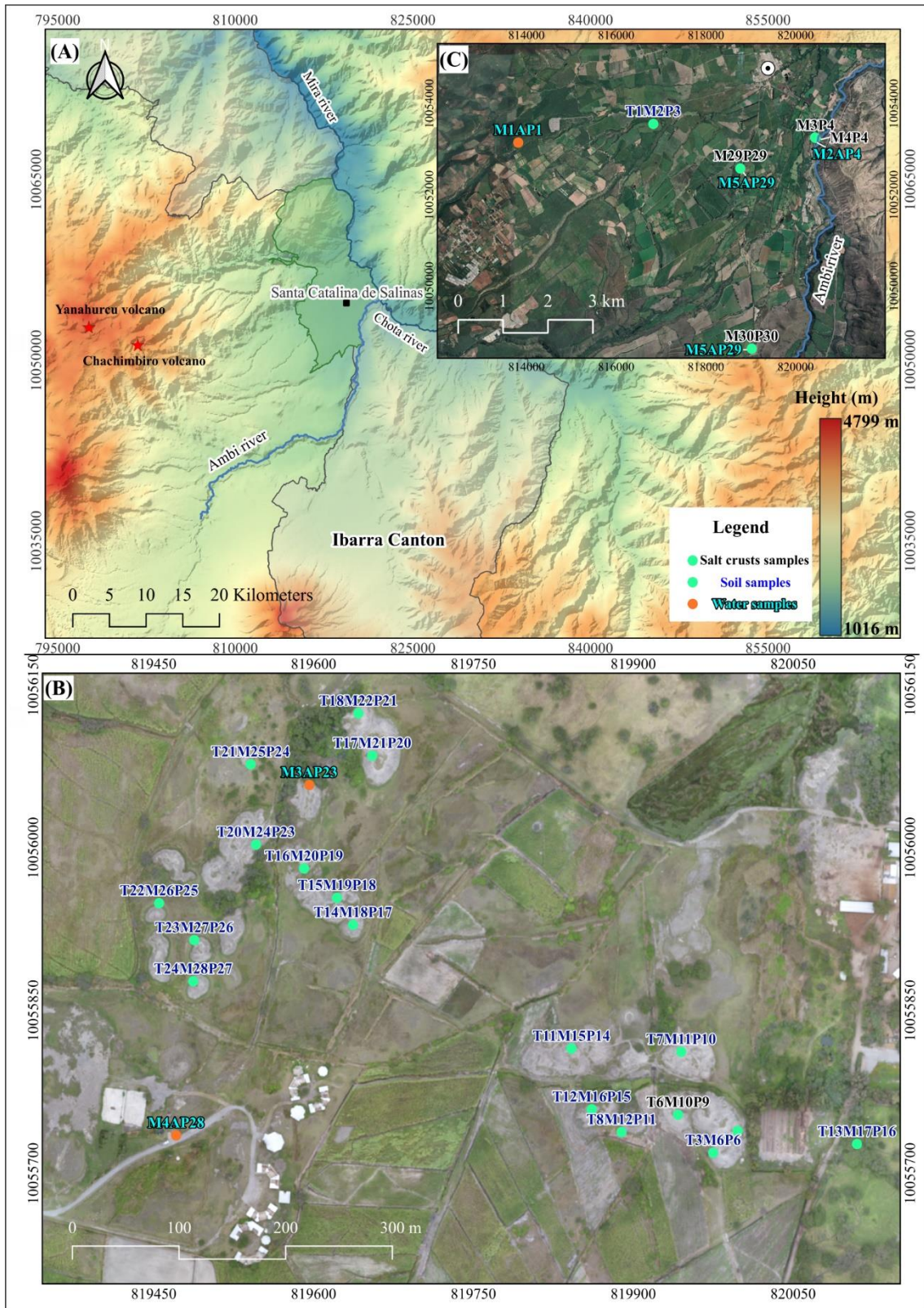


**Figure 1.** Location map and elevation model of the study area within the province of Imbabura at a scale of 1:50,000 (A). Sample collection site of the 24 Tolas and salt crusts. Additionally, six water samples from natural and surface springs near and around Santa Catalina de Salinas (B) and (C).

## 1.9 Geomorphology

Geomorphology analyzes the Earth's surface shapes and the processes that shape them (Gilsanz, 1996). The shapes of the Earth's surface result from a dynamic balance between constructive and destructive processes such as geological, geographic, biotic, and anthropic (Gilsanz, 1996). One of the main events is the uplift of the continental crust. This event is given by the force of the terrestrial interior, which lifted a sea or continental shelf to generate fluvial agents that formed large reliefs and valleys. (Huggett, 2011). In Ecuador, several geomorphological processes, such as the weathering of volcanic materials and the transport of sediments in alluvial and fluvial environments, produce valleys and reliefs. On the other hand, Santa Catalina de Salinas has very dynamic and relevant geomorphological forms, which are associated with various processes of transport, weathering, and erosion of materials related to volcanic eruptions. These processes are represented by geomorphological units present in the study area (Cevallos, 2015; Garcia, 2020).

The study area has different geomorphological units that occupy the entire territory of the parish (Figure 2). These geoforms are essential for this research work because they allow us to identify the flat geomorphology of the parish and the source of the materials that filled the terraces. In addition, this is important with the general objective of seeing if the origin of the deposits of soluble salts is related to the volcanic materials located in the area. According to Garcia (2020), Salinas has different morphological units that cover the entire urban and rural zone (volcanic deposit plain, wavy volcanic relief, and mountain volcanic relief). There are reliefs of greater and lesser extent in the area. Besides, the unit that stands out the most is the mountainous volcanic relief because they are reliefs of ancient volcanic materials (Figure 2). Then, there is the morphological unit of the plain of volcanic deposits present within the sample collection area in the Tolas.

Additionally, it constitutes a form of plain located at the foot of the volcanic edifice where pyroclastic flows, such as ash, pumice, lapilli, and other, have been deposited. In addition, these materials are integrated into the alluvial environment forming valleys and terraces. Other geomorphological units are the wavy volcanic relief present in the southern part of the parish and the shallow hilly volcanic relief in the southeastern part of the parish. In addition, in the zone, there is a volcanic deposit plain slope unit within the central zone of Salinas. Finally, the remaining morphological units



are distributed in the area in small reliefs due to the variation and dynamics of the terrain's morphology (see Figure 2).

### **1.10 Climate conditions**

The variables that generally control climate and give rise to different climate changes are factors such as latitude, altitude, relief, precipitation, temperature, prevailing winds, distance from the sea, and ocean currents (Alvarino & Ocampo, 2016). In the Andes, altitude variations and orography are the main factors controlling the climate (Crespo et al., 2010). The climate present in the parish is due to its location in the subtropical region, which varies from dry, humid and semi-humid (Cevallos, 2015). The Santa Catalina de Salinas is part of the Inter Andean Valley, with the Oriental and Occidental mountain range. In addition, these two mountain ranges have different heights that do not allow the warm and humid winds from the west and east to enter the basins' interior, generating a wide variety of climates and considerable changes in the region (Garcia, 2020). Ecuador has two main climate variations: winter is the rainy season (October-May), and summer (June-September) is the dry season (Donoso, 2012). In this area, there are two climatic seasons each season: winter, with an average temperature of 18°C, and summer with the average temperature is 24°C (Donoso, 2012; Garcia, 2020). Another factor influencing the climate is the precipitation, which has a low annual rainfall of around 500 mm. This precipitation is due to the position conditions in the foothills of the Oriental and Occidental mountain ranges; because of the characteristics of the relief, precipitation is distributed by the orography (Pupiales, 2021). Precipitation and climatic variations allow the concentration of salts in the soil because when there is more rainfall, the salts in the surface layer of the earth decrease (winter season), while when there is less precipitation (summer season), the concentration of salts in the soil increases (Flores, 1991).

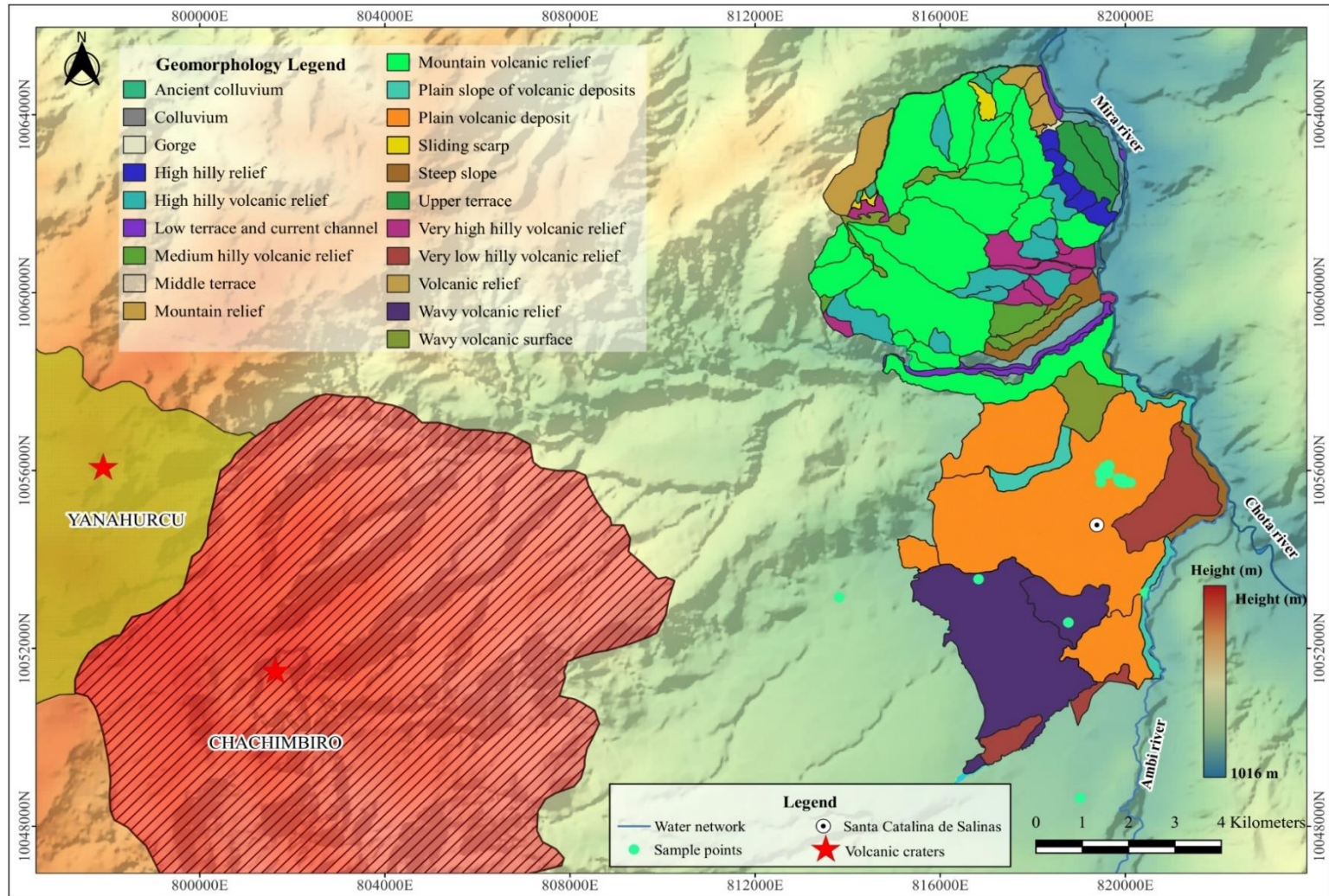


**Figure 2.** Representation of the geomorphological map of Santa Catalina de Salinas with a scale of 1:25000. This parish is settled on terraces filled with volcanoclastic materials. The most represented formations are mountainous volcanic reliefs and plains of volcanic deposits from the Chachimburo and Yanahurco volcanoes. Modified from García, 2020 and Instituto Geográfico Militar, 2016.

## 2 Chapter 2. Geological Framework

The Ecuadorian Sierra has three geological and morpho-structural structures that include: the Cordillera Real in the eastern zone, the Inter-Andean Valley in the central area, and the Cordillera Occidental located in the western foothills (Morocco & Winter, 1997; see Figure 3). This mountain range consists of a mafic-ultramafic basement that belongs to the oceanic plateau that contains mafic, extrusive, and intermediate intrusive composition, turbiditic deposits, and volcano-sedimentary successions developed from the Late Cretaceous to the Oligocene (Vallejo, 2007). Inter-Andean Valley is the graben or inter-Andean depression that occurred in the geological events between the Upper Miocene and Pliocene due to extensional tectonics (Hungerbhuler et al., 2002). This valley has several events, such as clastic sedimentary series and volcanic sequences, in which the deposits are linked to volcanic activity within the volcanic arc. The volcanic materials that occurred are andesitic lava flows with minor intercalations of pyroclastic flows and volcanic breccias (Hungerbhuler et al., 2002).

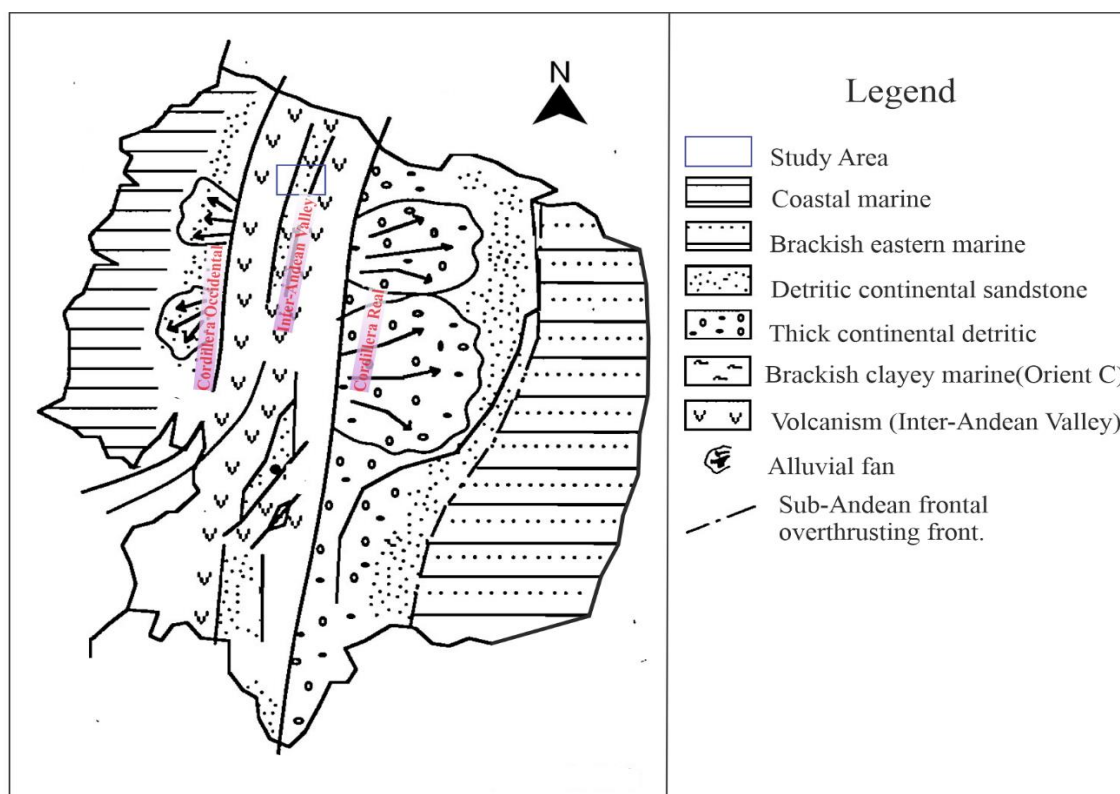


**Figure 3.** Tectonic setting of Ecuador. Model showing the structural subdivisions of the Andes Mountains in Ecuador: Cordillera Occidental, Inter-Andean Valley, Cordillera Real. Quaternary deposits are shown in the Inter-Andean depression, where the study area is recorded with the blue box. Modified from Morocco & Winter, 1997.

Imbabura province is constituted within the Inter-Andean Valley and limited to the Cordillera Occidental, which the main emission centers are stratovolcanoes and domes where longitudinal faults have allowed the ascent of magmas to form the current continental volcanic arc (Pupiales, 2021; Andrade et al.,2012). The predominant materials in these volcanic zones are pyroxenic andesites and hornblende dacites, and in small quantities are basalts and rhyodacites. In Imbabura, Quaternary volcanism has developed significantly through the formation of andesitic stratovolcanoes such as Cusín, Cushnirrumi, Yanahurco, Huanguillaró, Iguán, Cubilche, Imbabura, Pugarán, Cotacachi and Chachimbiro (Andrade et al.,2012). Therefore, the Chachimbiro and Yanahurco de Piñan volcanoes are the closest to the limits of the research area and constituted the main emission of volcanic materials to form the Santa Catalina de Salinas terrace.

The parish of Santa Catalina de Salinas is located in the Inter-Andean depression and predominantly volcanic materials and undifferentiated terraces with the presence of Chachimbiro and Yanahurco volcanic, which have recorded activities of several eruptive events (Figure 4). Santa Catalina de Salinas Parish comprises several geological units distributed throughout the rural and urban areas. Generally, the geologic units that outcrop the study area range from the oldest Tertiary to the most modern Quaternary units. These units correspond to granitic rocks, Macuchi Unit, Silante Chota Group, Angochahua volcanic, volcanic breccias, undifferentiated terraces, Yanahurco and Chachimbiro volcanic, alluvial deposits, and Cangahua. According to Pupiales (2021), in parish territory, the area's most predominant geologic units are undifferentiated terraces (1-3), Yanahurco volcanic, Alluvial deposits, Volcanic breccias, and Cangahua (Figure 4).

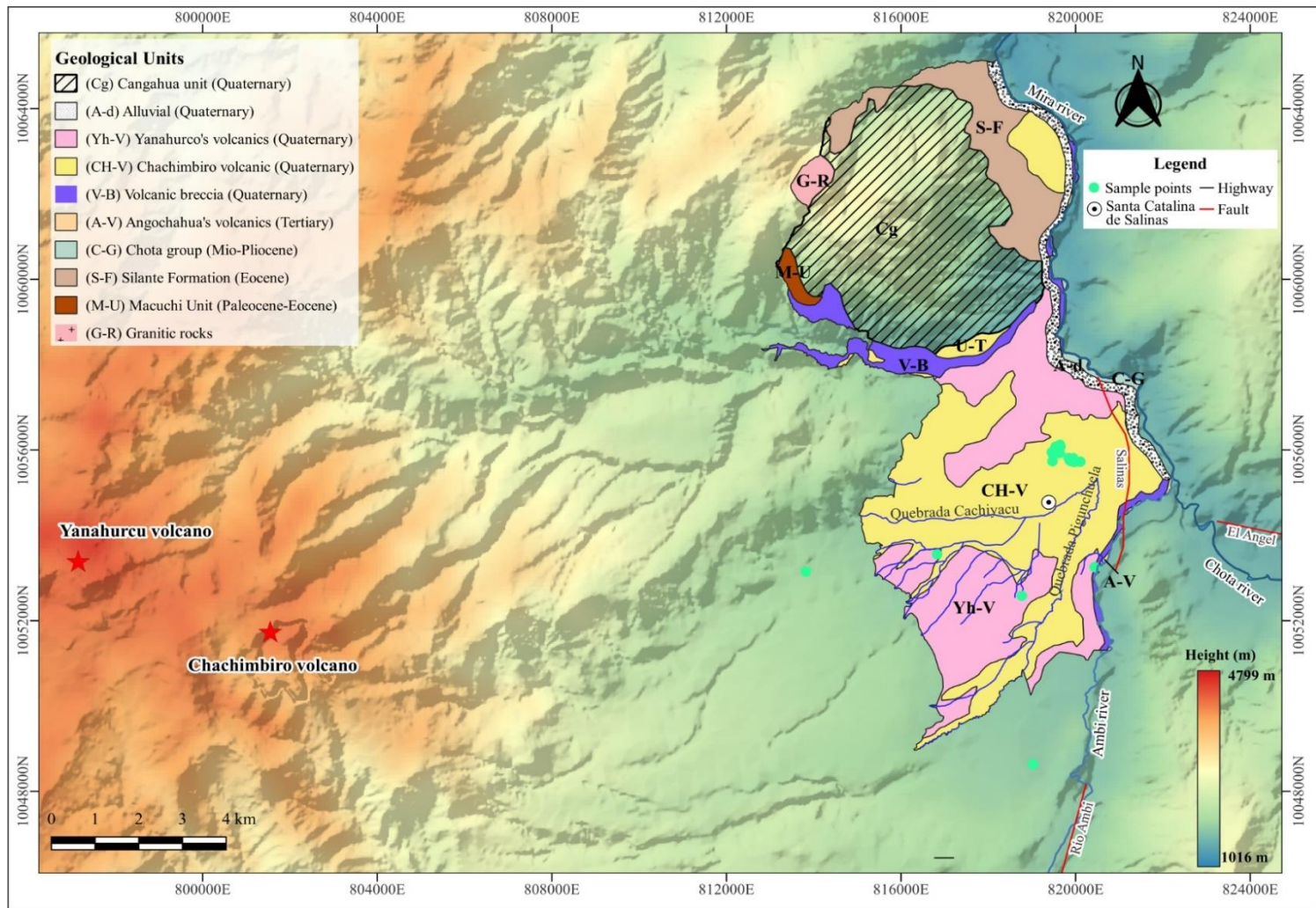


**Figure 4.** Geological map of Santa Catalina de Salinas, Imbabura province. The most representative units are the undifferentiated terraces such as Chachimbiro (CH-V-2) and Yanahurco volcanic (Yh-V). These units are associated with alluvial deposits in terrace fills. Adapted from Instituto de Investigación Geológica and Energética, 2018; Pupiales, 2021.

### ***Granitic Rocks (G-R)***

Granitic Rock is located in the northwestern area of the parish, with a percentage of 0.80% of the total area (Cevallos,2015). It originated essentially from magma's crystallization, giving the form an excellent structure and resistance to decomposition because it is associated with granitic rocks and granodiorite. In addition, they are associated with coarse, medium, or fine-grained rocks with feldspar and micas elements (Pupiales,2021).

### ***Macuchi Unit (M-U)***

The Macuchi Unit is located in the northwestern part of the parish, with 0.64% between the limits of the Cangahua and volcanic breccias (Figure 4). This unit is characterized as a volcanic arc that originated detrital material from ancient areas (Garcia, 2020). They are associated with basaltic and andesitic rocks, which are formed in a massive form and formed by volcanic sedimentary and volcanic rocks (Pupiales,2021).

### ***Silante Formation (S-F)***

Silante Formation (S-F) is located between the Mira River and the northern part of the parish. It has a high abundance of volcanic minerals and material derived from the continental crust, with 1.77% of the territory (Garcia,2020). Polymictic conglomerates, supported clasts, and subangular and green volcanic clasts mainly characterize it. In addition, it has rich concentrations of volcanic material such as breccias, sandstones, and shales. Also, there are dextral faults on the Salinas-Lita highway (Andrade et al., 2012).

### ***Chota Group (C-G)***

The Chota Group (C-G) is exposed in the central part of the Mira River basin, where the metamorphic basement lies discordant between the limits of the Chota River and the Salinas parish. This unit is located in the eastern zone with 0.48% (Cevallos,2015). This geological formation contains volcanic breccias and conglomerates associated with volcanic sandstone sediments and, on several occasions, has very fine limestone strata.

### ***Angochagua Volcanic (A-V)***

The Angochagua Volcanic (A-V) is located in the southern part of the parish and does not have a higher concentration of materials for the area, with 0.07% (Pupiales, 2021). This unit is composed of lavas, volcanic breccias, and tuffs derived from Pliocene eruptions. The rocks are andesites and basalts containing plagioclase phenocrysts, orthopyroxenes, and clinopyroxenes (Garcia,2020).

#### ***Volcanic Breccias (V-B)***

Volcanic Breccias (V-B) are found to the north, center, and south of Salinas, with a percentage of 5.27% of the entire parish territory (Cevallos, 2015). The volcanic Breccias are generated by explosive eruptions where there is the breakage of the rock of box or lava plugs. They are also pyroclastic igneous rocks where large rock particles are formed and compacted with ashes. They can also be associated with the extrusion of domes and some dykes (Pupiales, 2021).

#### ***Undifferentiated terraces (1-3, U-T)***

Undifferentiated terraces are found in the central part and a little in the south of the parish territory, with 53.14% (Garcia, 2020, see Figure 4). There are considered terraces that occurred in the geological age of the Pleistocene, which is located in large drainages along the Mira River. These terraces are characterized by terraces 1-3, representing volcanic materials such as lavas, andesites, and sediments eroded over time by the formations in the areas (Pupiales,2021). These materials are transported to the south area, which is part of Salinas, and the materials come from the high stakes of the western mountain range and the Inter-Andean valley. The emission sources are located in these high areas and are associated with volcanism with pyroclastic flows consisting of ash, lapilli, and tuffs. The origin of the materials deposited in the different volcanic activities is detailed to identify more about the undifferentiated terraces.

#### ***Chachimbiro volcanic (CH-V)***

Chachimbiro volcanic unit (CH-V) is located on the eastern edge of the Cordillera Occidental on the border with the Inter-Andean valley. The evolution and formation of this volcanic complex are given by magmatic activity during the Quaternary (Tipantásig,2017). In addition, this covers an extensive area with volcanic materials such as pyroclastic and is located in the Pablo Arenas to Cahuasquí sector. The tuff and lapilli

materials of greater quantity are located in the southeastern area of the Inter-Andean Valley (see Figure 4). Andesitic volcanic breccias predominate in sectors of Pablo Arenas (Andrade et al., 2012). Finally, the following eruption events of the Chachimbiro Volcano are considered;

*Chachimbiro 1 (CH-1)* is composed of an andesitic stratovolcano with large effusive andesitic lava flows that descended from the eruptive center forming the first stage of the Chachimbiro volcanic complex. Then, during the middle Pleistocene, the stratovolcano underwent a landslide and generated a debris avalanche of volcanic and andesitic rocks flowing eastward from the volcano (Bernard et al., 2009).

*Chachimbiro 2 (CH-2)* consists of the resurgence of volcanism after having suffered the collapse of the caldera. Several materials, such as dacitic and andesitic domes and pyroclastic flows, were created in this event. Following this event, the Tumbatú volcano was made, but there was an explosion event where the volcano, as mentioned above, collapsed in an easterly direction (Bernard et al., 2009).

*Chachimbiro 3 (CH-3)* is the last event where new dacitic and andesitic composition cupolas formed. This process gave rise to two new domes as, Hugá and Albuji. These domes were located in the same place as the second landslide (Villagomez et al., 2010).

#### ***Yanahurco Volcanic (Yh- V)***

Yanahurco Volcanic (Yh-V) is found in the center and south of Santa Catalina de Salinas, representing 20.85% of the parochial surface (Garcia, 2020). Yanahurco was an eroded volcanic center constituted by two Pleistocene-age domes and underlying Pliocene units, all part of the Quaternary period. It is one of the most frontal volcanoes of the volcanic arc and is between the limits of the Pilavo volcano and surrounded by the Chachimbiro volcano (Figure 4). Yanahurco consists of andesitic lavas and pyroclastic flows and contains andesitic porphyritic rocks associated with phenocrysts of the plagioclase group and minerals related to amphibole, quartz, and biotite (Beguelin et al., 2015).

#### ***Alluvial deposits (A-d)***

Alluvial deposits (A-d) are located in north to south of Santa Catalina de Salinas; these materials comprise 6.21% of the parish territory (Garcia, 2020, see Figure 4). It



consists of the formation of alluvial soils by deposition and transport of detrital material through the action of the fluvial system such as the river, in which they are deposited at the end of a slope or gradient and occupy riverbeds, plains, and paleochannels in the form of fans (Pupiales, 2021). The materials found in these deposits are sands, clays, granules, pebbles, and blocks of very variable shapes, such as angular to subangular. These materials comprise 6.21% of the parish territory (Garcia, 2020).

### ***Cangahua (Cg)***

Cangahua (CG) is located in the northern part of the parish and covers 34.88% of the area (Garcia,2020, see Figure 4). This unit is approximately three meters thick and lies on an unconformable contact above the volcanic breccia units. According to Vera (1992), mentions that to form soft and porous rocks through partial diagenesis of fine explosive material of pyroclastic flows origin, smaller than the size of ash. Cangahua has mineralogical compositions associated with andesitic rocks and dacites by having a high content of minerals such as andesine which is the feldspar group (Leon,2016). This formation occurred in the Imbabura volcanic complex, subjected to various erosive episodes and reworked materials that generated Cangahua.

### 3 Chapter 3. Experimental procedure

#### 3.1 Materials and Equipment

The materials used to develop the field and laboratory work are allowed to collect and process the samples in the study area through various methods. These materials are essential to have calibrated and selected according to the research work to be carried out to meet the objectives established in Santa Catalina de Salinas, Ibarra (Table 8).

**Table 8.** *Materials used to carry out research work both in the field and laboratory.*

Material	
Plastic bags (Ziploc)	Spatula
Brush	Filter paper
Geological magnifying glass	Hydrochloric acid
GPS	Plastic bottle 750 ml
Camera	MDT
Permanent marker	ArcMap

The equipment was used to collect and analyze the soil and water samples collected in different outcrops in the fieldwork. This equipment was obtained from the School of Earth Sciences, Energy, and Environment laboratories of Yachay Tech University. Each piece of equipment must be calibrated to the research terms, especially the X-ray diffraction equipment (Table 9).

**Table 9.** *Equipment used to carry out research work both in the field and laboratory.*

Equipment	
X-Ray Diffraction	Drone
Sieve Shaker	Disc Mill
Portable digital pH Meter	Ultrasonic (water bath)
Laboratory balance	Incubator (drying)
Stove	Agate and porcelain mortar
Precipitation beaker	Heating plate

#### 3.2 Methodology

The geological characterization of the mineral phase composition is the object of study of the salt's chemical functional groups to identify the salt's possible origin using several processes and methods detailed in the following paragraphs. This study's main points of interest were the different areas of Tolas, some outcrops, and areas of natural and artificial water sources (Figures 1 and 5). In addition, the fieldwork for collecting samples and geological information was done in a single day, November 21, 2022, in the parish of Santa Catalina de Salinas in the province of Imbabura. The field trip started at 9:00 am and lasted until 16:00. The weather during this day was warm (25°) with abundant sun and wind, which allowed us to collect samples in a dry state, a good point for the analysis of the samples.



**Figure 5.** *The main points of interest in the sample collection. (A) The zone of tolas resulting from the residues of soil piles from the salt extraction process, (B) Tolas showing heights up to 10 meters, and (C) Water sampling zone in natural springs.*

For this study were taking 35 samples, including soil, salt crusts, and water samples at varying zones. These samples were sorted into 26 saline sediment samples in 24 different tolas (Figure 1B), some at the base, middle, and top. Besides, three crust samples and two salt samples were collected in small quantities, and five samples of water

from natural and surface springs, 750ml (Figure 1C). In addition, the amount of material collected varies from 1 kg for soil and a few grams of salt crusts and soluble salts in situ form. Besides, all the characteristics of the samples, such as coordinates, code, description, and location, are included in Table 10.

**Table 10.** Description of samples collected from Santa Catalina of Salinas, Ibarra. Samples of water, soil, and salt crusts are present in the study area.

Code of sample	Sample description	UTM X	UTM Y	Location	Height (m)	Weight (kg)
T1M2P3	Sample 2-top	816828.1	53557.4	Tumbabiro - Salinas highway	6	1.000
M3P4	Sample 3 (Crusts)	820447.7	53252.5	Main bridge to Salinas-Lita	50	1.000
M4P4	Sample 4 (Salts)	820435.3	53257.4	Main bridge to Salinas-Lita	3	-
T2M5P5	Sample 5-base	819998.9	55739.7	Tola zone (Palenque ranch)	3	1.000
T3M6P6	Sample 6-top	819975.3	55719.8	Tola zone (Palenque ranch)	10	1.000
T4M7P7	Sample 7-top	819982.5	55747.9	Tola zone (Palenque ranch)	10	1.000
T5M8P8	Sample 8-top	819982.5	55756.2	Tola zone (Palenque ranch)	9	1.000
T6M9P9	Sample 9-top	819942.2	55754.1	Tola zone (Palenque ranch)	8	1.000
T6M10P9	Sample 10 (Crusts)	819942.2	55754.1	Tola zone (Palenque ranch)	8	1.000
T7M11P10	Sample 11-top	819945.7	55812.9	Tola zone (Palenque ranch)	10	1.000
T8M12P11	Sample 12-top	819889.9	55738.5	Tola zone (Palenque ranch)	5	1.000
T9M13P12	Sample 13-top	819893.5	55811.1	Tola zone (Palenque ranch)	5	1.000
T10M14P13	Sample 14-top	819846	55826.6	Tola zone (Palenque ranch)	10	1.000
T11M15P14	Sample 15-top	819842.6	55815	Tola zone (Palenque ranch)	8	1.000
T12M16P15	Sample 16-top	819861.3	55759.5	Tola zone (Palenque ranch)	8	1.000
T13M17P16	Sample 17-top	820110.7	55727.3	Palenque ranch (Income)	4	1.000
T14M18P17	Sample 18-top	819877.7	55991.1	Tola zone (C. alto rendimiento)	5	1.000
T15M19P18	Sample 19-base	819622.7	55954.8	Tola zone (C. alto rendimiento)	3	1.000
T16M20P19	Sample 20-top	819591.4	55981.7	Tola zone (C. alto rendimiento)	5	1.000
T17M21P20	Sample 21-top	819655.7	56085.8	Tola zone (C. alto rendimiento)	10	1.000
T18M22P21	Sample 22-top	820003.6	56120.2	Tola zone (C. alto rendimiento)	8	1.000
T19M23P22	Sample 23-top	819596.3	56058.9	Tola zone (C. alto rendimiento)	8	1.000
T20M24P23	Sample 24-top	819546.6	56003.6	Tola zone (C. alto rendimiento)	4	1.000
T21M25P24	Sample 25-medium	819541.7	56077.9	Tola zone (C. alto rendimiento)	4	1.000
T22M26P25	Sample 26-top	819455.7	55949.1	Tola zone (C. alto rendimiento)	7	1.000
T23M27P26	Sample 27-medium	819488	55915.2	Tola zone (C. alto rendimiento)	10	1.000
T24M28P27	Sample 28-top	819487.5	55877.7	Tola zone (C. alto rendimiento)	9	1.000
M29P29	Sample 29 (Crusts)	818769	52582.1	Secondary road from Salinas	-	0.500
M30P30	Sample 30 (Salts)	819024.6	48635.7	Secondary road from Salinas	-	0.005
M1AP1	irrigation water	813818.8	53148.7	Farm and water reservoir	-	-
M2AP4	Spring water	820447.7	53252.5	Main bridge to Salinas-Lita	-	-
M3AP23	Superficial water	819596.30	56058.80	Tola zone (C. alto rendimiento)	-	-
M4AP28	Spring water	819471.30	55735.60	Tola zone (C. alto rendimiento)	-	-
M5AP29	Spring water	818769	52582.1	Secondary road from Salinas	-	-
M6AP30	Spring water	819024.6	48635.7	Secondary road from Salinas	-	-

### 3.2.1 Laboratory work

The laboratory work was carried out at the Yachay Tech University facilities. In the laboratory, we developed an analysis of the pH classification of the water, separation of salt samples, the sieving technique, extraction of salt in an artisanal way, crushing method, and quantitative analysis of the minerals of the chemical group of salts by X-ray diffraction. Processing the samples collected in the laboratories with all the appropriate equipment is necessary. Follow all the steps of the different methods to be applied to identify which piece has a salt concentration and how to classify it. Therefore, each of the processes and methods involved in this research is described in the following paragraphs.

### 3.2.2 pH analysis

Six water samples were collected in different natural or surface springs areas at various points in Santa Catalina de Salinas (Figure 1C). In order to classify the type of water, the pH method was applied, which is an index of the concentration of hydrogen ions (H<sup>+</sup>) in the water. Water temperature is the only variable measured more frequently than pH. In addition, the characteristics of salt water are different from those of fresh water. The pH measurement scale is logarithmic, with values 0-14 with a pH value of 7 as the midpoint. The scale is divided into acidic, neutral, and basic. pH values below 7 represent acidic reactions, and pH values above seven represent progressively more basic or alkaline reactions. However, the pH of neutral (pure) water is 7 only at a temperature of 25°C. At lower temperatures, the pH is above 7; at higher temperatures, the pH is below 7 (Boyd et al., 2011). Besides, the pH allows for identifying the classification of the soil if it is acid, neutral, or alkaline so that in different areas, the pH tends to vary the scale of 0-14 (Smith & Doran, 1996).

### 3.2.3 Salt sample separation

During the preparation of samples for different analyses, four essential points were identified in the study area to develop a characterization of the salt sample separation. First, in the tola zones, soil sediment samples were collected in plastic bags of about 1 kg (Figure 6A). Second, in watershed areas, salt crust samples were collected in plastic bags of about 250 grams (Figure 6B). Third, about 20 g of salts were collected from soil sediment samples in outcrops or in situ form. Water transport forms these

samples as soluble salts (Figures 6C and 6D). This zoned sample selection aims to determine the characterization of the mineral phases present in each sample. Therefore, the samples collected in the tolas must pass through the sieving process to identify the different granulometric fractions. After this process of separation of the material, X-ray diffraction analysis (XRD) must be performed. Additionally, for the X-ray diffraction analysis, the samples must go through the drying and crushing process to correctly identify the salts.



**Figure 6.** Different points where the samples were collected, (A) Samples of 1kg salts with sediments in soils, (B) Salt crusts in natural water sources, (C) Areas made up of salts in the soil, (D) Salt zones with fragments of volcanic rocks such as pumice and volcanic tuffs.

### 3.2.4 Sieving methods

The soil samples collected show variations in particle size. To classify samples taking into account the texture of the soil and work with different fractions, especially the sieving method was applied, which consists of separating a sample to organize it according to particle size. This process is carried out using a sieve, either manually or by mechanical force (see Figure 7). The different properties of this process, such as intensity, time, direction, and force, vary greatly depending on the sieving method chosen (Lucka,2016). In addition, the passage of different particles will depend on the size ratio and the different mesh openings of the sieve (Figure 7a). This process's main criterion is obtaining several fractions of the analyzed material, so the set of sieves will be applied from the smallest to the largest mesh size, called cascade sieving. The particle size must consider when choosing the sieving method since samples from 40  $\mu\text{m}$  to 125 mm can be sieved by the dry sieving method. However, if the size is below the mentioned limit, it will be sieved by the wet sieving method until the size of 20  $\mu\text{m}$  is reached. Finally, Figure 7b shows that the air jet sieving method can be applied if the samples are very fine (Retsch GmbH Haan, 2016).

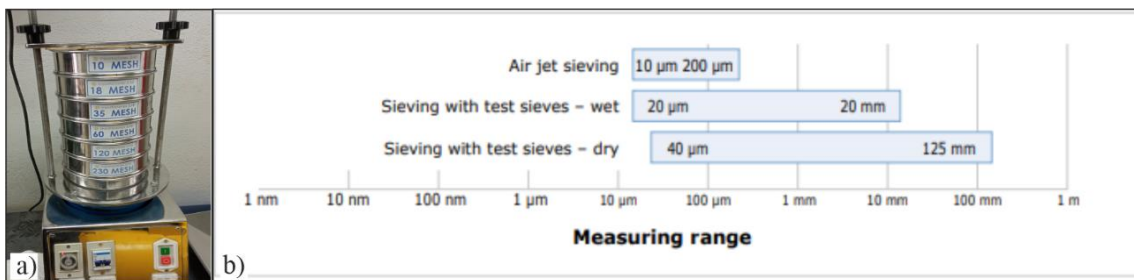


**Figure 7.** The sieving method, (a) Sieving mechanic with different mesh size, (b) Measuring range to samples analysis. Figure 7b; modified from Retsch GmbH Haan (2016).

The laboratory of the Faculty of Earth, Energy, and Environmental Sciences of Yachay Tech University allowed the drying and sieving process for the samples collected in Santa Catalina de Salinas. The samples contain their identification code to make the process more accurate with the different sieves that vary the mesh size from 10 (2mm) to 230 (0.062mm). In addition, for each Tola sample, the dry sieving process was applied, so the samples were dried using the incubator at a temperature of 85° for 2 to 3 hours according to each sample's amount and state of humidity (Figure 8A). Subsequently, to carry out the sieving process, the weight control was carried out with a total amount of 1000gr for each tola sample (Figure 8B). The sieving process was carried out for 30 to 40

minutes per tola sample to meet the objective of texture classification for each of the samples in the different meshes.



**Figure 8.** The samples are dried in an incubator at 85° for 4 hours (A). B) After drying, the samples can be sieved on sieves from 10 to 450 mesh.

### 3.2.5 Granulometric analysis

The granulometric analysis of the soil consists of the division of several fractions according to their size, thus identifying the texture of the soil. The granulometric scale allows classifying the size in several percentage fractions, such as the smallest particles corresponding to the fraction of clays (< 0.004 mm), silts (0.002-0.032 mm), and sands (0.04-2.0 mm). Particles of larger diameters correspond to gravel sediments (> 2.0 mm), where pebbles are present (Rzasa & Owczarzak, 2013; see Table 11).



**Table 11.** Classification of sediments by grain size proposed in 1922 by C. K. Wentworth. Adapted from Ingemmet, 2015.

Clast or crystal size in mm	Clasts	Sediments	Volcaniclastic fragments	Crystalline, igneous, sedimentary or metamorphic rocks	Rock type
256	Boulder	GRAVEL	Blocks/ Bombs	Very coarse grain	Conglomerate/ Breccia
64	Cobble		Lapili		
4	Pebble			Coarse grain	
2	Granule				
1	Very coarse sand	SAND	Coarse Ash	Medium grain	Sandstone
0.5	Coarse sand				
0.25	Medium sand			Fine grain	
0.125	Fine sand				
0.032	Very line sand				
0.004	Silt	MUD	Fine Ash	Very fine grain	Siltstone
	Clay			Cryptocrystalline	Claystone

In this same context, the collected samples were processed by the sieving method to obtain the weight data according to each sieve size. The total weight used by the sieves was 1kg (see Table 12). During the sieving process, the granulometric classification was achieved according to the different established meshes packed in each plastic bag with their respective code, date, and weight. Subsequently, these samples of tolas and salt crusts can be crushed and then analyzed by X-ray diffraction (XRD).

**Table 12.** Representing to the data of the total weight of the sample and the total weight remaining for each particle size fraction. The light blue row is from the first method and the yellow row is from the second method.

Sample	10	18	35	60	120	230	Total Result	Total sample (gr)
T1	131.9	186.8	213.25	222.89	20.48	15.3	810.62	1000
T2	131.68	155.56	184.76	178.74	114.25	63.54	832.53	1000
T3	150.08	194.7	154.69	175.33	145.9	37.26	857.96	1000
T4	118.9	158.16	194.16	168.31	135.23	59.71	834.47	1000
T5	117.21	137.96	187.5	194	148.1	51.81	836.58	1000
T6	168.11	203.82	163.89	225.17	95.06	25.8	881.85	1000
T7	167.24	187.72	211.18	179.72	76.48	46.5	868.84	1000
T8	230.41	266.02	162.84	107.88	26.66	12.4	806.21	1000
T9	177.93	157.4	206.24	165.56	80.77	24	811.9	1000
T10	132.93	68.72	86.17	119.86	90.02	19.67	517.37	550
T11	167.66	191.37	223.3	193.52	66.87	23.2	865.92	1000
T12	166.99	191.55	209.67	210.73	10.5	0	789.44	1000
T13	123.1	151.9	170	217.3	170.6	65.18	898.02	1000
T14	117.72	183.55	204.3	177.83	113.88	19.11	816.39	1000
T15	207.69	192.96	155.64	194.66	173.95	27.36	952.26	1000
T16	190.36	196.44	165.32	177.55	78.19	48.6	856.46	1000
T17	171.54	185.97	195.13	196.42	114.98	31	895.04	1000
T18	139.27	174.85	156.54	237.48	94.95	42	845.09	1000
T19	141.75	143.15	118.46	243.56	118.1	52.22	817.24	1000
T20	78.74	178.14	166.8	288.68	169.68	36.79	918.83	1000
T21	97.18	190.61	286.66	210.86	56.15	34.4	875.86	1000
T22	213.47	150.39	157.1	202.36	62.6	25	810.92	1000
T23	200.5	169.3	220.02	137.5	26.4	85.4	839.12	1000
T24	153	86.44	141.58	106.83	73.16	13.76	574.77	600

On the other hand, in the granulometric classification of the Tolas samples, two methodologies of soil analysis were applied by X-ray diffraction (XRD). These two methodologies allow us to examine the composition of salt mineral phases found in mixed materials with soils, the first method, and the extraction of salt from the soil, the second method, in which all the samples are from the Tolas area. In the first method, we only want to see the concentration of soluble salt minerals associated with volcanoclastic materials. In the second method, we want to separate the soil material and the soluble salts to check later if it is related to the first method.

**First method.** - It consists of selecting and analyzing randomly selected samples using a fast algorithm in the online programming language Python to identify the seven most representative samples out of the twenty-four total samples (see Figure 9). This method allows performing the analysis on all the selected mixed saline sediment samples in which complete results of the mineral compositional phases and chemical functional groups will be identified in a general way.

```

main.py
1 import random
2 from random import sample
3 Totalsamples = sample(range(1,24),7)
4 for samples in Totalsamples:
5     print('Tola', samples)
6
Shell
Tola 1
Tola 4
Tola 20
Tola 9
Tola 6
Tola 13
Tola 23
> |

```

**Figure 9.** It consists of an online Python programming language to identify random samples. The random code generates random numbers that fit a uniform distribution over a range of integers (1,24).

As a result of the seven randomly selected samples, the Tolas 1, 4, 6, 9, 13, 20, and 23 were obtained. In addition, these samples were considered the most representative according to the location of the different tola zones. Subsequently, the samples will be crushed by various crushing equipment until they are converted into finer sizes as powder.

**Second method.** - Randomly and representatively selecting eight samples without counting the samples already selected in the previous method. Similarly, the samples were selected by applying a random code algorithm in the Python online programming language (see Figure 10).

```

main.py
1 import random
2 from random import sample
3 SamplesTotal = sample(range(2,24),8)
4 for sample in SamplesTotal:
5     print('T', sample)
Shell
T 22
T 11
T 8
T 16
T 21
T 15
T 2
T 5
> |

```

**Figure 10.** It consists of an online Python programming language to identify random samples. The random code generates random numbers that fit a uniform distribution over a range of integers (2,24).

The objective of this method is to take one of the eight samples selected to perform the artisanal process of salt extraction, applying some changes to the process performed

by the community of Salinas. The representative sample chosen is Tola 16 because it is located in the area with the highest concentration of tolas and is close to natural springs.

### 3.2.6 Artisanal extraction of salt

This process involves adapting of the artisanal salt extraction method in the Santa Catalina de Salinas community. Therefore, this method was carried out in the laboratories of Yachay Tech University, where the processes were performed as follows; First, collect the samples in the study area (Figure 11, step 1). Second, place the six fractions with their respective weights in each beaker, then put about 400 ml of distilled water (see Figure 11, steps 2 and 3). Before this, check the pH and temperature of the water, which has a pH of 5.8 and T of 20.8°C. Next, mix the whole sample with a glass rod for about five minutes to concentrate the water and sediments. Then, let it stand for twenty-four hour to decant of the solid-liquid mixture (see Figure 11, step 4). Next, separate the solid and liquid in a beaker where the liquid of each fraction is in the range of 300ml (see Figure 11, step 5). Next, the obtained liquid sample was placed on a hot plate at a temperature of 150°C, and for 4 hours per sample to evaporite the water (see Figure 11, step 6). Finally, obtain the salt solids for each fraction (Figure 11, step 7).

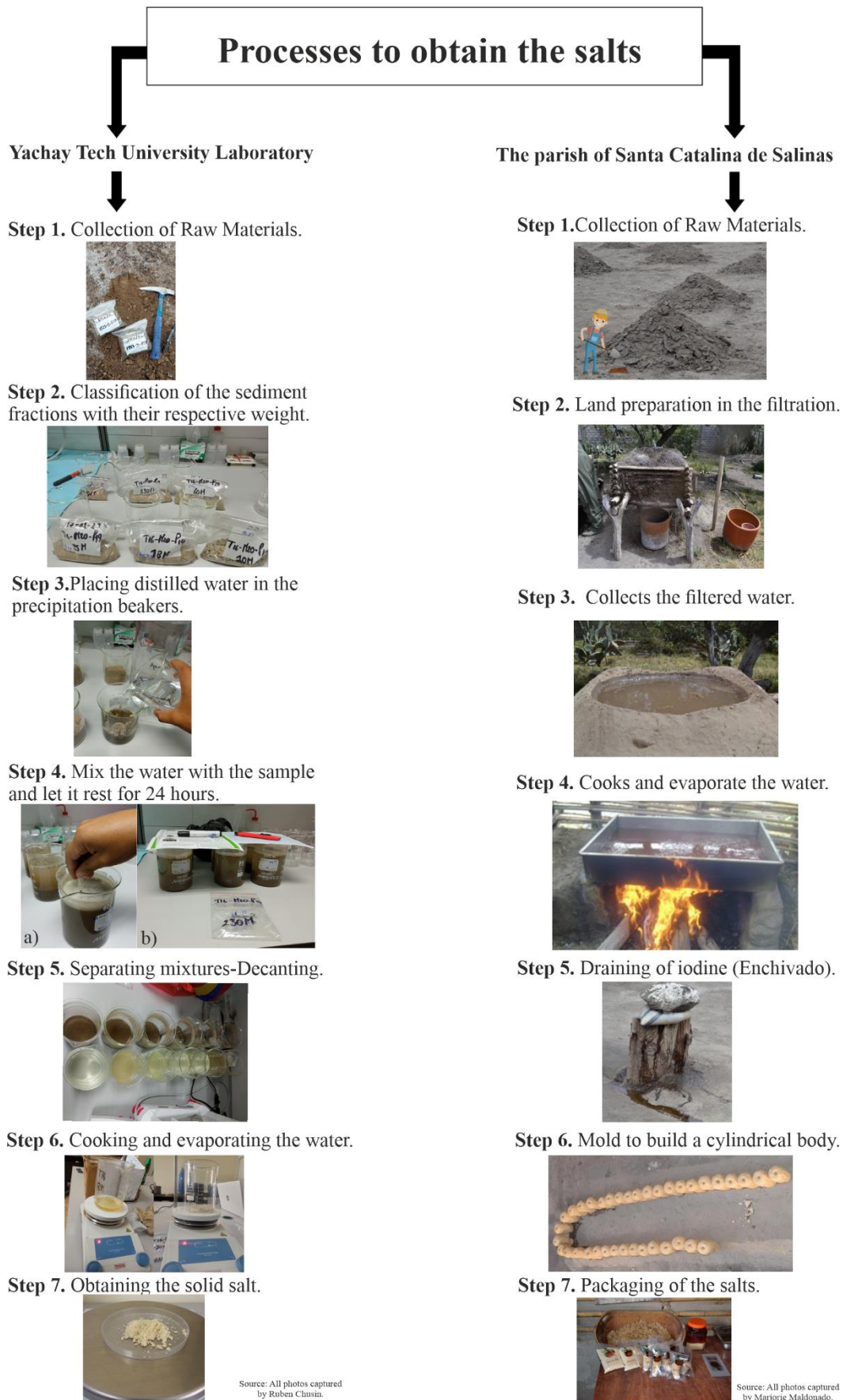


**Figure 11.** Workflow of the artisanal salt extraction process in Santa Catalina de Salinas and in the laboratories of Yachay Tech University. This diagram shows the different processes from soil collection to salt production.

### 3.2.7 Crushing process

The crushing process allows for obtaining finer-size samples by applying other equipment, such as disc mills or mortars. In this case, most of the samples collected and classified are of various granulometric fractions. These samples were subjected to a crushing process in which the disc mill, agate mortar, and porcelain mortar were applied. The disc mill was used to crush the different selected Tolas. This equipment was used for one minute for each Tola fraction since small portions of samples should be placed to avoid losing more samples (see Figure 12A). In addition, for a better crushing process, the samples must be dehydrated and clean so that the result does not present organic material and the larger samples become powder (Figure 12B).



**Figure 12.** *Crushing of samples using the disc mill (A). The pieces must be well dried so the crushing is homogeneous (B) and not mixed with organic matter.*

The agate and porcelain mortar allows the samples to pass into a more homogeneous powder. The friction process with the mortars is essential in the study because the samples collected are not very fine particles. It is necessary to pass the mortar for about 5 minutes per sample; however, this will depend on the particle size (Figure 13A). During this preparation stage, some samples only need to be passed through the mortar, and subjecting the sample to any finer sieving process is optional. However, some samples must be passed through the mortar and then through the 450-mesh sieve to obtain

a result equal to talc (Figure 13B). In addition, grinding the samples is essential with the different materials because it allows for achieving a texture similar to talc to reduce the roughness on the surface of the sample mounted in the XRD (Betancourth et al., 2010).



**Figure 13.** Sample preparation by crushing the agate mortar (A). Samples should be turned into a powder so they are passed on the 450-mesh sieve.

### 3.2.8 X-ray diffraction analysis (XRD)

The X-ray diffraction method is essential in mineral identification studies in soil and rock. It consists of a monochromatic X-ray beam directed at a sample turned into powder in a sample holder of various sizes. The diffraction intensity is measured as the detector moves at different angles (Hernandez, 2017). This technique helps to analyze, identify and quantify crystalline structures as minerals present in various samples in crystalline and non-crystalline solid states (Benavente et al., 2012). On the other hand, the x-ray diffraction method by powder technique can be performed for various parameters by photographic or diffractometric means. In addition, it is applied to various particle sizes of soil samples such as silt, clay, and sand (Justo & Murillo, 1999).

The scattering of radiation generates X-ray diffraction through the different atoms. This technique presents experimental results that allow identifying a diffraction profile. The information on the diffraction peaks is extracted from the interaction processes between electrons and electromagnetic radiation (Benavente et al., 2012). The width of the diffraction peaks can extract. Therefore, the information allows for generating

properties of the crystal size, micro deformations, and, above all, determining the different preferential orientations of the crystals analyzed; in addition, allowing both to quantify and identify all the phases structured in the material to observe whether it is of mineral or natural origin of the samples (Quiroga, 2021).

On the other hand, these samples were analyzed in the materials characterization laboratory of the School of Chemical Sciences and Engineering of Yachay Tech University. The X-ray diffraction analysis (XRD) was performed on a total of sixty-three samples divided as follows; forty-five samples from seven different tolas, five samples of crusts and salts, and six samples of salts obtained from a tola and seven samples of sediments remaining from obtaining the salt. In addition, each slab is separated granulometric by six fractions according to the sample size. The following steps were performed to obtain the final result of each sample analyzed:

First, the selected samples must be dry, for which the incubator of the E2E3 geology laboratory was used for 4 hours with a temperature of 85°C for each tola (see Figure 14A). Then, some samples were crushed using the agate mortar, and others were sieved with the 450-mesh size (see Figure 14B). Then, the sample turned into powder must have a quantity greater than 1 g to be placed in the sample holders since there are several sizes of sample holders, and each has its margin of error. Thus, for the sample preparation, the most profound sample holder was selected for its respective analysis (Figure 14C). After these processes, eight samples were introduced into the XRD equipment for each treatment, and the analysis time was four hours with certain measurement conditions, such as; an X-ray generator operated at 40 kV and 15 mA. CuK(alpha) radiation source (sealed tube), a Theta/2Theta scanning axis, 0.005° step width, 5-100° scanning range in 2Theta, and Ultra2 D/tex detector in 1D scanning mode were used for data acquisition. Finally, after four hours of analysis, a document is obtained in text format (txt). A list of the mineral phases was identified according to the 2θ parameters and the intensity of the peaks for each sample analyzed (see Figures 14D and 14E).



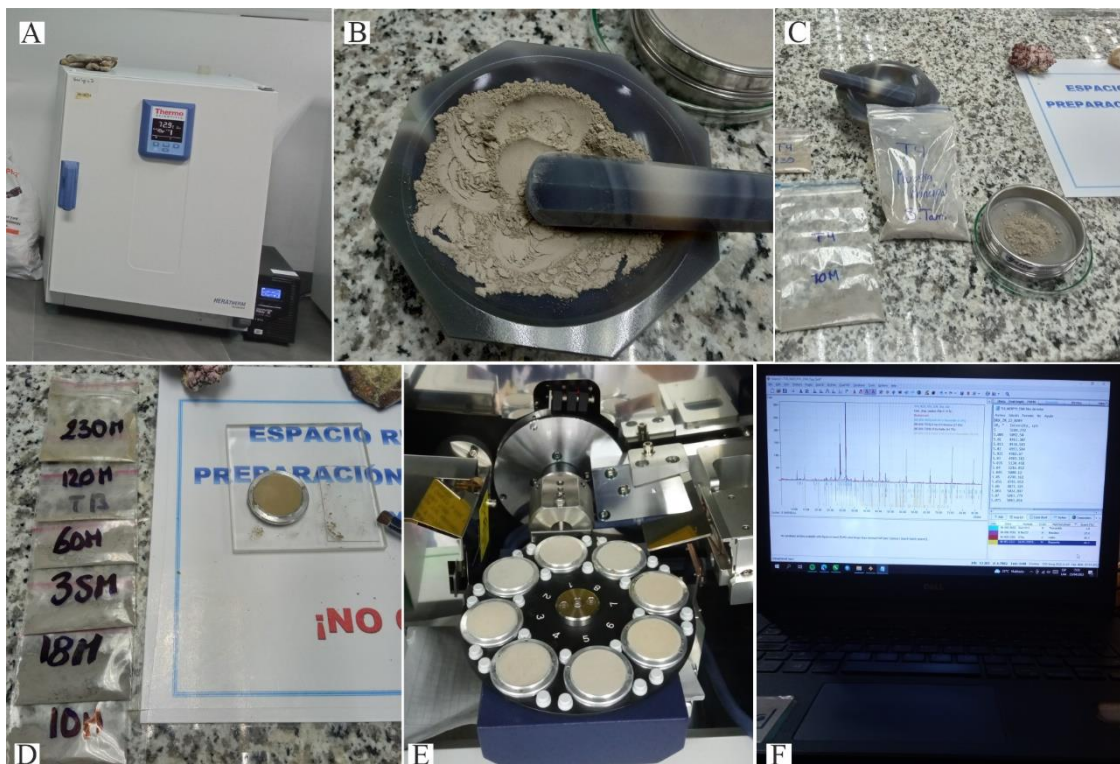


**Figure 14.** Processes to prepare the samples and then put them in the XRD. (A), drying of samples moisture. (B) Crushing in the agate mortar. (C) Passing through the smallest sieve to obtain a powder-type sample. (D) Placing in the sample holder. (E) Analyze the samples for 4 hours according to the XRD parameters. Finally, analyze by Match program the mineralogical composition phases (F).

The MiniFlex benchtop X-ray diffraction (XRD) instrument was used to analyze the mineral phases. This instrument allows the analysis of powder diffractions to determine and quantify the crystalline phases with their crystallinity percentages, size, formula, Rietveld refinement, and others. In addition, this instrument has these features as Cu K $\alpha$  radiation ( $\lambda = 1.5418740 \text{ \AA}$ ), X-ray diffractometer for polycrystalline samples, provided with a 600W X-ray tube, Bragg-Brentano goniometer with 8-position autosampler, D/teX Ultra detector, SmartLab Studio II software. The results obtained with this instrument were analyzed and characterized using Match! Software version 3.15 Build 262. This software has the download conditions for Windows 7, 8, 10, or 11 (64-bit) and Match-3-windows-x64-installer.exe (Figure 15F). Moreover, the identification of mineral phases was carried out using Crystallography Open Database (COD), especially COD-Inorg 2012.11.07 (Crystal Impact GbR, 2022).

## **4. Chapter 4. Result and Discussion**

### **4.1 Stratigraphic column of the study area**

A generalized stratigraphic column was made to understand the stratigraphy of the salt terrace where the salt extraction activity mainly takes place (Fig 15). A stratigraphic column was surveyed along the Santa Catalina area of Salinas de Ibarra. This column shows approximately 103m of thickness. It comprises facies during the Quaternary period, such as volcanic breccias, andesitic lava flows, and pyroclastic material of ash composition, such as tuffs, lapilli, and fine silt Cangahua unit (Fig 15). We briefly describe the stratigraphic column, such as lithology, texture, classification, units, and environment.

First, the basal part has 47m of thickness and is constituted of volcanic breccia block material with a fining-grained upward sequence. These materials are composed of gray breccias with angular to subangular textured clasts, where the clasts are of ashy grain size (Fig 15D). Through discordant contact, breccias is located at the top of this unit with refined matrix-supported ash-sized grains. These brecciated materials have a good to moderate classification, starting from the base. In addition, all these volcanoclastic materials are undifferentiated terrace fills by alluvial deposits resulting from volcanic collapse, so the materials have yet to be transported much. Then, we have a channel fill layer approximately 4 meters thick that follows the breccias' continuity to form lenticular bodies of conglomerate lenses with clasts of decreasing grain size (Fig 15C). In addition, the clasts have some rounded to subangular texture.

At the top of this unit, through a discordant contact, we have a 40 meters thick layer representing chaotic deposits of andesitic lava flows consisting in the base part of subangular clasts supported by ash type grain size, and in the upper part, there is the presence of fine matrix supported by ash-type, there are some fractures of andesitic rocks. All these materials are classified as moderate to well throughout the layer (Fig 15B). Above this layer is a discordant contact comprising volcanic materials such as dark brown tuffs, mainly composed of ash. The size of the tuffs contains fine sand particles and fine matrix support. Then, we have a 6m thick layer comprising lapilli deposits of fine to medium sand particle size associated with pumice materials. The colors of this layer are white and yellow. It has texture clasts supported by pumices and a good grading. Finally, At the top of this unit, through a discordant contact, is located a thickness of 3m of Cangahua materials, which are pyroclastic deposits, and the clast's size classification is

fine silt and yellow color (Figure 15A). In this same context, the upper part of the whole column is dominated by finer materials that are volcanoclastic environments.

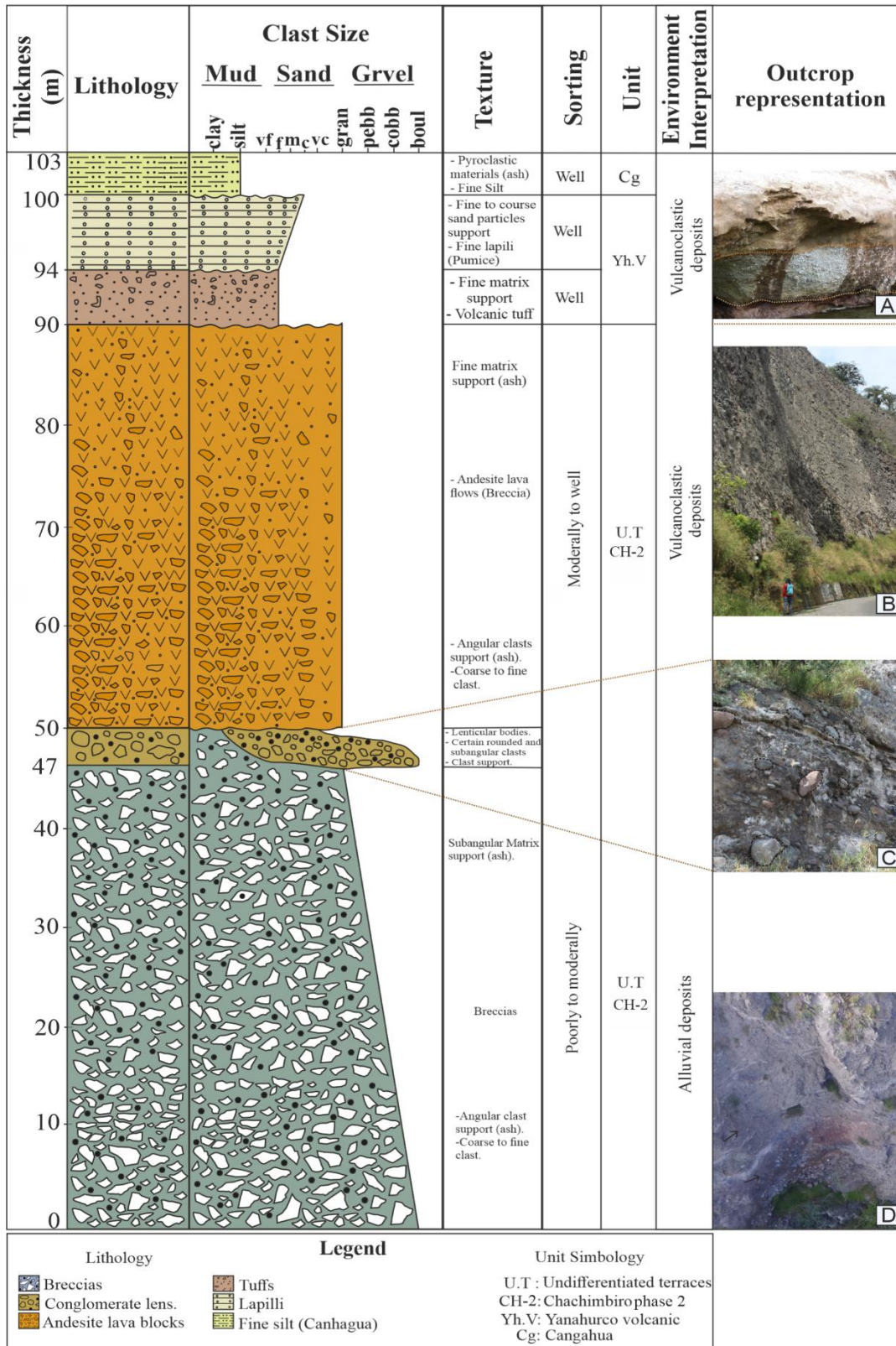


**Figure 15.** The stratigraphic position of the samples in the undifferentiated terrace which has a thickness of 103m. Image a) represents the upper part of the column composed of pyroclastic flows between tuffs, lapilli, and Cangahua. b) represents blocks of andesitic lava flows with ash-supported matrix. c) represents a channel filled with the lenticular body through conglomerate lenses. d) represents the base of the terrace with the presence of volcanic breccias.

## 4.2 Granulometric analysis

The data obtained by the sieving method correspond to the twenty-four different tolas. There is a granulometric classification by different sizes, such as lithic with fractions of fine, medium, and coarse sands, silts, and clays (see Table 11). Due to the different sizes of the sediments, a tola sample can be divided into six fractions representing 10 mesh sizes up to 230. In some cases, the particles are very fine and usually pass through all sieves. At the same time, there are samples with large fragments that do not pass through the sieves in considerable quantity, especially in the 230-mesh size, because the sample may not be homogeneous (Figure 16).

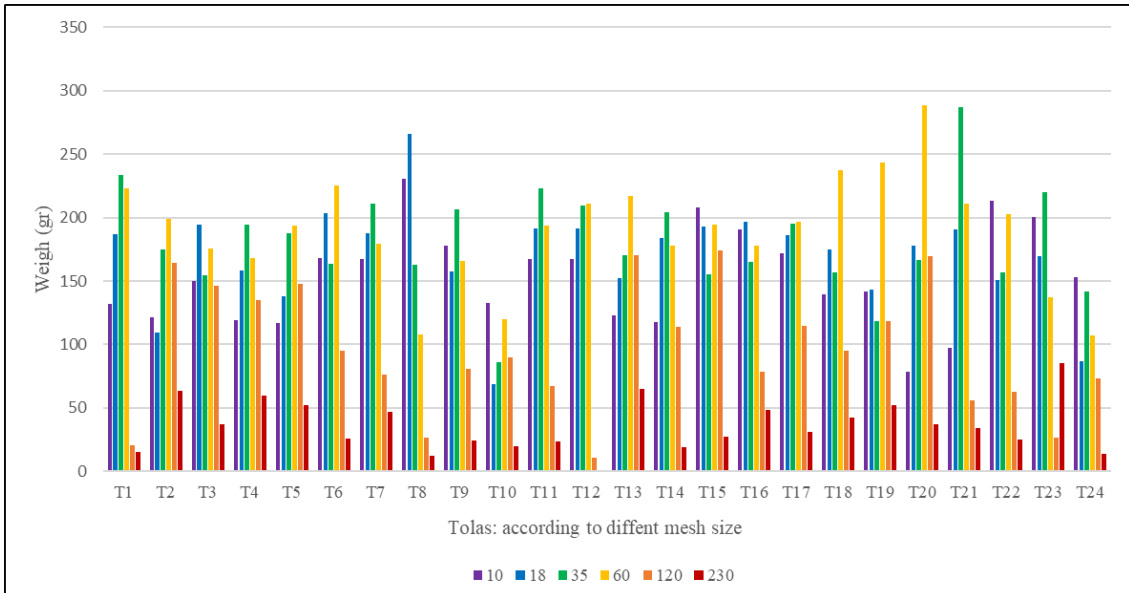


**Figure 16.** Representation of fractions recorded on all tolas according to their accumulation in the established fractions.

The sieved samples with the highest concentration in the following are Tolas 8, 19, 20, 21, and 23. The most predominant fractions in all the Tolas are the 18-mesh number which represents 1mm, fraction 35, which represents 0.5mm, fraction 60, which represents 0.25mm and 120, which means 0.125mm. According to the granulometric classification of the sediments, the most predominant in the study area correspond to the fractions divided into fraction 35 as coarse sand, fraction 60, and fraction 120 as fine sand.

### ***Artisanal extraction of salt***

The salt solids samples obtained should be weighed on a precision balance to obtain a figure representing how the weight (grams) varies and to identify in which fraction there is a higher salt concentration (see Figure 17). Finally, the salts must be well dried to obtain excellent sizes using an agate mortar to perform x-ray diffraction (XRD). The highest concentration of soluble salts is found in fractions of 18 and 35 for tola 16. In a total of 400 ml of distilled water mixed with soil, a salt range of 3 gr to 5.7 gr was obtained.

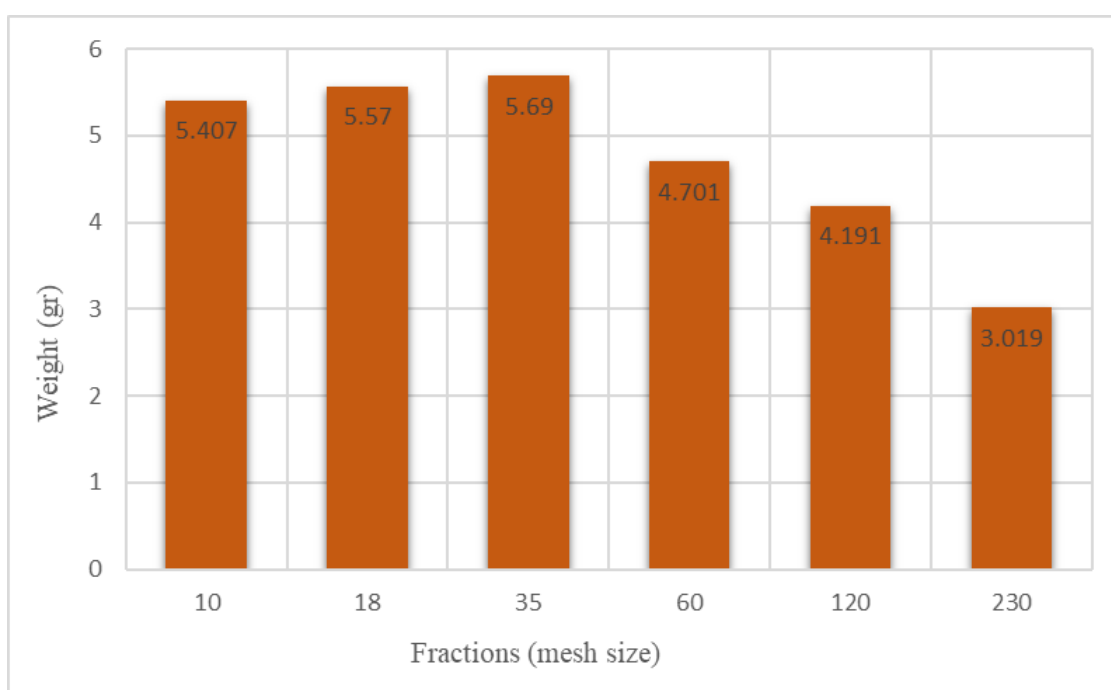


**Figure 17.** The salt concentration was obtained for each fraction according to the sieve mesh size. The highest salt concentration is in fractions 18 and 35 and the lowest in 230 mesh size.

### **4.3 pH analysis**

Data collection through water pH analysis allows us to identify the five water samples collected from natural springs, such as M2AP4, M4AP28, M5AP29, and M6AP30, and surface springs, such as M1AP1 and M3AP23 (Table 13). The water samples were analyzed at an average temperature of 20°C, where they were classified as neutral, basic, and very basic. There is more water of neutral classification in samples M2AP4, M4AP28, M5AP29, and M6AP30. On the other hand, there are basic to very basic classification water, such as M1AP1 and M3AP23. In this way, this neutral classification is because the source where it was collected is natural springs. However,

the basic to very basic water samples because the catchment source is surface springs in areas of tolas, and the irrigation drainage water could be associated with a concentration of soluble salts.

**Table 13.** Result of the classification of water by pH. There is a higher concentration of natural spring water, so it is neutral.

Sample	Descriptions	Temperature °C	Water pH	Water
M1AP1	Irrigation water	20.6	8.25	Basic
M2AP4	Spring water	20.8	7.5	Neutral
M3AP23	Superficial water	20.7	9.43	Very basic
M4AP28	Spring water	20.7	7.44	Neutral
M5AP29	Spring water	20.8	7.34	Neutral
M6AP30	Spring water	20.8	7.63	Neutral

#### 4.4 X- Ray Diffraction result

In this technique, diffractograms were provided from the samples converted into powder. The material analyzed was from areas of Tolas, outcrops, and around natural springs in the study area. Consequently, the sample analysis is a semi-quantitative estimation of the mineral composition phase where the reference intensities ratio (RIR) method was applied (Toraya, 2018). This method allows for comparing the intensity scale factors of the identified mineral content. In addition, all the highest and standard peaks, relative to the highest peak intensity, were considered in the XRD analysis to determine whether or not the minerals are part of the mineral composition phases (Morales et al., 2012).

In this study, two methodologies were applied; In the first method, seven representative Tolas were randomly selected from the 24 Tolas, where six fractions per Tola were analyzed. In the second method, eight Tolas were randomly selected from the remaining Tolas, where Tola 16 was randomly selected because it was in the most representative study area. A total of sixty-one samples were analyzed with their respective diffractograms. The codes of the different samples selected are T1P3, T4P7, T6P9, T9P12, T13P16, T16P19, T20P23, T23P26 and M3P4Crusts, M4P4 Salts, T6M10 Crusts, M29P29, M30P30. Fractions separated each Tola sample from 10 (2mm) mesh to 230 (0.063mm). In addition, each fraction shows different colors, such as fractions 10 is purple, 18 is blue, 35 is green, 60 is yellow, 120 is orange, and 230 is red.

Finally, the results obtained from the diffraction analysis are for eight general tolas; however, in this result, we present as an example Tola 23P26-Medium Sample of the first method, which has the same mineral identification pattern applied to the other Tolas. Then, the second method is presented by Tola 16, and finally, the analyzed samples of salt crusts. In the following writings, the description of the representative tolas was made, which was classified by general information about the sample; the diffractogram pattern represents the semiquantitative analysis following the concentration of the highest peaks. In addition, graphs of the semiquantitative value of the mineral phase composition and chemical functional group are presented. These graphs are examples of the classification of the different minerals identified for each Tola, outcrop, and salt crust.

#### *T23P26-Medium Sample (first method)*

In this example, the recorded data were identified by a diffractogram pattern where the highest peak intensity was considered for each mineral phase, depending on the percentage composition. The semi-quantitative analysis by XRD diffractogram for T23P26-230M Medium. The diffractogram allows identifying the majority and minority phase intensity peaks in which the following are detailed; the most intense peak is located at  $2\theta = 27.76^\circ, 21.99^\circ, 23.73^\circ, 24.44^\circ$  and  $31.48^\circ$  which corresponds to andesine mineral. In addition, the peaks of higher intensity for barrerite are represented at  $2\theta = 29.56^\circ$  and  $36.14^\circ$ . Furthermore, there is the presence of a peak of higher concentration at  $2\theta = 31.55^\circ$  and  $45.44^\circ$  represented by berlinite. Finally, higher peak intensity is identified at  $2\theta = 31.70^\circ, 45.45^\circ, 56.46^\circ$ , and  $75.31^\circ$  for the halite mineral, which is part of the chlorides (Figure 18). Additionally, the diffractograms in general of the other Tola samples, such as T4, T6, T9, and T20, have a relationship of presenting the peaks of higher intensity at  $2\theta$  between  $25^\circ$  to  $60^\circ$ . Thus, these represent several minerals such as thenardite, gypsum, sassolite, calcite, anhydrite, and others.

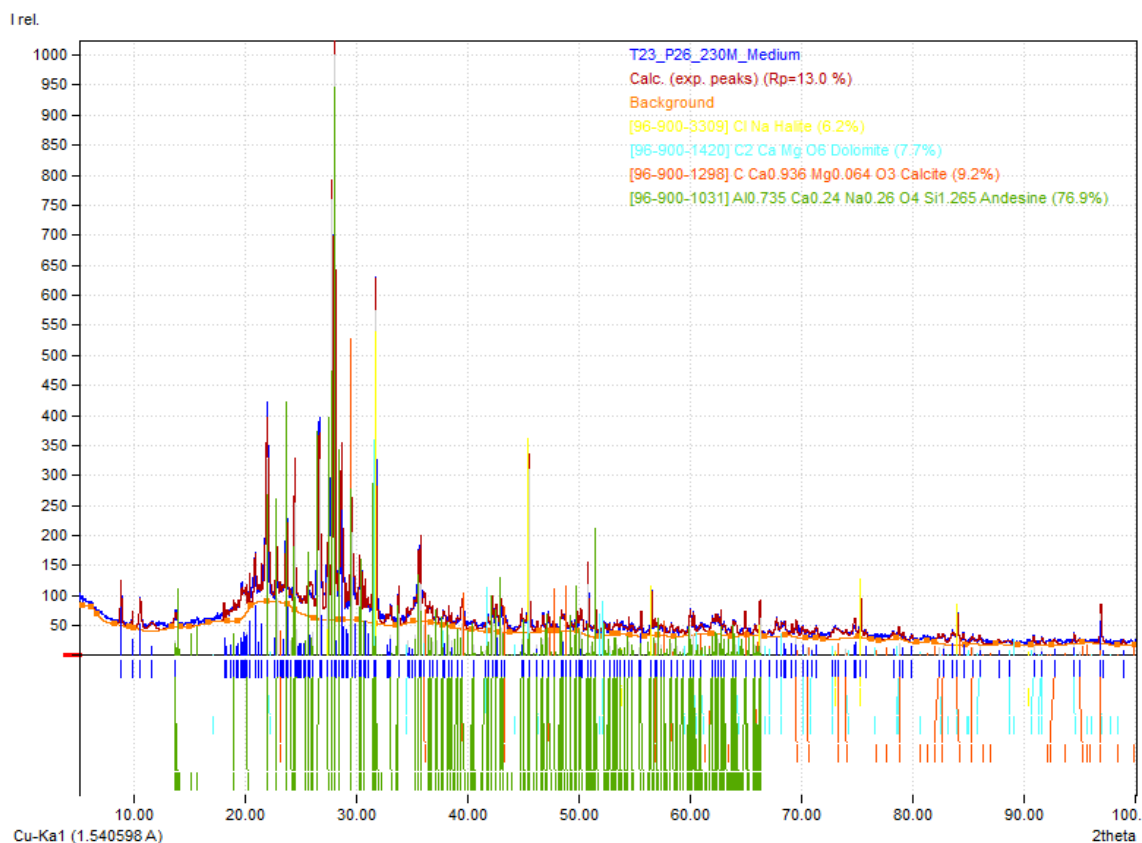


**Figure 18.** Diffractogram determined with the XRD pattern of the sample T23P26-230M medium. It is constituted that the presence of the highest intensity peaks of the minerals, such as halite, dolomite, calcite and andesine (silicate group).

On the other hand, in the samples analyzed, there are six different fractions per each Tola. Twenty-four mineral phases composition are recorded; some are repeated in other granulometric fractions and Tolas (Table 14). In addition, the identified minerals have the entry code for each mineral to more quickly determine the same mineral for each Tola in the Match program. This Tola contains more abundant salt minerals related to the other Tola samples analyzed, such as thenardite, calciolangbeinite, calcite, dolomite, halite, and nitratine. Finally, in all the fractions of T23, there are four mineral phases with different compositions in percentages (Table 14); this may vary according to the other Tola samples.



**Table 14.** General detail of the mineral phases detected in the T23P26-Medium sample divided into each granulometric fraction.

Mesh size	Entry #	Formula	Mineral phase	Phase composition (%)	Chemical functional group	Lithic fragments	Rocks or associated minerals
10	96-900-1031	(Na,Ca)[Al(Si,Al)Si <sub>2</sub> O <sub>8</sub> ]	Andesine	50.1	Silicates	Igneous rock	Diorites/Andesites
	96-900-7488	Ca <sub>4</sub> Be <sub>2</sub> Al <sub>2</sub> Si <sub>9</sub> O <sub>26</sub> (OH) <sub>2</sub>	Bavenite	15.1	Silicates	Miarolitic cavities	Granites
	96-900-0526	Na (AlSi <sub>3</sub> O <sub>8</sub> )	Albite	21.5	Silicates	Igneous rock	Granites/Syenite
	96-900-3309	NaCl	Halite	13.3	Chlorides	Sedimentary deposit	salt beds/salt domes
18	96-900-1031	(Na,Ca)[Al(Si,Al)Si <sub>2</sub> O <sub>8</sub> ]	Andesine	48.5	Silicates	Igneous rock	Diorites/Andesites
	96-900-0745	(Ca,Na)[Al(Al,Si)Si <sub>2</sub> O <sub>8</sub> ]	Labradorite	40.9	Silicates	Igneous rock	Gabbros/Anorthosites
	96-900-5023	SiO <sub>2</sub>	Quartz	7.6	Silicates	Igneous rock	Widespread
	96-900-3309	NaCl	Halite	3	Chlorides	Sedimentary deposit	Salt beds/salt domes
35	96-900-0745	(Ca, Na)[Al(Al,Si)Si <sub>2</sub> O <sub>8</sub> ]	Labradorite	58.4	Silicates	Igneous rock	Gabbros/Anorthosites
	96-900-1031	(Na, Ca)[Al(Si,Al)Si <sub>2</sub> O <sub>8</sub> ]	Andesine	18.7	Silicates	Igneous rock	Diorites/Andesites
	96-901-6688	K <sub>2</sub> Ca <sub>2</sub> (SO <sub>4</sub> ) <sub>3</sub>	Calciolangbeinite	20.8	Sulfates	Volcanic fumarole	Hematite/Rutile
	96-900-3309	NaCl	Halite	2.1	Chlorides	Sedimentary deposit	Salt beds/salt domes
60	96-900-1031	(Na,Ca)[Al(Si,Al)Si <sub>2</sub> O <sub>8</sub> ]	Andesine	48.9	Silicates	Igneous rock	Diorites/Andesites
	96-900-1259	Ca(Al <sub>2</sub> Si <sub>2</sub> O <sub>8</sub> )	Anorthite	45.8	Silicates	Plutonic rock	Datolite
	96-900-4093	Na <sub>2</sub> SO <sub>4</sub>	Thenardite	2.8	Sulfates	Volcanic fumarole	Mirabilite
	96-900-3309	NaCl	Halite	2.6	Chlorides	Sedimentary deposit	Salt beds/salt domes
120	96-900-1031	(Na,Ca)[Al(Si,Al)Si <sub>2</sub> O <sub>8</sub> ]	Andesine	60	Silicates	Igneous rock	Diorites/Andesites
	96-900-1259	Ca (Al <sub>2</sub> Si <sub>2</sub> O <sub>8</sub> )	Anorthite	28.5	Silicates	Plutonic rock	Datolite
	96-900-3309	NaCl	Halite	8.5	Chlorides	Sedimentary deposit	Salt beds/salt domes
	96-900-7555	NaNO <sub>3</sub>	Nitratine	2.9	Nitrates	Surficial deposits	Niter/Anhydrite
230	96-900-1031	(Na, Ca)[Al(Si,Al)Si <sub>2</sub> O <sub>8</sub> ]	Andesine	76.9	Silicates	Igneous rock	Diorites/Andesites
	96-900-1298	CaCO <sub>3</sub>	Calcite	9.2	Carbonates	All environment	Limestone/Carbonatites
	96-900-1420	CaMg(CO <sub>3</sub> ) <sub>2</sub>	Dolomite	7.7	Carbonates	All environment	Limestone/Carbonatite
	96-900-3309	NaCl	Halite	6.2	Chlorides	Sedimentary deposit	Salt beds/salt domes

### Mineral phase composition

The results are based on the semi-quantitative analysis of the mineral phase composition versus the different granulometric fractions (Figure 19). In this section, the following percentages for the mineral phase composition of the group of salts most commonly identified, such as thenardite, calciolangbeinite, calcite, dolomite, halite, and nitratine. In the same context, the minerals phase composition is divided into; fraction 10 (2mm), and halite (13.3%). In fraction 18 (1mm), halite (3%). In fraction 35 (0.5mm), calciolangbeinite (20.8%) and halite (2.1%) are present. In fraction 60 (0.25mm), the mineral with the highest concentration is thenardite (2.8%) and halite (2.6%). In fraction 120 (0.125 mm), halite (8.5%), and nitratine (2.9%) are present. In fraction 230 (0.063mm), the highest concentration mineral identified in the peaks of the more excellent range is calcite (9.2%), dolomite (7.7%), and halite (6.2%). Additionally, it should be considered that these mineralogical composition phase results are unidentified in other sample fractions for each Tola, as is the case of thenardite, which is visualized in Tolas 4,6,13, and 20.

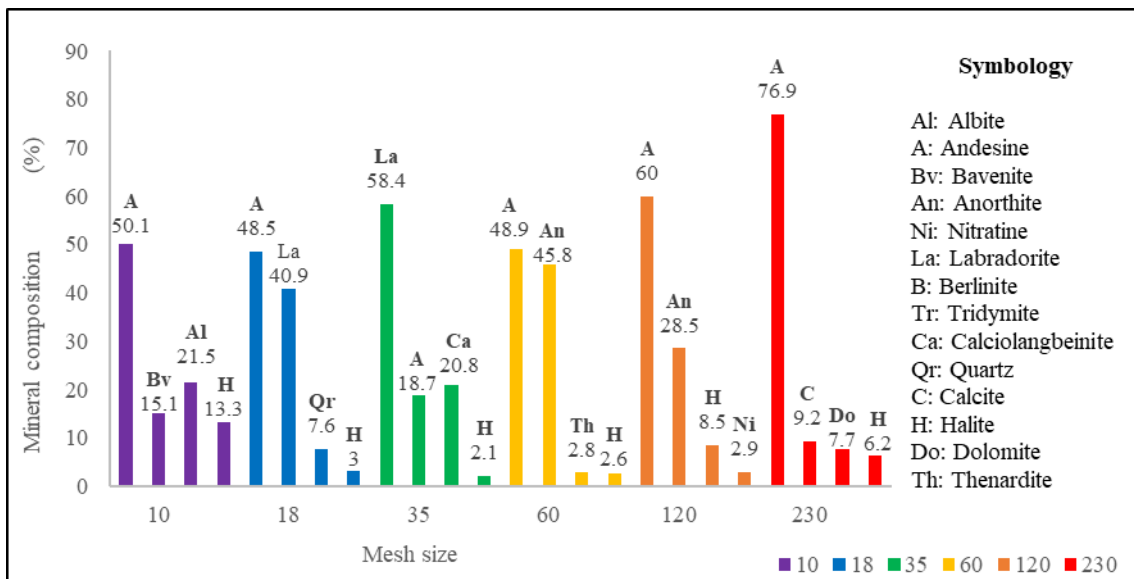


**Figure 19.** XRD percentage of the mineral phase composition versus sieve mesh size classification of 21 mineral phases of the saline soils. In this samples, there are higher concentrations of salt minerals such as dolomite, thenardite, halite and calciolangbeinite.

### Chemical functional group

X-ray diffraction (XRD) analyses represent the chemical functional group as sulfates, carbonates, chlorides, nitrates, and silicates are identified in the general mineral classification group. Below, percentages are divided into 50% for the soluble salts group and 50% for the silicates group (Figure 20). In these analyzed samples, it is identified that the group of silicates is the most abundant. However, it is customary to find these minerals because the location of the study area is a volcanic terrain, thus corroborating that the salts are associated with volcanic environments. However, we do not discuss silicate minerals because it does not contribute anything to identifying the groups of soluble salts. On the other hand, there are sulfate groups with calciolangbeinite and thenardite and carbonates with calcite and dolomite; both groups represent 17%. Likewise, the nitrate and chloride groups have the same percentage of 8% and present a mineral phase (Figure 20). In addition, the mineral halite of the chloride or halide group is present in all the granulometric fractions of the same Tola 23 (Table 14). These minerals of the salts group can be identified and related to results from other Tolas such as Tolas 1,4,6,13, and 20.

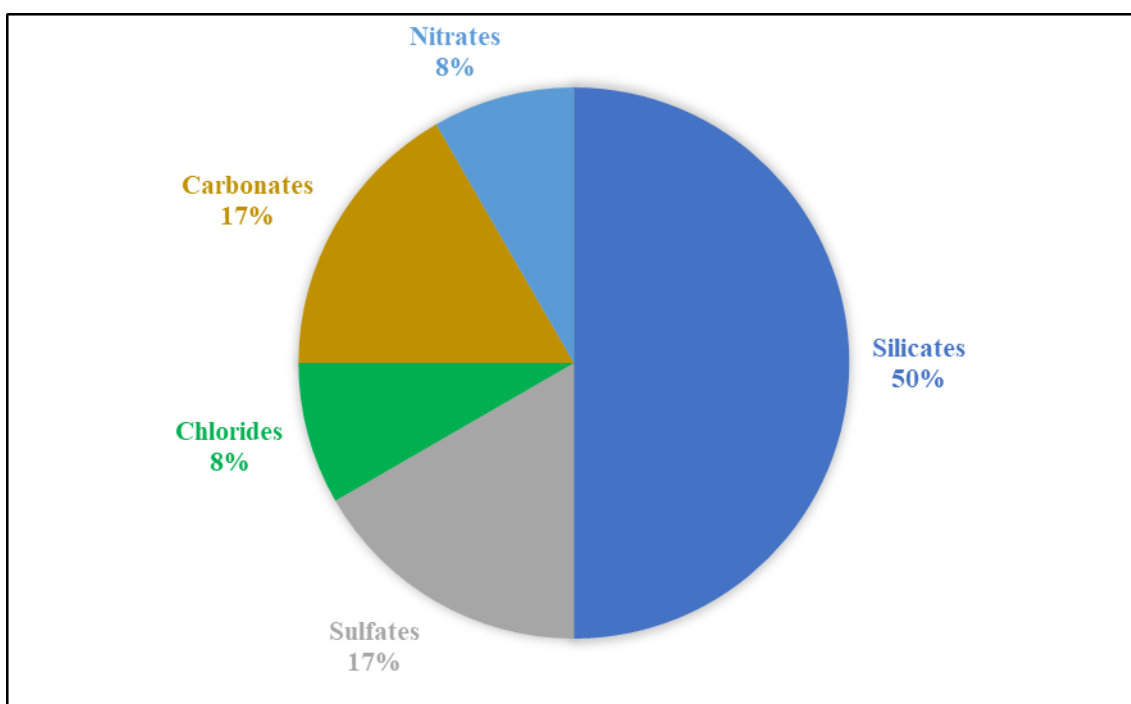


**Figure 20.** Percentage concentrations of functional chemical groups of 21 mineral phases within the T23P26 - medium. Considering the silicate groups as the main chemical functional group of the whole tola samples, but the main chemical functional groups for the salts are carbonate and sulfates.

#### 4.4.1 Second methodology: Salt extraction

One tola was randomly selected from the 24 Tola samples in this method. From the results obtained during various salt extraction processes and using X-ray diffraction equipment, the majority and minority phases were identified from the intensity of the

peaks in the diffractogram pattern. The semi-quantitative analysis was developed by XRD diffractogram for T16P19-Top Salts (Fig 21). Through this method, it is possible to identify the majority and minority phase intensity of the peaks. So, the following is detailed; the most intense peak is located at  $2\theta = 31.71^\circ$ ,  $45.44^\circ$ ,  $56.46^\circ$ ,  $75.29^\circ$  and  $83.98^\circ$  which corresponds to halite mineral. In addition, the peaks of highest intensity for nitratine are represent at  $2\theta = 29.37^\circ$ ,  $38.96^\circ$  and  $47.92^\circ$ . Besides, a peak was observed at  $2\theta = 25.42^\circ$  representing calcite. Finally, a peak at  $2\theta = 31.35^\circ$  was identified that represents syngenite.

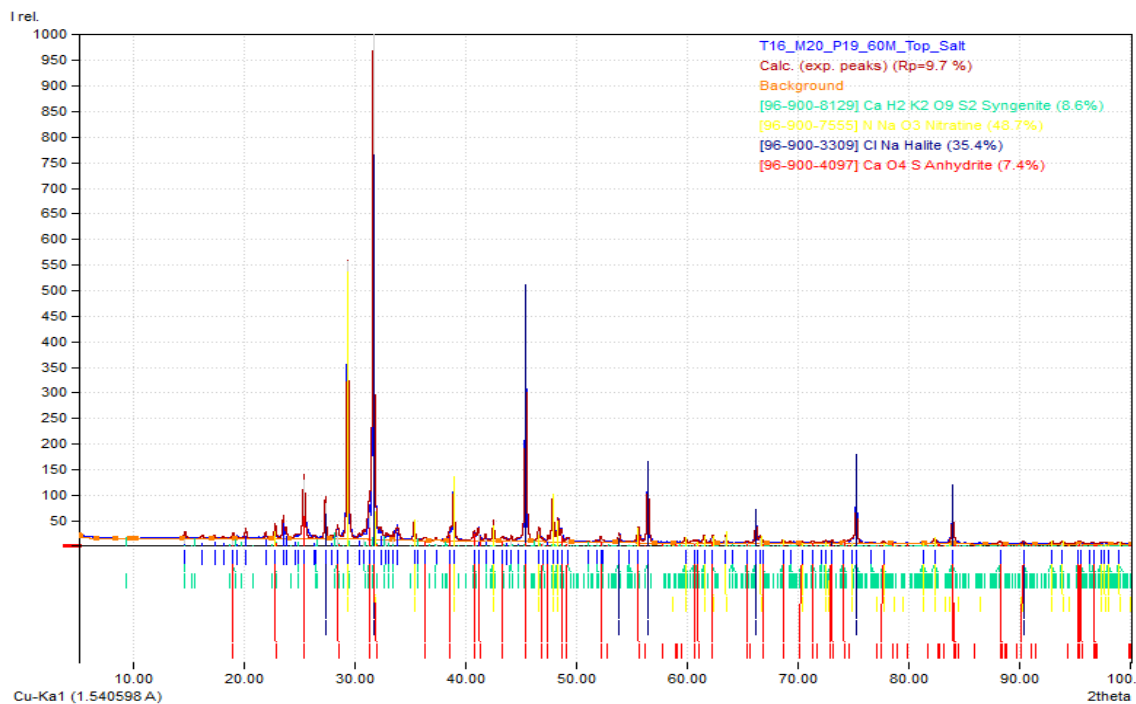


**Figure 21.** Diffractogram determined with the XRD pattern of the T16M20P19-60M- Top sample. It can be observed that the presence of the highest intensity peaks of the minerals, such as syngenite, nitratine, halite, and anhydrite.

Twenty-seven mineral phases were recorded from the six fractions, some repeated in other grain size fractions and Tolas. These are classified into different chemical functional groups within the salts (Table 15). In addition, the identified minerals have the entry code for each mineral to more quickly determine the same mineral for each Tola in the Match program. In this Tola, more abundant salt minerals such as thenardite, calcite, barrerite, gypsum, halite, syngenite, and nitratine are related to the other Tola samples analyzed.

**Table 15.** General detail of the mineral phases detected in the T23P26-Medium sample divided into each granulometric fraction.

Mesh size	Entry #	Formula	Mineral phase	Phase composition (%)	Chemical functional group	Lithic fragments	Rocks or associated minerals
10	96-900-7555	NaNO <sub>3</sub>	Nitratine	47.9	Nitrates	Surficial deposits	Niter/Anhydrite
	96-900-3309	NaCl	Halite	47.5	Chlorides	Sedimentary deposits	Salt beds/salt domes
	96-900-4097	CaSO <sub>4</sub>	Anhydrite	2.3	Sulfates	Evaporite deposits	Salt domes
	96-900-4093	Na <sub>2</sub> SO <sub>4</sub>	Thenardite	2.2	Sulfates	Volcanic fumarole	Mirabilite
18	96-900-7555	NaNO <sub>3</sub>	Nitratine	40.3	Nitrates	Surficial deposits	Niter/Anhydrite
	96-900-3309	NaCl	Halite	36	Chlorides	Sedimentary deposits	Salt beds/salt domes
	96-901-2211	Ca(SO <sub>4</sub> ) · 0.5H <sub>2</sub> O	Bassanite	22.2	Sulfates	Volcanic rock	Leucite/Tephrite blocks
	96-901-3166	CaSO <sub>4</sub> · 2H <sub>2</sub> O	Gypsum	1.5	Sulfates	Fumarole/evaporite	Brushite/Limestone
35	96-900-3309	NaCl	Halite	44.7	Chlorides	Sedimentary deposit	Salt beds/salt domes
	96-900-7555	NaNO <sub>3</sub>	Nitratine	27	Nitrates	Surficial deposits	Niter/Anhydrite
	96-901-2211	Ca(SO <sub>4</sub> ) · 0.5H <sub>2</sub> O	Bassanite	26.4	Sulfates	Volcanic rock	Leucite/Tephrite blocks
	96-900-4093	Na <sub>2</sub> SO <sub>4</sub>	Thenardite	1.8	Sulfates	Volcanic fumarole	Mirabilite
60	96-900-7555	NaNO <sub>3</sub>	Nitratine	48.7	Nitrates	Surficial deposits	Niter/Anhydrite
	96-900-3309	NaCl	Halite	35.4	Chlorides	Sedimentary deposit	Salt beds/salt domes
	96-900-8129	K <sub>2</sub> Ca(SO <sub>4</sub> ) <sub>2</sub> · H <sub>2</sub> O	Syngenite	8.6	Sulfates	Volcanic rock	Halite/Uricite
	96-900-4097	CaSO <sub>4</sub>	Anhydrite	7.4	Sulfates	Evaporite deposit	Salt domes
120	96-900-7555	NaNO <sub>3</sub>	Nitratine	44.5	Nitrates	Surficial deposits	Niter/Anhydrite
	96-900-3309	NaCl	Halite	34.2	Chlorides	Sedimentary deposit	Salt beds/salt domes
	96-901-2211	Ca(SO <sub>4</sub> ) · 0.5H <sub>2</sub> O	Bassanite	9.5	Sulfates	Volcanic rock	Leucite/Tephrite blocks
	96-900-8129	K <sub>2</sub> Ca(SO <sub>4</sub> ) <sub>2</sub> · H <sub>2</sub> O	Syngenite	6.8	Sulfates	Volcanic rock	Halite/Uricite
	96-901-3166	CaSO <sub>4</sub> · 2H <sub>2</sub> O	Gypsum	5	Sulfates	Fumarole/evaporite	Brushite/Limestone
230	96-900-4097	CaSO <sub>4</sub>	Anhydrite	40.4	Sulfates	Evaporite deposit	Salt domes
	96-901-3166	CaSO <sub>4</sub> · 2H <sub>2</sub> O	Gypsum	24.3	Sulfates	Fumarole/evaporite	Brushite/Limestone
	96-900-7555	NaNO <sub>3</sub>	Nitratine	12.2	Nitrates	Surficial deposits	Niter/Anhydrite
	96-900-1298	CaCO <sub>3</sub>	Calcite	11.3	Carbonates	All environment	Limestone/Carbonatites
	96-900-3309	NaCl	Halite	8.8	Chlorides	Sedimentary deposit	Salt beds/salt domes
	96-900-3137	KCl	Sylvite	2.9	Chlorides	Evaporite deposit	Salt beds/ fumaroles

The mineral phase composition represents in all six-grain size fractions ranging from 10 (2mm) to 230 (0.063mm) mesh (Figure 22). The following percentages constitute the minerals with the highest concentration in all granulometric fractions; nitratine, 48.7%, and halite, 47.5%, are found in the 60 (0.063mm) and 10 (2mm) mesh sizes. In the same context, the minerals are divided into fractions 10 (2mm), nitratine (47.9%), halite (47.5%), anhydrite (2.3%), and thenardite (2.2%). In fraction 18 (1mm), nitratine (40.3%), halite (36%), bassanite (22.2%), and gypsum (1.5%). In fraction 35 (0.5mm), halite (44.7%), nitratine (27%), bassanite (26.4%), and thenardite (1.8%) are present. In fraction 60 (0.25mm), there is the highest concentration mineral identified in the peaks of the more excellent range, such as nitratine (48.7%), halite (35.4%), syngenite (8.6%) and anhydrite (7.4%). In fraction 120 (0.125mm), nitratine (44.5%), halite (34.2%), bassanite (9.5%), syngenite (6.8%), and gypsum (5%) are present. In fraction 230 (0.063mm), anhydrite (40.4%), gypsum (24.3%), nitratine (12.2%), calcite (11.3%), halite (8.8%), and sylvite (2.9%) are present. Additionally, these mineral phase composition results are unidentified in other sample fractions for each Tola, as is the case of thenardite, which is visualized in Tolas 4,6,13, 20, 23 and salt crusts.

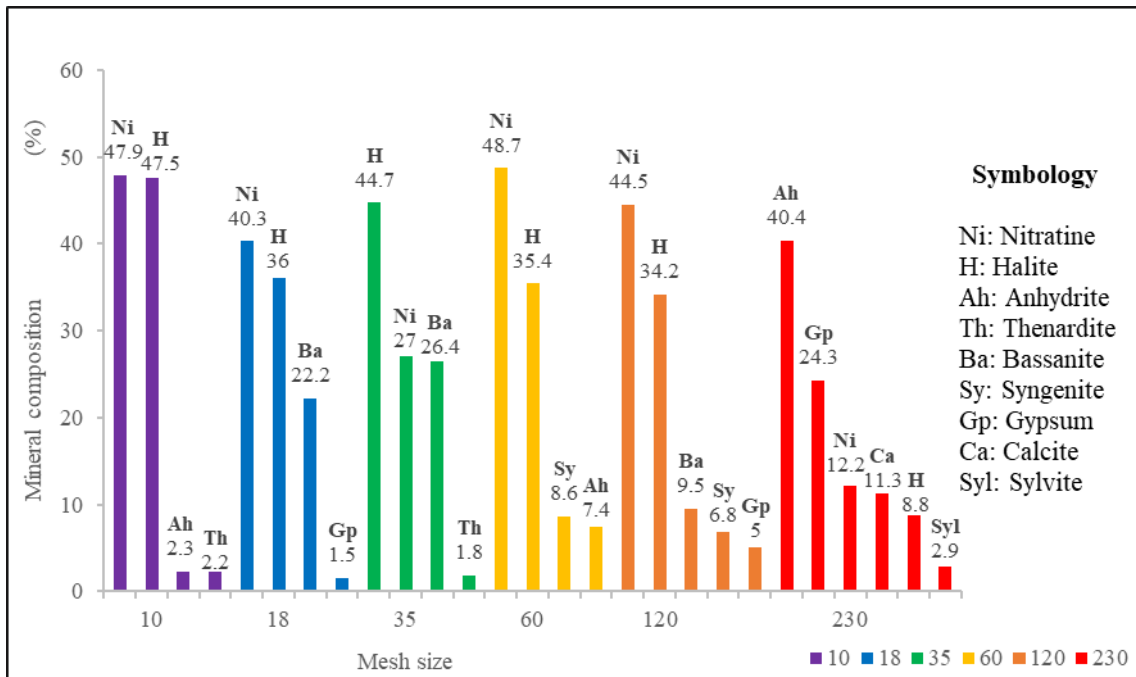


**Figure 22.** Represents the percentages of mineral phase composition versus sieve mesh size classification. In addition, twenty-seven mineral phases were identified by X-ray diffraction analysis (XRD). The studied samples were extracted by the salt leaching process in saline soils.

The chemical functional groups in this Tola sample include sulfates, carbonates, chlorides, and nitrates. In these samples, the chemical group with the highest concentration is; sulfates, with 60%, containing five mineral phases. Then, the chloride group follows this with 20% and two mineral phases. Finally, the group of nitrates and carbonates have the same percentage of 10%, which identified one mineral phase (Figure 23). These minerals of the salts group can be identified and related to results from other Tolas, such as Tolas 1, 4, 6, 9, 13, 20, 23, and salts crusts.

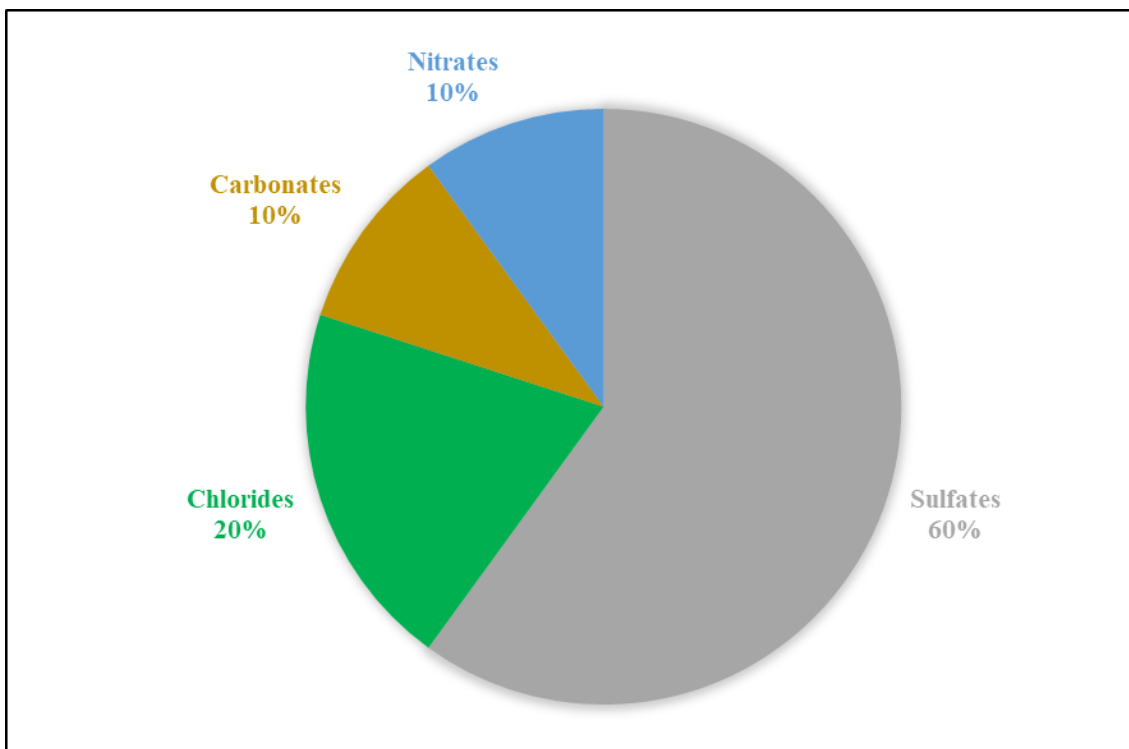


**Figure 23.** Percentage concentrations of functional chemical groups of 27 mineral phases within the T16P19 – top salt. Considering the main chemical functional group for the salts are found as sulfates, chlorides, carbonates and nitrates.

#### 4.4.2 Salt Crusts Samples

The salt crust samples were collected in the different outcrops, tolas, and springs to carry out semiquantitative analysis by XRD later. The diffractograms pattern represents the majority and minority phases of the intensity of the peaks; the semiquantitative analysis by XRD diffractogram for M4P4 Salts. Through this, the diffractogram identifies the majority and minority phase intensity of the peaks (Figure 24). Besides, the following is detailed; the most intense peak is located at  $2\theta = 27.78^\circ$ ,  $21.97^\circ$  and  $23.74^\circ$  which corresponds to Albite mineral. In addition, the highest intensity peaks for the ezcurrite are represented at  $2\theta = 28.87^\circ$  and  $34.72^\circ$ . Also, several prominent peaks were identified at

$2\theta = 33.88^\circ$ ,  $32.10^\circ$ ,  $19.03^\circ$  and  $42.82^\circ$ , which represents thenardite. Finally, two peaks were observed at  $2\theta = 41.19^\circ$  and  $29.02^\circ$  representing sylvite.

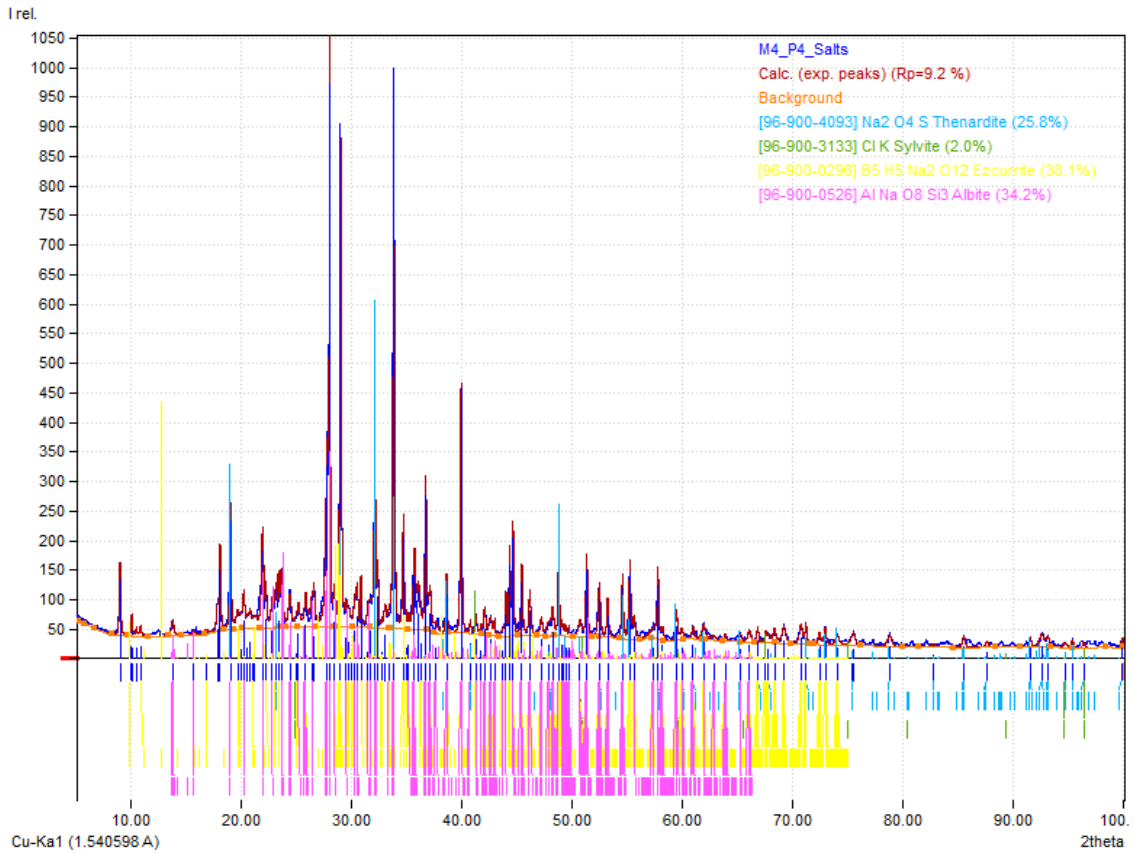


**Figure 24.** Diffractogram determined with the XRD pattern of the M4P4 Salts samples. It can be observed that the presence of the highest intensity peaks of the minerals, such as thenardite, sylvite, ezcurrite, and albite.

Twenty-one mineral phases were identified, some repeated in other samples of salts and crusts. The lithic fragments vary their possible environment of origin due to the presence of chemical functional groups for soluble salt minerals and solid minerals that could be found in weathered materials, geologic settings, or influenced by anthropogenic origin (Table 16). In this Tola, more abundant salt minerals such as thenardite, calcite, dolomite, sylvite, bassanite, halite, ezcurrite, and nitratine are related to the other Tola samples analyzed.



**Table 16.** General detail of the mineral phases detected in the Crusts and salts samples divided into each granulometric fraction.

Mesh size	Entry #	Formula	Mineral phase	Phase composition (%)	Chemical functional group	Lithic fragments	Rocks or associated minerals
M3_P4 Crusts	96-900-4093	Na <sub>2</sub> SO <sub>4</sub>	Thenardite	54.5	Sulfates	Volcanic fumarole	Mirabilite
	96-900-1298	CaCO <sub>3</sub>	Calcite	22.3	Carbonates	All environment	Limestone/Marbles
	96-900-1031	(Na, Ca)[Al(Si,Al)Si <sub>2</sub> O <sub>8</sub> ]	Andesine	14	Silicates	Igneous rock	Diorites/Andesites
	96-900-7555	NaNO <sub>3</sub>	Nitratine	6.1	Nitrates	Surficial deposits	Niter/Anhydrite
	96-900-1420	CaMg (CO <sub>3</sub> ) <sub>2</sub>	Dolomite	3.1	Carbonates	All environment	Limestone/Marbles
M4_P4 Salts	96-900-0296	Na <sub>4</sub> B <sub>10</sub> O <sub>17</sub> · 7H <sub>2</sub> O	Ezcurrite	38	Borates	Folded playa deposit	Siltstones/Sandstones
	96-900-0526	Na (AlSi <sub>3</sub> O <sub>8</sub> )	Albite	34.2	Silicates	Igneous rock	Granites/Syenite
	96-900-4093	Na <sub>2</sub> SO <sub>4</sub>	Thenardite	25.8	Sulfates	Volcanic fumarole	Mirabilite
	96-900-3137	KCl	Sylvite	2	Chlorides	Evaporite deposit	Salt beds/ fumaroles
T6_M9_P9 Crusts	96-901-6407	α-Fe <sup>3+</sup> O(OH)	Goethite	64.5	Oxides	Weathering product	Diaspore/Basalt
	96-900-2319	Fe <sup>2+</sup> Fe <sup>3+</sup> <sub>2</sub> O <sub>4</sub>	Magnetite	34	Oxides	Igneous accessory	Chromite
	96-900-1470	MgFe <sup>3+</sup> <sub>2</sub> O <sub>4</sub>	Magnesioferrite	1.5	Oxides	Fumaroles	Gahnite/Hematite
M29_P29 Crusts	96-900-1259	Ca (Al <sub>2</sub> Si <sub>2</sub> O <sub>8</sub> )	Anorthite	38.1	Silicates	Plutonic rock	Datolite
	96-900-1298	CaCO <sub>3</sub>	Calcite	28.1	Carbonates	All environment	Limestone/Marbles
	96-900-0526	Na (AlSi <sub>3</sub> O <sub>8</sub> )	Albite	31.3	Silicates	Igneous rock	Granites/Syenite
	96-900-7555	NaNO <sub>3</sub>	Nitratine	2.3	Nitrates	Surficial deposits	Niter/Anhydrite
M30_P30 Pumice/salts	96-900-5023	SiO <sub>2</sub>	Quartz	34.9	Silicates	Igneous rock	Widespread
	96-901-3187	K(AlSi <sub>2</sub> O <sub>6</sub> )	Leucite	29.8	Silicates	Volcanic rock	Syenite/Trachyte
	96-900-1259	Ca (Al <sub>2</sub> Si <sub>2</sub> O <sub>8</sub> )	Anorthite	19.1	Silicates	Plutonic rock	Datolite
	96-901-1103	Na <sub>2</sub> CO <sub>3</sub> · 10H <sub>2</sub> O	Natron	11	Carbonates	Soda lakes	Trona/Gypsum
	96-901-2211	Ca (SO <sub>4</sub> ) · 0.5H <sub>2</sub> O	Bassanite	5.2	Sulfates	Volcanic rock	Leucite/Tephrite

*M3P4 Crusts* is registered in brown color where the phases of mineral composition were identified with the following percentages; the mineral that represents the highest intensity in the peaks is thenardite with 54.5 %, followed by calcite which has 22.4%, nitratine with 6.1% and dolomite with 3.1% (Figure 25).

*M4P4 Salts* is shown in gray color where the mineral composition phases are identified with the following percentages; the mineral with the highest intensity is ezcurrite at 38%, then, thenardite at 25.8 %, and sylvite at 2%.

*T6M10P9 Crusts* are present in red color in which the phases of mineral composition are found with the following percentages; the mineral with the highest intensity is goethite at 64.5%, followed by magnetite at 34% and magnesioferrite at 1.5%.

*M29P29 Crusts* represent yellow color in which the phases of mineral composition are identified with the following percentages; the mineral that represents the highest intensity in the peaks is calcite at 28.1%, and nitratine at 2.3 %.

*M30P30 Pumice/salts* are represented in light blue color in the bar column figures, where the phases of mineral composition are identified with the following percentages; the mineral that represents the highest intensity is quartz with 34.9%. Then, natron at 11%, and bassanite at 5.2% (Figure 25).

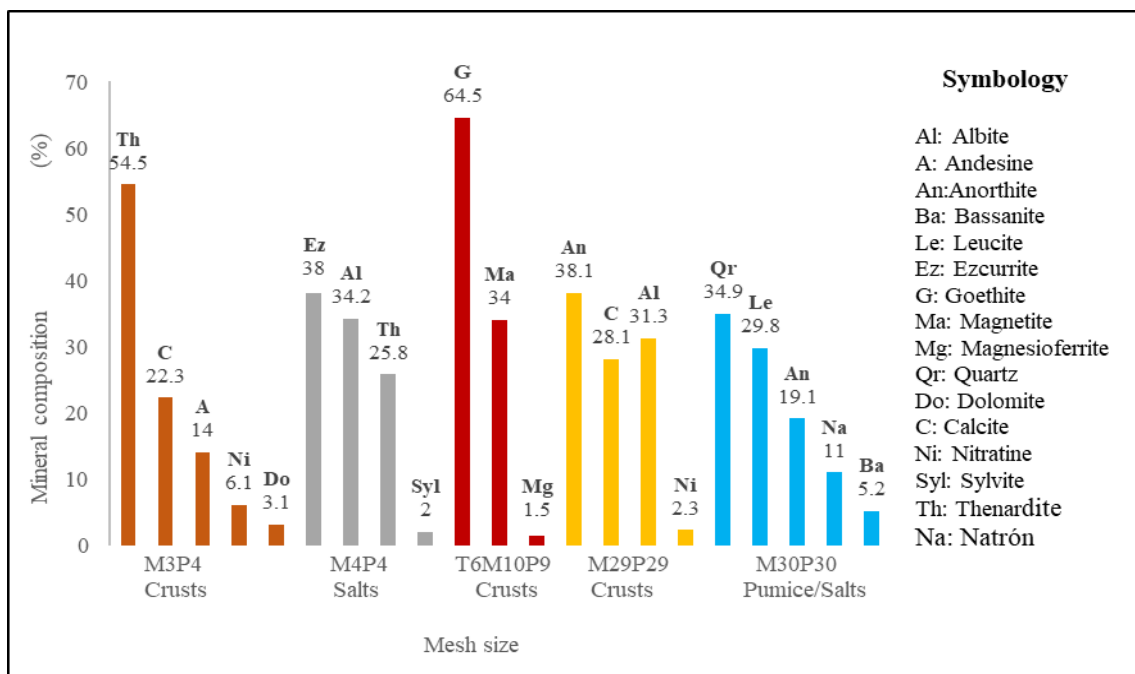


**Figure 25.** It represents the percentages of the mineral phases' composition identified with the samples of crusts and secondary salts. In addition, twenty-one mineral phases were identified by X-ray diffraction analysis (XRD). The studied samples were collected at different sampling points, such as in areas of Tolas and natural springs.

The chemical functional group is classified into groups of soluble salts such as sulfates, carbonates, nitrates, chlorides, and borates. In another part, these groups were divided into solid minerals containing another formation environment, such as silicates and oxides (Figure 26).

*In M3P4 Crust's samples*, five mineral phases are present and represent four functional groups such as; the most predominant chemical functional group is carbonate, with 40 %, and has two mineral phases. Then they are with a single mineral phase for sulfates, nitrates, and silicates and contain 20 % for all.

*M4P4 Salts samples*, four mineral phases are present and represent four functional groups where no chemical functional group predominates. However, all minerals are with a single mineral phase. The groups present in the samples are borates, sulfates, chlorides, and silicates, representing 25% of the total percentage.

*In T6M10P9 Crust's samples*, three different mineral phases are identified, but all of the same chemical functional group as oxide with 100%. These samples are oxides due to the presence of ferruginous crusts collected in high of the Tola 6.

*In M29P29 Crust's samples* are classified by several chemical functional groups such as silicates with 50%, nitrates, and carbonates with 25% each. The most predominant minerals are calcite and nitratine.

In the *M30P30 Pumice/Salts samples*, three different functional groups are recorded as silicates with 60%, and carbonate, and sulfates represent 20%. The most predominant minerals are natron and bassanite.

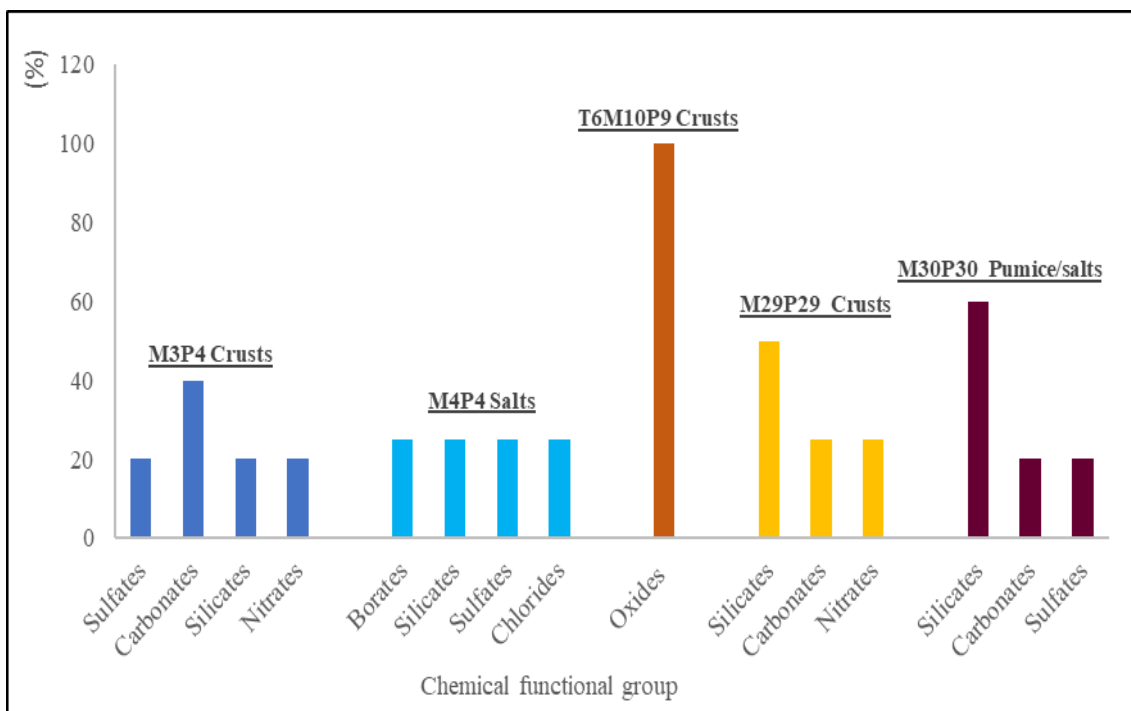


**Figure 26.** Represents the percentage concentrations of chemical functional groups of 21 mineral phases in the Crusts and salts samples. Considering the main chemical functional groups are found as sulfates, carbonates, nitrates, borates, chlorides, silicates, and oxides.

## 4.5 Discussion

### 4.5.1 Salt deposits based on the stratigraphy of the area.

In the stratigraphic column, most materials of volcanoclastic origin were identified, such as volcanic breccias of coarse size in the lower level of the terrace. In the middle part, lenticular bodies of conglomerates were found due to channel filling; additionally, in the upper level, volcanic material was identified as andesitic lavas with pyroclastic material such as ash, tuff, and lapilli (see Figure 15). Therefore, the salt deposits identified in the study area are found in different geological units, such as; the highest concentration of salts in the Chachimbiro volcanic terraces and eruptive event 2 (CH-2). In this unit, most samples were collected from Tola 2 to 24. The chemical functional groups identified are sulfates and carbonates, especially thenardite and calcite minerals (Table 17). Then, there is part of the Yanahurco volcanic collapse (Yh-V); in this unit, some samples were collected from Tola 1 and salt crusts that allowed us to identify mainly borates and sulfates; the minerals identified are sassolite, gowerite, and

calciolangbeinite (Tables 16 and 17). Finally, samples of salt crusts (M3P4, M4P4, M29P29, and M30P30) were collected in the alluvial depositional units, volcanic breccias, and some parts of the Cangahua unit. These units mainly identified sulfates, borates, carbonates, nitrates, and chlorides, especially thenardite, calcite, natron, nitrates, ezcurrite, and sylvite minerals (Tables 16 and 17).

On the other hand, the entire study area is formed by terraces of alluvial deposits from the erosion of volcanoclastic materials. Additionally, in the geologic context, the most representative units in the area are volcanic breccias, undefended terraces composed of volcanic material from the Chachimbiro 2 (CH-2) event and Yanahurco volcanic, as well as part of the Cangahua unit (Figure 29). Thus, these identified units are related to the study conducted by the National Institute of Meteorology and Hydrology (2015) mentions that the units present in Santa Catalina de Salinas are formed by terraces of alluvial deposits of volcanic origin with the lavas, tuffs, volcanic breccias of various sizes and Cangahua unit.

In this same context, the materials identified result from the collapse of the Chachimbiro volcanic edifices, eruptive event 2 (see Figure 29). This eruptive event (CH-2) consists of the formation of a second unit Tumbatú which are covered much of the east and northwest areas such as Cahuasquí, Tumbabiro, Urcuquí, and part of Santa Catalina de Salinas (Andrade et al., 2010; Bernard et al., 2011). This eruptive event occurred in two periods; the first is characterized by the extraction of dacitic domes that exploded pyroclastic flows of ash and blocks. The second period had more acidic lava flows with pyroclastic ash and pumice material (Bernard et al., 2011). Finally, in the parish, salt exploitation is not sea salt or rock salt but salt that permeates the valley floor and water systems, which are also associated with volcanic materials, climatic conditions, and soil salinity (Caillavet, 2000).

#### **4.5.2 Granulometric fractions**

Six fractions were identified in all the tolas, which the most representative fractions, according to the sample weight of all 24 tolas, are concentrated in fraction 35 (0.5mm), fraction 60 (0.25mm), and fraction 120 (0.125mm) (see Figure 16). However, the eight randomly selected Tolas are also concentrated in some of the abovementioned fractions 18, 35, 60, and 120. The most repeated grain size fractions are as follows (Figure

16); Fraction 35 is concentrated in T1, T4, T6, T16, and T23. On the other hand, in fraction 120, the chemical functional group such as sulfate, carbonate, and borates (Table 15 and 16) are concentrated and repeated in T4, T6, T9, T13, T20, T16, and T23. This fraction has a sediment size classification of 0.125mm and represents fine sand clasts. In fraction 230, mineral composition phases predominate in the T9, T13, T23, and T16 (Figure 16). The particle size classification is 0.063mm, corresponding to the limit between the very fine sand and coarse silt size clasts.

Finally, the classification of the granulometric scale shows that the studied samples are within the range of coarse sand to coarse silt clasts. Therefore, the classification of volcanoclastic deposits mentions that the ash-type fragments could be classified from coarse to fine clasts (Murcia et al., 2013). Consequently, the fractions samples obtained are secondary volcanoclastic deposits from undifferentiated debris avalanches and pyroclastic flows of the CH-2 eruptive phase (Chachimbiro volcanic; see Figure 29). This process is also associated with gravitational action or water acting directly in removing and accumulating from a volcanic deposit to the lower zones as alluvial plains (Villagómez et al., 2011; Bellver-Baca et al., 2019).

#### **4.5.3 Mineral phase group of the samples**

The most common minerals are thenardite, syngenite, halite, calcite, dolomite, berlinite, nitratine, and sassolite. These minerals form part of the following chemical functional groups found in the samples: sulfates, carbonates, chlorides, borates, nitrates, and phosphates, which behave differently in the natural environment. So, these samples are soluble salt minerals of sediments (Table 17). In addition, no clear pattern of some mineral phases was found for the distribution of all minerals in each Tola and fraction. However, X-ray diffraction analysis was possible to recognize some patterns of mineral composition phases that are repeated among some Tolas and fractions. Next, we propose a table identifying the X-ray diffraction patterns with their respective mineral phase composition and chemical functional group of all the analyzed samples (see Table 17).

**Table 17.** The most predominant compositional phase per semi-quantitative XRD analysis. The most common functional groups are sulfate, carbonate, and borates. The most predominant minerals are thenardite, calcite, calciolangbeinite, sassolite, and gypsum. These minerals represent the soluble salts in the study area.

Chemical functional group	T1P3	T4P7	T6P9	T9P12	T1316	T20P23	T23P26	T16P19 Salts	T16P19 Sediments	Crusts and Salts
	Mineral phases									
Sulfates	Ca	Th	Th	Sy	Sy	Ca	Th	Ah	-	Th
	-	Ep	Ca	Gp	Th	Th	Ca	Sy	-	Ba
	-	-	-	-	-	-	-	Th	-	-
	-	-	-	-	-	-	-	Ba	-	-
	-	-	-	-	-	-	-	Gp	-	-
Carbonates	-	C	-	C	-	C	C	C	-	Do
	-	-	-	-	-	-	Do	-	-	C
	-	-	-	-	-	-	-	-	-	Na
Chlorides	-	-	-	H	-	-	H	H	-	Syl
	-	-	-	-	-	-	-	Syl	-	-
Phosphates	B	B	Fl	B	B	B	-	-	B	-
	-	-	B	-	-	-	-	-	-	-
Borates	Sa	-	-	-	Sa	-	-	-	Sa	Ez
	Go	-	-	-	-	-	-	-	-	-
Nitrates	-	-	-	Ni	-	N	Ni	Ni		Ni
Silicates	Al	Al	La	Al	A	Al	Bv	-	Al	Qrz
	A	A	Qrz	Anr	Cr	A	A	-	A	A
	La	Cr	A	A	Qrz	La	La	-	La	Al
	An	E	Le	Tr	Le	Qrz	An	-	Le	An
	Le	Tr	Al	Ka	Al	Cr	Qrz	-	Tr	Le

**Mineral Phase Symbology:** Ca: Calciolangbeinite, Th: Thenardite, Sy: Syngenite, H: Halite, Syl: Sylvite, C: Calcite, Ah: Anhydrite, Gp: Gypsum, Ep: Epsomite, Ba: Bassanite, Na: Natrón; Do: Dolomite, Ez: Ezcurreite, Sa: Sassolite, Go: Gowerite, B: Berlinite, Fl: Fluorapatite, Ni: Nitratine, N: Nitrocalcite, Al: Albite, A: Andesine, Bv: Bavenite, An: Anorthite, La: Labradorite, Tr: Tridymite, Qrz: Quartz, Cr: Cristobalite, Le: Leucite, E: Enstatite, Ka: Kalsilite, Anr: Anorthoclase, Bo: Boehmite.

On the other hand, the presence of salts in the area of Santa Catalina de Salinas occurs because it is made up of cations (+) sodium, calcium, and magnesium, and anions (-) chloride, sulfate, and carbonate and in some cases nitrate and borate (Figure 2). In this area, there is the presence of saline soils due to the accumulation of soluble salts on the surface, which are formed by the evaporation of groundwater or aquifers where they accumulate in a shallow phreatic layer to later rise by capillarity to the soil surface, forming white salt crusts (Grumberger, 1995; Figure 27).



**Figure 27.** *The presence of soluble salt crusts on the surface is due to the capillarity process in areas with saline soils. This process can occur more frequently in dry precipitation due to the evaporation-transpiration of water to the surface. This saline soil is located in Tolas Zone (T17M21P20; see Figure 1B).*

To ratify the identification of saline soils and the possible origin of the salts deposit in the study area, we briefly explain the chemical functional groups identified in the X-ray diffraction data analysis (XRD). In the sulfate chemical functional group, it was identified that the most predominant mineral phase is thenardite, which is sodium sulfate. This mineral is found mainly in almost all the samples and fractions studied in the first method, such as T4, T6, T13, T20, and T23; in the second salt extraction method, thenardite is also found and additionally, in the samples of salts crusts. After this, we have the calciolangbeinite mineral in T1, T6, T20 and T23. This mineral is followed by syngenite found in T9, T13, and T16. Finally, we have in small concentrations the phases of minerals such as gypsum, which represents calcium sulfate hydrate in tola T9 and T16; epsomite, which is magnesium sulfate hydrate and is found in tola 4 (see Table 17). In addition, it is verified that there is a relationship between the mineral phases identified in the sediment samples without salt extraction and with the salt extraction sample (T16). The related minerals of the sulfate group are thenardite, syngenite, gypsum, and anhydrite.

Moreover, the dominant presence of thenardite is found as soluble salt and is transported and dissolved in water. Thenardite has a rhombic structure in the presence of



white to colorless color and can be generated in salt flats or volcanic exhalations (Zappettini et al., 2003). Thenardite can be a primary or secondary mineral. However, this study is a sample of a secondary mineral because it can be transformed from other minerals during diagenesis, as in the case of mirabilite (Last, 1994). On the other hand, a higher concentration of the thenardite mineral phase allows us to identify whether the area is saline soil. The sulfate group is constituted by the thenardite mineral that, according to micromorphological investigations, is frequently identified during saline soils in mineral salts and salt crusts (Mees & Tursina, 2018).

In the carbonate chemical functional group shows that three minerals were identified as Calcite, a Calcium Magnesium Carbonate and the most predominant in samples T4, T9, T20, T23, T16, M3P4 crusts, M29P29 pumice/salts, and M30P30 pumice/salts (Table 17). Then, the dolomite mineral representing Calcite magnesian Magnesium was found in samples T23 and M3P4 crusts. Finally, the mineral natron was identified in one of the samples of salts and pumice (M30P30). Compared with the second salt extraction method (T16) and the other samples analyzed, there is a relationship between the identified mineral phase composition, mainly, calcite mineral. In this same context, calcite originates in specific environments such as caves and some rare carbonate-rich igneous rocks but is mainly common due to weathering (Perkins, 2014). According to Grumberger (1995), in natural springs associated with the neo-volcanic in the zone of Mexico, in the State of Texcoco, salts are generated from groups of sodium carbonates and sodium chlorides such as the minerals natron, trona, and thermonatrite where deeper salty layers concentrated the salts due to past evaporation that was exposed on the surface of the soil by erosion influenced by temperature and CO<sub>2</sub> pressure, through a continental cycle. Therefore, we have a mineral identified as Natron found in one of the salt samples with pumice material (M30/P30), collected in natural springs. This result allows us to verify that the salt samples collected in the study area are influenced by the evaporation of water springs, which could be generated by continental origin associated with volcanism.

The chloride chemical functional group shows two mineral phases composition as Halite, a natural sodium chloride, also known as salt rock. This mineral is the most predominant in this chemical group which is found in samples T9, T23, and T16 (Table 17). Then, sylvite is also part of the halide groups found in samples T16 and M4P4 Salts.

These two minerals are found in most of the fractions of the samples mentioned above. In addition, there is a relationship of the mineral halite between the first method of sample selection and the second method.

On the other hand, Halite (NaCl) is a rock salt with a cubic crystalline structure. Its possible origin is in specific saline environments, sedimentary beds, and salt domes (Zappettini et al., 2003). As deposits of volcanic gases, they are associated with minerals and salts such as gypsum, calcite, sylvite, and clay (Perkins, 2014). In addition, halite deposition can occur in a closed continental or marine basin. According to Henneberg et al., (2020), in the North German basin, they mention that rock salt (halite) is quite soluble in water and it was not only generated by marine environments yet, groundwater of continental origin, where it served as the primary source of the formation of halite.

Besides, groundwater has a high content of salts because in continental basins, the content of anion, chloride, and cation, sodium, is generated; however, if there is the presence of a higher concentration of sodium chloride (halite), the conditions would be due to sedimentation formations of marine origin Grumberger, (1995). Therefore, the results obtained in the study area show a lower concentration of sodium chlorides such as halite, which rules out the possibility that the salts were sedimented in a sedimentary environment occurring in the sea; on the contrary, it could be of continental origin. Finally, in the study area, there are natural and superficial springs that could be of continental origin or associated with human-made irrigation drainage.

In nitrates, the chemical functional group presented two nitrate minerals associated with the compound sodium nitrate (Nitratine) and nitrocalcite. The nitratine mineral comprises a Na<sup>+</sup> cation and a (NO<sub>3</sub>)<sup>-</sup> anion, the most predominant mineral in the following samples; T9, T16, T23, and M29P29 crusts (Table 17). Additionally, nitratine has a higher concentration in sample T16 and is found in all fractions from 10 to 230 mesh size. Nitratine is a soluble salt mineral because it is transported by water, and its processes are chemical. Then, the nitrocalcite is in sample T16, corresponding to the second method. Therefore, we can see if there is a relationship with the other samples without extracting the salt. According to Perkins (2014), nitratine is highly soluble in water; it can also be found in arid regions where it can be associated with other evaporite continental minerals, as is the case of niter (Saltpeter).

In the borate chemical functional group, there were three phases of minerals such as, sassolite, gowerite, and ezcurrite. The most predominant sassolite mineral was found in T1, T13, and M4P4 salts (Table 17). In this case, minerals of the borate group are related to the sediments left over from the salt extraction, as sassolite is above the other minerals mentioned above. To identify the possible origin of the environment where these minerals occur, for example, sassolite. So, this mineral can be found in evaporite or sublimate environments around hot springs and volcanic vents (Perkins, 2014). The salts of Andean origin are located in the Volcanic Arc (CVZ) of the Quaternary of the Antiplano-Puna, Argentina, which consists of a higher concentration of boratiferous sedimentation that makes the difference of saline environments in its formation with groups of minerals represented by carbonates (travertine), sulfates (Mirabilite, gypsum), borates (sassolite and borax) and chlorides (halite). This salt deposit has the highest concentration of the borates group, which refers to the chemical-evaporitic sedimentation of continental environments in arid or semi-arid zones associated with active volcanism, as considered by the facies analysis and the different salt deposition models in Andean basins (Alonso, 2006). Therefore, the salts of the Salinas, Ibarra parish are located within the Volcanic Arc called Inter-Andean Valley, where the formation of all groups of salts was identified and influenced by various volcanic and alluvial events.

The chemical functional group of phosphates is identified as two mineral phases: berlinite and fluorapatite. In this case, the mineral berlinite was found in most of the samples, except for the T23 and T16 salts and in the granulometric fractions that vary according to the classification from fine sand to coarse silt (Table 17 and Figure 16). Then, we have the fluorapatite mineral found in Tola 6. In this case, the minerals of the phosphate group are related to the sediments left over from salt extraction, such as berlinite, which is above the fluorapatite. In this same context, the occurrence of the mineral berlinite is considered a rare high-temperature hydrothermal or metasomatic mineral where it would be associated with a cave in compacted phosphate-bearing clay sediments (Mineralogical Society of America, 2021).

Finally, we can find the chemical functional group of the salt samples analyzed by semi-quantitative XRD is divided into different percentages, such as sulfates at 41%, carbonates at 19%, borates at 13%, and phosphates, nitrates, and chlorides at 9%. The

most predominant chemical groups are sulfates, carbonates, and borates, represented in red squares (see Figure 28).

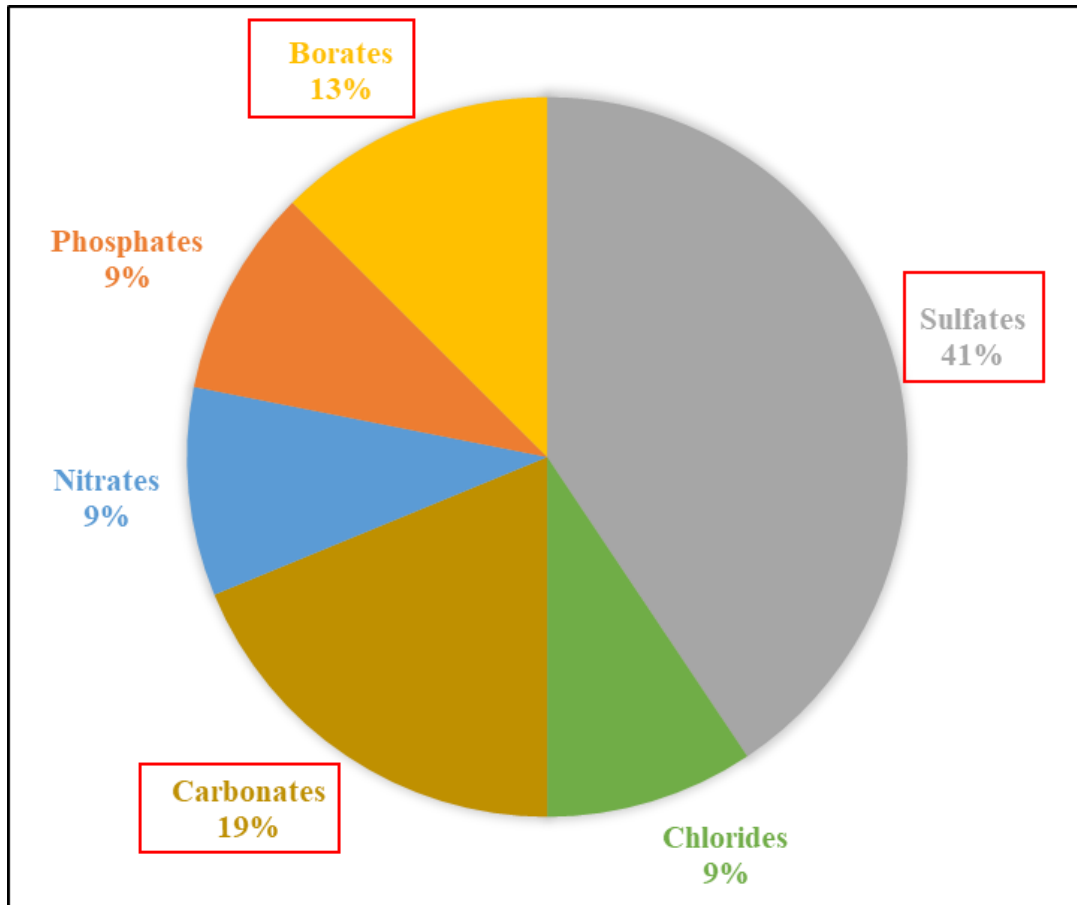


**Figure 28.** It represents the percentage of functional chemical concentrations of eight tolas and five salt crust samples. The main groups are sulfates, carbonates, and borates, marked in a red box because they are the most predominant in the area. Each group is represented by minerals such as thenardite, calcite, dolomite, and sassolite, identified semi-quantitatively by x-ray diffraction.

According to all the samples obtained as a result, we can see that there is a relationship between the phases of mineral composition in the chemical group of salts with the results of the research work of Gonzales (2021), which mentions that the most predominant minerals in the Santa Catalina de Salinas are composed of Halite, Nitratine, Gypsum, Calcite, Syngenite, and Anhydrite. These minerals were collected from tolas at the base, middle, and top heights and then analyzed by XRD diffractogram. Therefore, it can verify that the methods applied to obtain the mineral's phase composition are valid and agree with the results of Gonzalez.

Therefore, the knowledge of the origin of soluble salts deposit has been given throughout the different geological epochs where there have been exchanges of soluble

salts between oceanic and continental environments. The differentiation of soluble salts is provided by the degree of solubility so that an accumulation of chlorides is obtained in marine origin. At the same time, in continental zones, the domain belongs to sulfates and carbonates (Montañas, 1977). In this way, we can identify that the continental environment gives the origin of the soluble salts in Santa Catalina de Salinas because the samples studied have a higher concentration of soluble salts of sulfates and carbonates. The accumulation of soluble salts in the study area was generated by the movement of distribution and assembly, where the topography hinders drainage and has low permeability, especially throughout the parish. In addition, the salts found in the area are secondary minerals through saline sediments, the salinization cycle, associated with volcanoclastic deposits that release cations and anions during eruptive activity as in the case of eruptive phase 2 (CH-2) of the Chachimbiro volcano (see Figure 29).

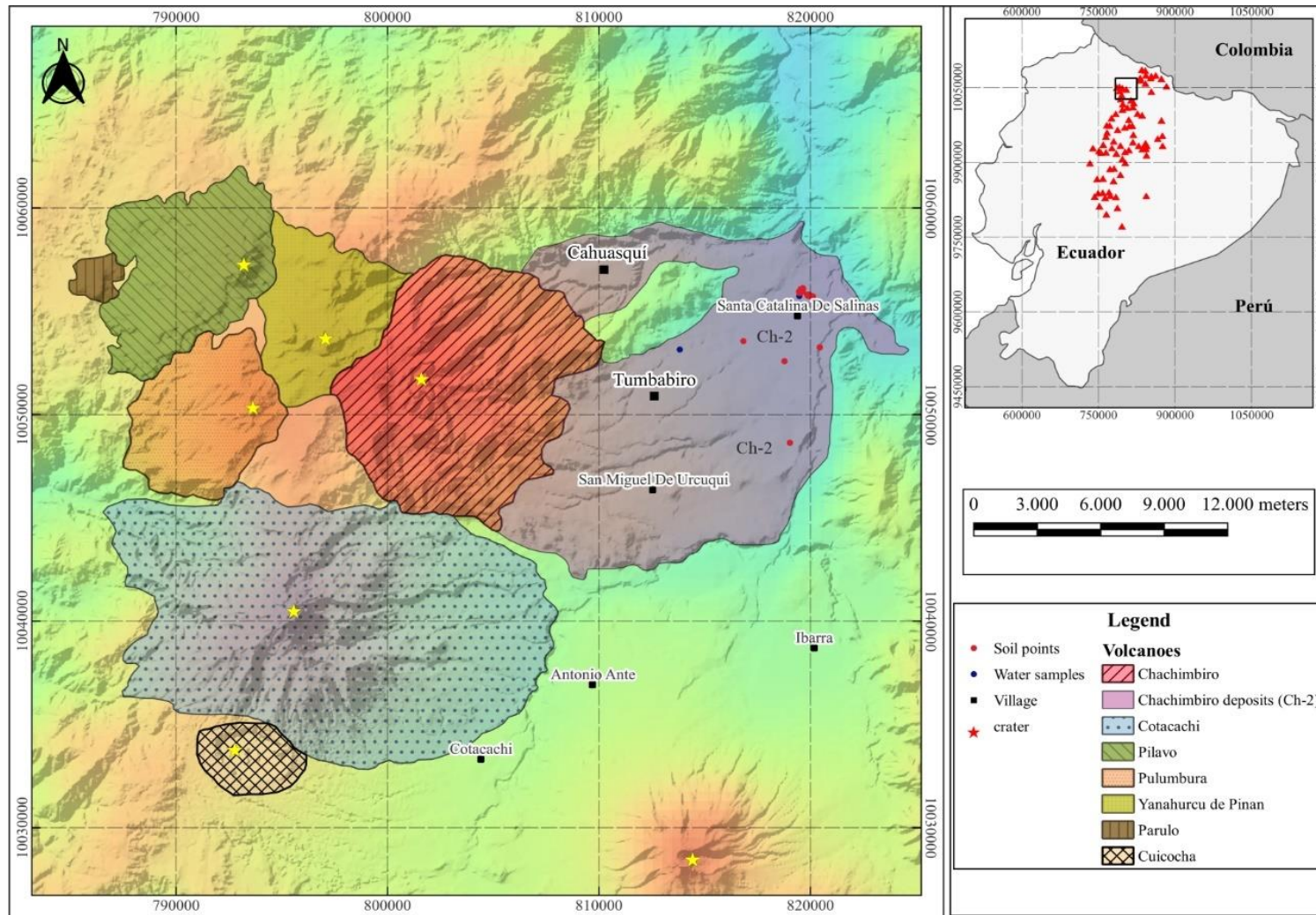


**Figure 29.** Geologic map of the different volcanic deposits, especially the Chachimburo volcano of the eruptive phase 2 (CH-2) and Yanahurco volcanic deposits. In the study area, it can be seen that there is a higher concentration of debris flow deposits due to the eruptive activity. The geomorphological formation of Santa Catalina is a plateau of volcanic deposits. The different samples collected in the area are within the CH-2 polygon. Modified from Bernard et al., 2011 and Bellver-Baca et al., 2019.

## **5. Chapter 5. Conclusions and Recommendation**

### **5.1 Conclusions**

- Santa Catalina de Salinas is located in the depression zone of the Quaternary Inter-Andean Valley in northern Ecuador. Our study was focused in the central and southwest area of the general polygon of the parish, where are located the greatest concentration of Tolas, salt crusts, and water samples from natural and superficial springs.
- Twenty-four tolas analyzed allowed us to identify, according to the granulometric classification, the most predominant of soil classification correspond to fraction 35, which is 0.5mm, fraction 60, 0.25mm, and fraction 120, which is 0.125. These fractions correspond to particles from coarse sand to fine silt. These materials proved to come from volcanoclastic deposits such as pyroclastic flows, especially of the ash type.
- This study analyzed 61 samples using X-ray diffraction; determining that the most predominant chemical functional group correspond to sulfates with 41% of presence, carbonates with 19%, and borates with 13%. Therefore, in sulfates, the most predominant mineral is thenardite, which is soluble salt found in higher concentrations in samples of tolas than in salt crusts. This mineral can crystalize in saline soils due to capillary processes on the soil surface.
- These group of salts such as sulfate, carbonate and borates, comes from continental origin due to the presence of volcanic materials, groundwater, precipitation, and humidity in the studied area's environment.
- The geological context related to the studied area and the analysis developed in this research allowed us to identify the concentrations of different groups of salts in the geologic units we can find in this area. Therefore, the salts predominating in the Santa Catalina de Salinas come from undifferentiated terraces constituted by Chachimbiro volcanic, phase 2 event (CH-2), and Yanahurco volcanic. These terraces resulted from the collapse of volcanic buildings through alluvial deposits, which represent in the lower part of the terrace presents brecciated material of coarse clasts and in the upper part the fine material of pyroclastic flows of volcanoclastic deposits.

- The most abundant chemical functional groups in the study area correspond to sulfates, carbonates, and borates, so the formation of salts in Santa Catalina de Salinas has a continental origin. The soluble salt deposits are associated with the climatic conditions, especially with semi-arid climates. In addition, the salt formation is associated with the weathering of secondary deposits related to volcanic events, since they reworked volcanic materials in the parish from the Chachimbiro and Yanahurco volcanoes.

## 5.2 Recommendations

- These results can help in efforts to limit soluble salt concentrations in a variety of scenarios, whether continental or anthropogenic origin, in order to identify what type of salts are present in the area and how this may affect water resources, agriculture, and human health. Therefore, to identify where there is a higher concentration of salts and how to remedy these negative effects on land use, it is recommended to analyze crops and the entire Santa Catalina de Salinas polygon.
- The water networks should be analyzed in detail to identify human consumption of natural springs.
- I recommend that this product be considered in the Imbabura Geopark within the Salinas-Lita geosite due to that the community can know the origins of the salt also, cultural and social heritage.
- I recommend analyzing the trace elements of the salts studied to determine if a concentration of components harms health outside acceptable limits.

## 6. References

- Alonso, R. N. (2006). Continental Evaporitic Environments of Argentina. *Serie Correlación Geológica*, 21(2), 155–170.
- Andrade, G., Carranco, A., Pachacama, F., & Rodriguez, O. (2012). Contributions to the Ibarra Geological Sheet Project: Salinas - LA Merced Scale 1: 50,000. 1–24.
- Barale, V., Grade, Martin. (2008). The European marginal and enclosed seas: an overview. *Remote sensing of the European seas*, 3-22.
- Béguelin, P., Chiaradia, M., Beate, B., & Spikings, R. (2015). The Yanaurcu volcano



- (Western Cordillera, Ecuador): A field, petrographic, geochemical, isotopic and geochronological study. *Lithos*, 218–219, 37–53. <https://doi.org/10.1016/j.lithos.2015.01.014>
- Bellver-Baca, M. T., Chiaradía, M., Beate, B., Beguelin, P., Deriaz, B., Mendez-Chazarra, N., & Villagómez, D. (2020). Geochemical evolution of the Quaternary Chachimbiro Volcanic Complex (frontal volcanic arc of Ecuador). *Lithos*, 356–357, 105237. <https://doi.org/10.1016/j.lithos.2019.105237>
- Benavente, D., Cañaveras, J. C., Martínez-martínez, J., Cervera, C. M., Ángel, M., & García, R. (2012). Identificación de minerales mediante difracción de rayos X utilizando bases de datos online de libre acceso. *Enseñanza de Las Ciencias de La Tierra*, 20(3), 280–289.
- Bernard, B., Robin, C., Beate, B., & Hidalgo, S. (2009). Nuevo modelo evolutivo y actividad reciente del volcán Chachimbiro. *December 2013*, 1988–1991.
- Betancourth, D., Gómez, J., Mosquera Julio César, & Tirado Mejía, L. (2010). X-ray Diffraction Analysis on Rocks from Emerald Mining Region. *Scientia et Technica*, 44, 257–260. <https://www.redalyc.org/pdf/849/84917316048.pdf>
- Bloch, M. R. (1976). Salt in human history. *Interdisciplinary Science Reviews*, 1(4), 336–352. <https://doi.org/10.1179/030801876789768282>
- Buder, T. A., Davis, J. G., & Waskom, R. M. (2014). Managing Saline Soils. *Colorado State University Extension, Fact Sheet 0.503*, 0, 5.
- Bukowski, K., & Czapowski, G. (2009). Salt geology and mining traditions: Kalush and Stebnyk mines (Fore-Carpathian region, Ukraine). *Geotourism/Geoturystyka*, 18(1), 27–34. <https://doi.org/10.7494/geotour.2009.18.3.27>
- Caillavet, C. (2000). La sal de Otavalo . Continuidades indígenas y ruturas coloniales. *Institut Francais Détudes Andines*, 1–36.
- Cevallos, M. (2015). Plan de Desarrollo y Ordenamiento Territorial de la Parroquial Rural “Santa Catalina de Salinas.” *Igarss 2014*, 1, 1–5.
- Chesworth, W. (2008). Encyclopedia of Soil Science. *Springer*, 33(4), 916. [https://doi.org/10.1007/978-1-4020-3995-9\\_140](https://doi.org/10.1007/978-1-4020-3995-9_140)
- Cirillo, Massimo; Capasso, Giovambattista; Leo, Vito Andrea Di; Santo, Natale Gaspare De (1994). A History of Salt. *American Journal of Nephrology*, 14(4-6), 426–431.
- Conant .J, F. . . (2012). A community guide to environmental health. In *Hesperian*. [https://en.hesperian.org/hhg/A\\_Community\\_Guide\\_to\\_Environmental\\_Health](https://en.hesperian.org/hhg/A_Community_Guide_to_Environmental_Health)
- Cosentino, N. J. (2018). Sr / 86 Sr en paleosuelos salinos como paleoaltímetro ; resultados

- preliminares para el norte de Chile ( 19-22 ° S ). *June*.
- Courel, G. (2019). Guia de estudio. Suelos Salinos y Sódicos. *Journal of Chemical Information and Modeling*, 53(9), 1689–1699. <https://webcache.googleusercontent.com/search?q=cache:bjR8L0Fx46AJ:https://www.edafologia.org/app/download/9026474176/Suelos%2BSalinos%2BBy%2Bs%25C3%25B3dicos%2B2019.pdf%3Ft%3D1563476239+&cd=1&hl=es-419&ct=clnk&gl=pe>
- Crespo, P., Célleri, R., Buytaert, W., Feyen, J., Iñiguez, V., Borja, P., & De Bievre, B. (2010). Land use change impacts on the hydrology of wet Andean páramo ecosystems. *IAHS-AISH Publication*, 336(April), 71–76. <https://doi.org/10.13140/2.1.5137.6320>
- Cuello, C. (2009). La industria salinera de la Península Ibérica crea el instituto de la sal. *Instituto de La Sal*.
- Doehne, E., The EU-China Energy and Environment programme, Okrusch, M., Frimmel, E. H., Henneberg, M., Linckens, J., Schramm, M., Hammer, J., Gerdes, A., Zulauf, G., Zappettini, E., Celeda, A., Pinto, A., Murcia, H. F., Borrero, C. A., Pardo, N., Alvarado, G. E., Arnosio, M., Scolamacchia, T., ... Czapowski, G. (2009). Salt Production - A reference book for the industry *Salt. Lithos*, 4(1), 29. <https://doi.org/10.1107/S1600576716010451>
- Donoso, E. (2012). Análisis del sistema ambiental según la metodología de SENPLADES, como aporte a la planificación y ordenamiento territorial del cantón Ibarra. *In Pontificia Universidad Católica del Ecuador Sede Ibarra*.
- Durack, E., Alonso-Gomez, Mercedes, & Wilkinson, M. G. (2008). Salt: A Review of its Role in Food Science and Public Health. *Current Nutrition & Food Science*, 4, 290–297.
- Fernandez, N., Duffy, O. B., Hudec, M. R., Martin P.A, J., Burg, G., Jackson, C. A. L., & Dooley, T. P. (2017). The origin of salt-encased sediment packages: Observations from the SE Precaspian Basin (Kazakhstan). *Journal of Structural Geology*, 97, 237–256. <https://doi.org/10.1016/j.jsg.2017.01.008>
- Flores, A. (1991). Suelos salinos y sodicos. *Journal of Property Research*, 32.
- Franzosi, C., & Montagna, S. (2007). Mercado y yacimientos de Nitratos.
- Garcia, J. R. (2020). Actualización del Plan de Desarrollo y Ordenamiento Territorial del Gobierno Autonomo Descentralizado Parroquial Rural de Santa Catalina de Salinas. *Gobierno Autónomo Descentralizado Parroquia Rural de Santa Catalina de*

*Salinas*, 112.

- Grumberger, O. (1995). *Los Tipos De Yacimientos De Sales En México Y Las Propiedades Químicas Que Influyen en la producción*.
- Henneberg, M., Linckens, J., Schramm, M., Hammer, J., Gerdes, A., & Zulauf, G. (2020). Structural evolution of continental and marine Permian rock salt of the North German Basin: constraints from microfabrics, geochemistry and U–Pb ages. *International Journal of Earth Sciences*, 109(7), 2369–2387. <https://doi.org/10.1007/s00531-020-01905-w>
- Herczeg, A. L., Dogramaci, S. S., & Leaney, F. W. J. (2001). Origin of dissolved salts in a large, semi-arid groundwater system: Murray Basin, Australia. *Marine and Freshwater Research*, 52(1), 41–52. <https://doi.org/10.1071/MF00040>
- Huerta, P., Armenteros, I., Recio, C., Carrasco-García, P., Rueda-Gualdrón, C., & Cidón-Trigo, A. (2021). The origin of the saline waters in the Villafáfila lakes (NW Spain). A hydrogeological, hydrochemical, and geophysical approach. *Science of the Total Environment*, 789. <https://doi.org/10.1016/j.scitotenv.2021.147909>
- Huggett, R. J. (2011). Fundamentals of Geomorphology. In *Fundamentals of Geomorphology*. <https://doi.org/10.4324/9780203860083>
- Hungerbühler, D., Steinmann, M., Winkler, W., Seward, D., Egüez, A., Peterson, D. E., Helg, U., & Hammer, C. (2002). Neogene stratigraphy and Andean geodynamics of southern Ecuador. *Earth-Science Reviews*, 57(1–2), 75–124. [https://doi.org/10.1016/S0012-8252\(01\)00071-X](https://doi.org/10.1016/S0012-8252(01)00071-X)
- Ibañez, C., Palomeque, S., & Fontúrbel, F. (2004). Elementos principales del suelo, geodinámica y dinámica de los principales componentes del suelo. *Isbn*, 99905–0.
- Iowa Department of Natural Resources. (2009). *Water Quality Standards Review: Chloride, Sulfate, and Total Dissolved Solids*. 79. [https://www.dnr.iowa.gov/~/media/2012/04/alpha\\_nt\\_cwq-assessment\\_minerals\\_papers\\_lit\\_studies\\_iowa](https://www.dnr.iowa.gov/~/media/2012/04/alpha_nt_cwq-assessment_minerals_papers_lit_studies_iowa)
- Jiang, X., Liu, C., Hu, Y., Shao, K., Tang, X., Gao, G., & Qin, B. (2022). Salinity-Linked Denitrification Potential in Endorheic Lake Bosten (China) and Its Sensitivity to Climate Change. *Frontiers in microbiology*, 13, 922546. <https://doi.org/10.3389/fmicb.2022.922546>
- Justo, Á., & Morillo, E. (1999). Técnicas de difracción de rayos X para la identificación cualitativa y cuantitativa de minerales de la arcilla. *Ciencia y Tecnología de Materiales*, 2, 77–86. [http://digital.csic.es/bitstream/10261/79501/4/Técnicas de difracción de rayos X.pdf](http://digital.csic.es/bitstream/10261/79501/4/Técnicas%20de%20difracción%20de%20rayos%20X.pdf)

- Kurlansky, M. (2011). Salt. Random House. Retrieved from <https://books.google.es/books?id=YbT64n3wYhoC&lpg=PA22&ots=uel86kfh18&dq=Salt%20&lr&hl=es&pg=PA22#v=onepage&q=Salt&f=false>
- Libretexts.com. (2014). Reactions of Main Group Elements with Oxygen - Chemistry LibreTexts. *Chem.Libretexts.Com*, 3, 1–4.
- Lucka, M. (2016). Sieve Analysis Different sieving methods for a variety of applications. *October*, 11. [www.retsch.com](http://www.retsch.com)
- Mackenzie, F. T. (2016). Carbonate minerals and the CO<sub>2</sub>-carbonic acid system. *Encyclopedia of Earth Sciences Series*, January 2016, 1–22. [https://doi.org/10.1007/978-3-319-39193-9\\_84-1](https://doi.org/10.1007/978-3-319-39193-9_84-1)
- Maldonado, M. C., & Mendieta, J. M. (2018). “Reintegración de la materia prima autóctona (cloruro sódico en la tierra) en la parroquia santa catalina de salinas de la provincia de Imbabura.” *UNIVERSIDAD DE GUAYAQUIL*, 114.
- Markowski, A., Vallance, J., Chiaradia, M., & Fontboté, L. (2006). Mineral zoning and gold occurrence in the Fortuna skarn mine, Namibia district, Ecuador. *Mineralium Deposita*, 41(4), 301–321. <https://doi.org/10.1007/s00126-006-0062-x>
- Marocco, T. & Winter, R. (1997). Bosquejo de la evolución geodinámica del Ecuador. 1.
- Martínez, V. R., Alonso, R. N., & Galli, C. I. (2020). Morfología de Las Costras Evaporíticas del Salar de Pozuelos (Puna Salteña). *Revista de La Asociación Geológica Argentina*, 77(1), 163–173.
- Mathieu, Colombier; Sebastian B. Mueller, Ulrich Kueppers, Bettina Scheu, P., Delmelle, Corrado Cimarelli, Shane J. Cronin, Richard J. Brown, Manuela Tost, A., & Dingwell, D. B. (2019). Diversity of soluble salt concentrations on volcanic ash aggregates from a variety of eruption types and deposits. 41(3), 251–253. <http://dx.doi.org/10.1037/xge0000076>
- Mees, F., & Tursina, T. V. (2018). Salt Minerals in Saline Soils and Salt Crusts. *In Interpretation of Micromorphological Features of Soils and Regoliths. Elsevier B.V.* <https://doi.org/10.1016/b978-0-444-63522-8.00011-5>
- Montañas, L. (1977). Suelos Salinos. *Departamento de Zaragoza*.
- Morales, J. (2013). Interacción de anhidrita (CaSO<sub>4</sub>) con soluciones acuosas: cristalización y relevancia medioambiental. 1–272.
- Murcia, H. F., Borrero, C. A., Pardo, N., Alvarado, G. E., Arnosio, M., & Scolamacchia, T. (2013). Términos y conceptos para una clasificación volcánoclastica deposits :

*terminology and concepts for a The University of Auckland , School of Environment , Auckland , Nueva Zelanda Massey University , Institute of Resources , Palmerston North , Nueva Zeland. 15–39.*

- Okrusch, M., & Frimmel, E. H. (2019). *Mineralogy: An Introduction to Minerals, Rocks and Mineral Deposits.*
- Osman, K. T. (2018). Management of soil problems. In *Management of Soil Problems.* <https://doi.org/10.1007/978-3-319-75527-4>
- Padilla, D. (2014). Procesos hidrogeoquímicos que dan origen a la salinidad en el sistema acuífero de Tierra Nueva, San Luis Potosí.
- Perkins, D. (2014). Mineralogy. In *British Library Cataloguing-in-Publication Data* (pp. 201–225).
- Pomeroy, C. (1988). The Salt of Highland Ecuador: Precious Product of a Female Domain. *Ethnohistory*, 35(2), 131. <https://doi.org/10.2307/482700>
- Pupiales, A. (2018). Identificación de áreas susceptibles a riesgos naturales y amenazas provocadas por deslizamientos de tierras mediante el uso de sig en el cantón Ibarra parroquias rurales Salinas- Lita.”. *Pontificia Universidad Católica Del Ecuador Sede Ibarra*, 1–41. <https://core.ac.uk/download/pdf/160757437.pdf>
- Quiroga, M. (2021). Evaluación del efecto térmico en arcillas por difracción de rayos X: análisis cuantitativo de fases por el método de Rietveld.
- Quinapallo García, C., & Ochoa Armijos, K. E. (2019). *La diversificación de producción de sal en el Ecuador.* 6.
- Ramón, M., Asensio, I., Blanquer, G., & Manuel, J. (2011). *Minerales carbonatados.* 1–9.
- Retsch GmbH Haan. (2016). Análisis por tamizado. *Verder Scientific*, 56.
- Rzaşa, S., & Owczarzak, W. (2013). Methods for the granulometric analysis of soil for science and practice. *Polish Journal Soil of Science*, XLVII, 1–50. [https://www.iuss.org/media/pjss\\_842-1674-1-sm.pdf](https://www.iuss.org/media/pjss_842-1674-1-sm.pdf)
- Salazar, E. (2010). Historia de la sal en el Ecuador Precolombino y Colonial. *Antropología Cuadernos de Investigación*, 10, 13. <https://doi.org/10.26807/ant.v0i10.46>
- Salvany, J. (1989). Las formaciones evaporíticas del terciario continental de la Cuenca del Ebro en Navarra y Rioja.
- Smith, J. L., & Doran, J. W. (2015). Measurement and use of pH and electrical conductivity for soil quality analysis. *Methods for Assessing Soil Quality*, 169–185.

<https://doi.org/10.2136/sssaspecpub49.c10>

- Soil Survey Staff. (1999). Soil taxonomy: A basic system of soil classification for making and interpreting soil surveys. In *Natural Resources Conservation Service. Agriculture Handbook*. <https://doi.org/10.1007/BF01574372>
- Song, C., Luo, S., Liu, K., Chen, T., Zhang, P., & Fan, C. (2022). Widespread declines in water salinity of the endorheic Tibetan Plateau lakes. *Environmental Research Communications*, 4(9), 091002
- Spalletti, Luis. A.(2006). Evaporites. *Cátedra de Sedimentología, Facultad de Ciencias Naturales y Museo, Universidad Nacional de La Plata*.
- Swanhart, S. L. (2013). Measuring soluble salts in soils via portable X-ray fluorescence Spectrometry. *December*.
- Taboada R.S., M. A. . L. (2009). Alteraciones de la fertilidad de los suelos. El halomorfismo, la acidez, el hidromorfismo y las inundaciones.
- The EU-China Energy and Environment programme. (2009). *Salt Production - A reference book for the industry Salt*.
- Tipantásig, H. (2017). Exploración gravimétrica del Complejo Volcánico Imbabura., Chachimbiro:Provincia de Imbabura.
- Titler, R. V, & Curry, P. (2011). Chemical Analysis of Major Constituents and Trace Contaminants of Rock Salt. *Pennsylvania Department of Environmental Protection Bureau of Water Standards and Facility Regulation*, 28.
- Toraya, H. (2016). A new method for quantitative phase analysis using X-ray powder diffraction: Direct derivation of weight fractions from observed integrated intensities and chemical compositions of individual phases. *Journal of Applied Crystallography*, 49(5), 1508–1516. <https://doi.org/10.1107/S1600576716010451>
- Torres, V. (2018). Manejo de suelos halomórficos. In *Energies* (Vol. 6, Issue 1). <http://journals.sagepub.com/doi/10.1177/1120700020921110%0Ahttps://doi.org/10.1016/j.reuma.2018.06.001%0Ahttps://doi.org/10.1016/j.arth.2018.03.044%0Ahttps://reader.elsevier.com/reader/sd/pii/S1063458420300078?token=C039B8B13922A2079230DC9AF11A333E295FCD8>
- U.S. Geological Survey, M. C. S. (2022). *SALT*. 703, 2022–2023.
- Vallejo, C. (2007). *Evolution of the Western Cordillera in the Andes of Ecuador (Late Cretaceous-Paleogene)*. 17023.
- Vera, R., & Lopez, R. (1992). Tipología de la cangahua, en *Tierra*, Vol. 10 (número especial: Suelos volcánicos endurecidos).

- Villagómez D., Hidalgo S., Bernard B. (2011). Geochronologic, Petrographic and geochemical report on the Chachimbiro volcano, Ecuador. 61 pp. plus appendices (in Spanish). *December 2011*. <https://doi.org/10.13140/RG.2.2.34182.83520>
- Villas, D. (1992). Suelos afectados por sales. *XIII*.
- Wicke, B., Smeets, E., Dornburg, V., Vashev, B., Gaiser, T., Turkenburg, W., & Faaij, A. (2011). The global technical and economic potential of bioenergy from salt-affected soils. *Energy and Environmental Science*, 4(8), 2669–2681. <https://doi.org/10.1039/c1ee01029h>
- Wolf, T. (1892). Geografía y Geología del Ecuador.
- Zappettini, E., Celeda, A., & Pinto, A. (2003). Sales. *SEGEMAR*.